

Faculty of engineering science and technology

Optimization of freeze-thaw durability testing for low-carbon concrete with VPI

Amber Steelandt

UiT & UGent student number: 16610012462 & 01805612

Supervisors: Associate Prof. Iveta Nováková (UiT), Prof. dr. ir Veerle Boel (UGent)

Counsellors: Boy-Arne Buyle (UiT)

Master's dissertation submitted in order to obtain the academic degree of
Master of Science in de industriële wetenschappen: bouwkunde at Ghent University
Course code UiT: BYG-3900

Academic year: 2023-2024



Preface

Embarking on the journey of writing a master's thesis in a foreign country is both daunting and immensely rewarding. It has not only deepened my understanding of low carbon concrete and its durability but it has also offered profound insights into the Norwegian culture beyond the confines of the laboratory.

Throughout this adventure, I have been fortunate to receive invaluable guidance and support from numerous individuals who have played crucial roles in shaping my academic and personal growth. Foremost among them are my thesis advisors, to whom I owe a debt of gratitude. I extend my heartfelt thanks to Prof. Dr. Ir. Veerle Boel (UGent) for her assistance in the preparatory phases and logistical planning prior to my relocation to Norway, as well as her eagerness to answer any concrete related questions I had. I am equally grateful to associate prof. Iveta Nováková (UiT) for generously sharing her expertise, providing crucial mix designs, and offering invaluable guidance on freeze-thaw testing protocols.

Special appreciation goes to Boy-Arne Buyle (UiT) for his indispensable assistance in navigating both the academic and cultural landscape of Narvik, making my Erasmus experience truly unforgettable. My appreciation also extends to Eirik Gjerlow for his instrumental support in setting up chloride migration tests and addressing practical concerns related to my thesis. Additionally, I am thankful to Magdalena Rajczakowska, PhD (Itu), for her guidance on curing methods and invaluable insights into freeze-thaw testing procedures. I am also deeply grateful to Klevis Xhura, Simen Andreassen, and Heike Almo for their unwavering assistance in the laboratory and their willingness to answer any lab related questions I had. I would also like to extend my thanks to Petter Thyholdt, senior engineer at Heidelberg Materials for answering any questions I had concerning the materials I used to make my concrete.

Lastly, I wish to express my profound gratitude to my family and friends whose support and encouragement have been the cornerstone of my journey. In particular, I would like to thank my parents for always believing in me and for their financial support, without which this adventure would not have been possible. Together, these individuals have made an indelible impact on my academic pursuits and personal development, for which I am truly grateful.

Amber Steelandt

Narvik, Norway- May 2024

Acknowledgement

The author gives permission to make this master dissertation available for consultation and to copy parts of this master dissertation for personal use. In all cases of other use, the copyright terms have to be respected, in particular with regard to the obligation to state explicitly the source when quoting results from this master dissertation.

10/05/2024

Remark on the master's dissertation and the oral presentation

This master's dissertation is part of an exam. Any comments formulated by the assessment committee during the oral presentation of the master's dissertation are not included in this text.

Optimization of freeze-thaw durability testing for low-carbon concrete with VPI

Amber Steelandt

Supervisors: Iveta Nováková, researcher (UiT), Prof. dr. ir Veerle Boel (UGent)

Counsellors: Boy-Arne Buyle (UiT)

Master's dissertation submitted in order to obtain the academic degree of
Master of Science in de industriële wetenschappen: bouwkunde at Ghent University

Academic year: 2023-2024

Abstract

Concrete, the most widely used building material, significantly impacts the environment, with cement production contributing up to 8% of global CO₂ emissions. To address this, low-carbon concrete (LCC) mixes with supplementary cementitious materials (SCMs) have been developed. Fly ash (FA) is a well-established SCM, but with the decline of coal-fired power plants, alternatives like volcanic pozzolans from Iceland (VPI) are needed. This research evaluated the durability of concrete with VPI through freeze-thaw (F-T) resistance, compressive strength, and chloride migration tests. Results showed VPI enhanced long-term strength more than FA, although higher VPI percentages reduced strength. VPI significantly improved chloride migration resistance, with higher percentages yielding greater resistance. Concrete with VPI performed well in F-T tests but generally worse than FA. Different curing methods significantly influenced F-T performance, with the effect dependent on factors such as air percentage, spacing factor, W/B ratio, specific surface area, and pore size distribution.

Keywords

Low carbon concrete • supplementary cementitious materials • volcanic pozzolan • VPI • fly ash • freeze-thaw • chloride migration • compressive strength

Extended abstract

Concrete is the most widely used building material, but its environmental impact is significant, with cement production contributing up to 8% of global CO₂ emissions. To address this, low-carbon concrete mixes incorporating supplementary cementitious materials (SCMs) have been developed. Fly ash (FA), a by-product of coal-fired power plants, is a well-established SCM. However, with the phasing out of these plants, alternative SCMs are needed. Natural pozzolans (NPs), such as volcanic pozzolans from Iceland (VPI) introduced by “Heidelberg Materials Sement Norge”, are promising alternatives.

This research evaluated the durability performance of concrete made with VPI through freeze-thaw (F-T) resistance, compressive strength, and chloride migration tests. The results showed that VPI enhanced strength development more after longer curing periods compared to FA, although strength decreased with higher VPI percentages. VPI also significantly improved chloride migration resistance, with higher percentages correlating to greater resistance.

While concrete with VPI performed well in F-T tests, it generally performed slightly worse than concrete with FA. Different curing methods significantly influenced F-T performance. However, the effect of the curing methods was highly dependent on various factors. The use of VPI did not show a consistent pattern of improved or worsened F-T performance under certain curing methods. This indicated that the binder alone did not dictate the effect of the curing method. It was essential to consider additional factors such as air percentage, spacing factor, W/B ratio, specific surface area, and pore size distribution.

In conclusion, VPI was found to be a viable SCM for enhancing concrete durability, but its performance was influenced by a complex interplay of factors. Further research is needed to optimize curing methods and mix designs to fully realize the potential of VPI in low-carbon concrete applications.

Keywords

Low carbon concrete • supplementary cementitious materials • volcanic pozzolan • VPI • fly ash • freeze-thaw • chloride migration • compressive strength

Dutch translation:

Beton is wereldwijd het meest gebruikte bouw materiaal, maar de milieu-impact ervan is aanzienlijk. Dit komt doordat de cementproductie bijdraagt aan maar liefst 8% van de wereldwijde CO₂-uitstoot. Om dit probleem aan te pakken, zijn laag-koolstof betonmengsels ontwikkeld die gebruik maken van supplementaire cementachtige materialen (SCM's). Vliegias, een bijproduct van kolengestookte elektriciteitscentrales, is een bekende SCM. Echter, nu deze centrales geleidelijk aan verdwijnen, zijn alternatieve SCM's nodig. Natuurlijke puzzolanen (NP's), zoals vulkanische puzzolanen uit IJsland (VPI) geïntroduceerd door "Heidelberg Materials Sement Norge", zijn veelbelovende alternatieven.

Deze thesis evalueerde de duurzaamheidsprestaties van beton gemaakt met VPI door middel van vorst-dooi (V-D) testen, druksterketesten en chloride migratietesten. De resultaten toonden aan dat VPI meer bijdroeg aan sterkteontwikkeling na langere uithardingsperioden vergeleken met vliegias, hoewel de sterkte afnam bij hogere VPI-percentages. VPI verbeterde ook significant de chloride migratieweerstand, waarbij hogere percentages aan VPI correleerden met een grotere weerstand.

Hoewel beton met VPI goed presteerde in vorst-dooi testen, presteerde het over het algemeen iets slechter dan beton met vliegias. Verschillende uithardingsmethoden hadden significant invloed op de V-D prestaties. Echter, het effect van de uithardingsmethoden was sterk afhankelijk van verschillende factoren. Het gebruik van VPI toonde geen consistent patroon van verbeterde of verslechterde V-D prestaties onder bepaalde uithardingsmethoden. Dit gaf aan dat het bindmiddel alleen niet het effect van de uithardingsmethode bepaalde. Het was essentieel om aanvullende factoren zoals luchtpercentage, afstandsfactor, W/B-verhouding, specifiek oppervlak en poriëngrootteverdeling in overweging te nemen.

Concluderend, VPI bleek een goede SCM te zijn voor het verbeteren van de duurzaamheid van beton, maar de prestaties werden beïnvloed door een complexe wisselwerking van factoren. Verder onderzoek is nodig om uithardingsmethoden en mengselsamenstellingen te optimaliseren om het volledige potentieel van VPI in laag-koolstof beton toepassingen te realiseren.

Kernwoorden:

Laag koolstof beton • aanvullende cementachtige materialen • vulkanische puzzolaan • VPI • vliegias • vorst-dooi • chloride migratie • druksterkte

Table of contents

<i>Preface</i>	<i>i</i>
<i>Acknowledgement</i>	<i>ii</i>
<i>Remark on the master’s dissertation and the oral presentation</i>	<i>iii</i>
<i>Abstract</i>	<i>iv</i>
<i>Extended abstract</i>	<i>v</i>
<i>Table of contents</i>	<i>vii</i>
Preliminary	1
1 Introductory	2
1.1 Introduction	2
1.2 Problem	3
1.3 Scope of the research and research questions	3
1.4 Research methodology	4
1.5 Thesis outline	5
2 Exploratory literature review	6
2.1 Ordinary Portland cement	6
2.2 Supplementary cementitious materials.....	8
2.2.1 Fly ash	9
2.2.2 Limestone powder	11
2.2.3 Natural pozzolans	12
2.3 What affects the durability of concrete?	21
2.3.1 Compressive strength	22
2.3.2 Freeze-thaw	23
2.3.3 Chloride induced corrosion	31
2.4 Durability improvement	34

Research	35
3 Test procedures	36
3.1 Fresh concrete tests	36
3.2 Compressive Strength	37
3.3 Chloride Migration	38
3.4 Freeze-thaw testing	40
4 Research Characteristics	43
4.1 Terminology for the mixes	43
4.2 Mix design and details about the used materials	44
4.3 Curing conditions	46
4.4 Test pieces	47
Results and Discussion	49
5 Results	50
5.1 Fresh concrete properties	50
5.2 Density evaluation	53
5.3 Compressive strength	54
5.4 Freeze-thaw	57
5.4.1 Results: graphs by curing condition	58
5.4.2 Results: graphs by concrete mix	61
5.5 Chloride migration	66
6 Discussion	68
6.1 Effect of mix design on workability	68
6.2 Effect of mix design on F-T resistance	68
6.3 Effect of mix design on compressive strength	69
6.4 Effect of mix design on chloride migration	69
6.5 Impact of curing conditions on F-T resistance	70

Conclusions	75
Conclusion.....	76
Sustainability reflection.....	77
Future perspectives.....	79
References	80
Appendices	i
A Detailed planning of lab work.....	ii
B Technical data sheets.....	xi
B.1 VPI	xi
B.2 CEM I.....	xii
B.3 CEM II.....	xiii
B.4 Dynamon SX-23.....	xiv
B.5 Mapei air	xvii
C Full mix design for 1 m ³ concrete	xix
D W/C-ratio and W/B ratio calculations	xx
E Compressive strength results.....	xxii
F Chloride migration results.....	xxv
G F-T result graphs and tables	xxvi
G.1 Normal curing samples.....	xxvi
G.2 CO ₂ -curing samples.....	xxix
G.3 Prolonged CO ₂ -curing samples	xxxii
H Pictures of F-T samples after testing.....	xxxv
H.1 Normal curing samples.....	xxxv
H.2 CO ₂ curing samples.....	xxxvi
H.3 CO ₂ and prolonged curing samples.....	xxxviii

I	Spacing factor and air percentage analysis on hardened concrete	xl
I.1	REF-360	xl
I.2	M 18/6-360.....	xli
I.3	M 18/6-300.....	xlii
I.4	M 25/10-360.....	xliii
J	Placement of samples in the F-T chambers.....	xliv

List of Tables

Table 1: chemical constituents of OPC	7
Table 2: types of volcanic rocks.....	15
Table 3: Pozzolanic activity of various types of VP according to literature.....	16
Table 4: chemical composition of volcanic pozzolans according to literature [wt-%].....	17
Table 5: Chemical composition of VPI.....	20
Table 6: compressive strength classes according to EN 206-1	23
Table 7: different pore types and their effect on F-T (Taylor et al., 2021).....	30
Table 8: code names given to the concrete mixes	43
Table 9: code names given to the curing conditions	43
Table 10: mix design of binder for 1 m ³ of concrete	44
Table 11: k-values of binders	45
Table 12: aggregates.....	46
Table 13: curing conditions per test	47
Table 14: test pieces	48
Table 15: overview number of test pieces per test	48
Table 16: fresh concrete properties	50
Table 17: results of test performed according to ASTM C457/457M-16.....	51
Table 18: comparison of amount of SP and free water	53
Table 19: density results for fresh concrete and hard concrete (2d,28d,56d)	53
Table 20: compressive strength results for cubes 100x100x100mm	55
Table 21: strength gain at different curing times [%]	56
Table 22: compressive strength comparison	57
Table 23: resistance to chloride migration according to NT BUILD-492	66
Table 24: chloride migration reduction percentages	67
Table 25: comparison of normal curing to CO ₂ -curing.....	71
Table 26: comparison of normal curing and prolonged CO ₂ curing	72
Table 27: comparison of CO ₂ curing and prolonged CO ₂ curing	72
Table 28: best and worst curing method for each mix	73

List of Figures

Figure 1: Research methodology..... 4

Figure 2: Lambafell Iceland (Norge, 2023) 19

Figure 3: common causes of deterioration ("EN 1504-9," 2008)..... 21

Figure 4: phases of F-T mechanism (R. J. Wang et al., 2022)..... 25

Figure 5: hydraulic pressure theory (Schutter, 2013)..... 26

Figure 6: crystallization theory (Schutter, 2013) 27

Figure 7: different types of pores (Honorio et al., 2018) 29

Figure 8: chloride induced corrosion (Belleghem, 2023) 32

Figure 9: chloride intrusion 33

Figure 10: PH reduction due to chloride migration..... 33

Figure 11: air pressure gauge ("NS-EN 12350-7," 2019) 37

Figure 12: compressive strength machine 37

Figure 13: vacuum pump..... 38

Figure 14: chloride migration test set-up 39

Figure 15: test piece split in half 39

Figure 16: test piece side profile 39

Figure 17: F-T test piece 41

Figure 18: samples in F-T chamber..... 41

Figure 19: CEM I product specification..... 46

Figure 20: CEM II product specification 46

Figure 21: surface of REF-360..... 51

Figure 22: surface of M 25/10-360 51

Figure 23: density progress of concrete samples 54

Figure 24: compressive strength for cubes 100x100x100mm (2d,28d,56d)..... 56

Figure 25: F-T results for regular curing..... 59

Figure 26: F-T results for CO₂ curing 60

Figure 27: results for prolonged CO₂ curing..... 61

Figure 28: F-T results for REF-360..... 62

Figure 29: F-T results for M 18/6-360 63

Figure 30: F-T results for M 18/6-300 64

Figure 31: F-T results for M 25/10-360 65

Figure 32: chloride migration at 28d and 56d 67

Figure 33: visual representation of scaling for different curing conditions 73

List of abbreviations

NP	Natural pozzolan	CPT	Chemical pozzolanicity test
SCM	Supplementary cementitious materials	ECM	Electrical conductivity method
VPI	Volcanic pozzolan Iceland	W/B	Water/binder
GGBFS	Ground granulated blast furnace slag	W/C	Water/cement
OPC	Ordinary Portland cement	VG	Volcanic glass
LCC	Low carbon concrete	SeP	Sedimentary pozzolan
MS	Micro-silica	VM	Volcanic material
SF	Silica fume	VR	Volcanic rocks
LP	Limestone powder	R	Rhyolite
FA	Fly ash	B	Basalt
SP	Superplasticizer	H	Hyaloclastite
VA	Volcanic Ash	P	Pumice
VP	Volcanic Pozzolans	F-T	Freeze-thaw
SAI	Strength activity index		
TGA	Thermo-gravimetric Analysis		
XRF	x-ray fluorescence		
XRD	x-ray diffraction		

List of chemical names

CO₂	Carbon dioxide	Ca(OH)₂	Calcium hydroxide
SiO₂	Silicon dioxide	C-S-H	Calcium silicate hydrate
Al₂O₃	Alumina oxide	C-A-S-H	Calcium-Alumino-Silicate-hydrate
Fe₂O₃	Ferric oxide		
CaO	Calcium oxide		
MgO	Magnesium oxide		
Na₂O	Sodium oxide		
K₂O	Potassium oxide		
SO₃	Sulfur trioxide		
TiO₂	Titanium dioxide		
P₂O₅	Phosphorus pentoxide		
Mn₂O₃	Manganic oxide		
CL	Chloride		
Na₂O eq⁻	Sodium oxide equivalent		

Part I
Preliminary

1

Introductory

1.1 Introduction

One of the most used construction materials worldwide is concrete, which is made by mixing a binder, aggregates, and water. During this process, the binder will react with the water, forming a matrix that binds the aggregates together. Typically, cement serves as the binder in traditional concrete production. (S.Druart & L.Taerwe, 2018) When focusing on the environmental impact that concrete has, it is noticeable that cement production is a prominent contributor to carbon dioxide (CO₂) emissions. It accounts for approximately seven to eight percent of the world's annual CO₂ emissions. (Singh et al., 2020) However, it wasn't until the 1990s that the construction industry, including the cement industry, began to acknowledge its environmental impact. (Nidheesh & Kumar, 2019)

In response to these environmental concerns, researchers have embraced the task of investigating alternatives to traditional cement in concrete production. This exploration has led to the formulation of low-carbon concrete (LCC), achieved by incorporating supplementary cementitious materials (SCMs) alongside ordinary Portland cement (OPC). (Nukah et al., 2022)

Research has shown that incorporating SCMs into concrete production can lead to a significant reduction of up to 80% in CO₂ emissions. This reduction is primarily attributed to the fact that cement production is the main source of CO₂ emissions associated with concrete manufacturing. Additionally, SCMs, often derived from waste products of other industrial processes, offer an environmentally friendly alternative to OPC. Unlike cement production, the manufacturing process for SCMs is typically less resource-intensive. (Singh et al., 2020)

The most widely recognized SCMs include fly ash (FA), ground granulated blast furnace slag (GGBFS), micro-silica/silica fume (MS/SF), and limestone powder (LP). Nevertheless, other materials can serve as alternatives to cement such as natural pozzolans (NP).

The research conducted in this thesis is part of the Ar2CorD project. This is a collaboration project between different Nordic countries to research the optimization of LCC with the use of both known and unknown SCMs. In this project mixes are used with a substitution percentage of at least 30% (UIT, 2023).

1.2 Problem

The most widely recognized and utilized SCM is FA. However, the availability of FA is decreasing due to the phasing out of coal-fired power plants. (Norge, 2023) This necessitates the exploration of alternative materials like NP. Within the group of NP, Volcanic pozzolans (VP) have emerged as a promising candidate for fulfilling the role of SCMs in concrete production. (Hamada et al., 2023)

As new types of SCMs, including VP, are being investigated, there is a pressing need for further research into their durability characteristics. Many natural SCMs remain unexplored, with limited data available regarding their durability performance. The properties of concrete are dependent on various factors such as curing conditions, the input materials, and the ratios in which they are used (S.Druart & L.Taerwe, 2018). Therefore it is crucial to investigate how altering these variables can impact the durability performance of concrete. This investigation can illuminate the mix designs that show the most promising results in terms of durability performance.

1.3 Scope of the research and research questions

The research conducted in this thesis was limited to four different concrete mixes. Three of these mixes were made with a NP, specifically a volcanic pozzolan (VP). The VP that is used in this thesis, originates from Iceland. It is referred to as Volcanic pozzolan Iceland or VPI. The fourth mix is a reference mix, made with FA-cement. Within the mix design different cement replacement ratios were used.

Since this research aims to evaluate the durability performance of LCC with VPI different durability tests were conducted. These tests were limited to freeze-thaw (F-T) tests under various curing conditions including CO₂ treatment and prolonged CO₂ curing, chloride migration (CM) tests, and compressive strength tests.

To conclude the following research questions were asked:

- What effect does the mix design have on the durability of low-carbon concrete?
 - How does concrete with VPI perform in terms of compressive strength compared to the reference mix?
 - How does concrete with VPI perform in terms of freeze-thaw resistance compared to the reference mix?
 - How does concrete with VPI perform in terms of chloride migration resistance compared to the reference mix?
 - How does the replacement ratio of VPI affect the durability performance
- What effect does the curing method have on the freeze-thaw performance of low-carbon concrete?
 - What effect does CO₂-curing have compared to normal curing?
 - What effect does prolonged CO₂-treatment have compared to normal curing?

1.4 Research methodology

This thesis consisted of two distinct phases: the initial stage involved preparation and planning, while the subsequent phase entailed conducting laboratory work and analyzing the results. Figure 1 shows the two phases divided over the entire school year along with the corresponding smaller work packets associated with each phase.

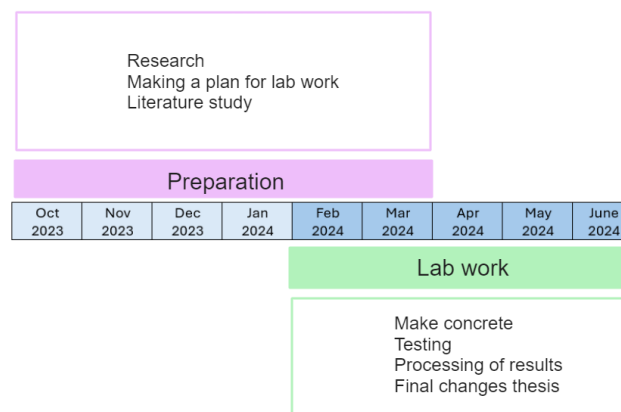


Figure 1: Research methodology

The majority of the preparation took place in Belgium at the University of Ghent, with a smaller portion of the preparation and the entirety of the laboratory work being conducted in Norway at the guest institution, UiT. Initially, research was undertaken to comprehend LCC by conducting a search on “Web of Science” for previously published studies on this topic.

Additionally, European standards were studied to enhance comprehension of the testing procedures planned for the second semester.

The second phase mainly consisted of laboratory work, which started with making the concrete mixes necessary for this research. Since this master thesis resides within the program of Ar2CorD it was important to create a mix design that aligns with the expectations of the project. The reference mix used in this thesis aligned with the one from Einar who resides in BM-Valla, Iceland. The other mixes, containing VPI had different substitution percentages based on the mix design that was provided by Iveta Nováková, associate professor at UiT. To investigate the impact of varying binder replacement ratios, mix designs were formulated with this as the sole differentiating factor. This means using identical admixtures and aggregates across all mix variations. The concrete aimed for a slump with a slump class of S4 (200-220 mm) and an air percentage of 4-6% which was tested on the fresh concrete according to standard procedures.

Furthermore, preparations were made to start the testing process of the three tests this thesis was limited to. This consisted of F-T tests, compressive strength tests and chloride migration tests. Since three different curing methods were used for the F-T tests, many of the samples had their own planning. This made it extremely difficult to keep up with the testing days. Therefore a very detailed plan was made to keep track of the different test pieces. This plan is shown in appendix A. More detailed information regarding the test procedures are given in section 3.

To answer the previously established research questions, the test results were compared with each other and with the reference mix. Despite the relative scarcity of VP as SCMs, several research papers have delved into their durability performance. By using previous studies it could be established whether the outcomes of the test results aligned with expectations.

1.5 Thesis outline

This thesis is structured into four primary sections. The first part is the preliminary, presenting the practical details about the thesis and conducting a literature review to delve into LCC and its ingredients. It also elucidates the concept of concrete durability and the factors impacting it. The second section entails the core research, detailing the tests, mix design, and other crucial aspects. Following that, the third part unveils the findings, while the fourth section offers the concluding remarks.

2

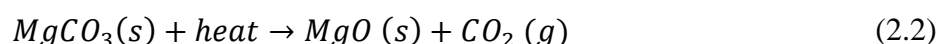
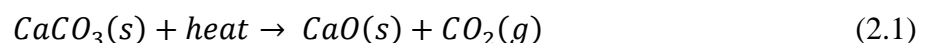
Exploratory literature review

Concrete, as previously mentioned, is composed of aggregates bonded together through a reaction between a binder and water. In efforts to mitigate the environmental impact associated with traditional concrete, researchers delved into the possibility of partially substituting OPC with SCMs. Over the years, a key research inquiry has been whether LCC can match or surpass the durability standards set by conventional concrete. It is crucial to explore alternative binders and their durability performance. Subsequent sections will provide a more detailed examination of various binders and the factors influencing the durability of concrete.

2.1 Ordinary Portland cement

Binders are the materials that are used within concrete to bind the inert materials such as sand or gravel together (Boel, 2006). There are two distinct categories. The first category is the hydraulic binders, which experience a hydration reaction. The second category involves pozzolanic binders, which undergo a pozzolanic reaction. The most used binder worldwide is OPC. It is classified as a hydraulic binder and undergoes a hydration reaction when mixed with water. This forms a paste that subsequently solidifies resulting in the making of concrete when mixed with aggregates. (S.Druart & L.Taerwe, 2018)

Portland cement is produced from Portland clinker, which is manufactured using either the wet or dry milling process. In both methods, limestone (CaCO_3), clay, and other clay-like materials are added into a rotating kiln. Water is included in the wet milling process. (Boel, 2006) The main reactions that take place when making Portland cement are shown in reactions 2.1 and 2.2.(Durastanti & Moretti, 2020)



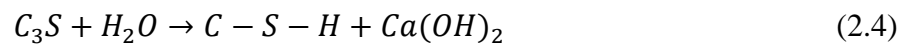
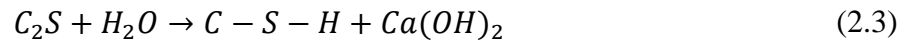
To produce OPC, the resulting clinker is ground, and gypsum (CaSO_4) is added. This final step ensures the desired properties of the cement. The fundamental elements of OPC include calcium silicates (C_2S , C_3S) and calcium aluminates (C_3A , C_4AF), which are generated through the heat-

induced reactions among the existing oxides present in the Portland clinker. The full chemical names for these elements are given in Table 1. (Boel, 2006)

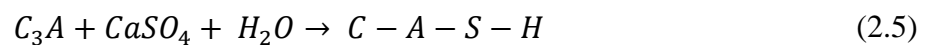
Table 1: chemical constituents of OPC

Abbreviation	Full chemical name
C ₂ S	2CaO.SiO ₂
C ₃ S	3CaO.SiO ₂
C ₃ A	3CaO.Al ₂ O ₃
C ₄ AF	4CaO.Al ₂ O ₃ .Fe ₂ O ₃

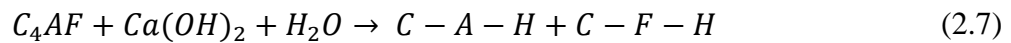
When OPC is used to make concrete, the calcium silicates will initiate a hydration reaction when combined with water leading to the formation of calcium silicate hydrate (C-S-H gel) and calcium hydroxide (Ca(OH)₂) as shown in the simplified reactions 2.3 and 2.4. The C-S-H gel plays a crucial role in interconnecting particles within the concrete, thereby influencing its strength and durability. The calcium hydroxide on the other hand is a by-product that does not directly influence the strength of the concrete. It does however, contribute to the alkalinity of the concrete. (S.Druart & L.Taerwe, 2018)



The calcium aluminates will immediately react when in contact with water, resulting in a high heat development and low strength. To avoid this, gypsum (CaSO₄) is added to the Portland cement as previously mentioned. This ensures that the reaction will slow down, thereby diminishing the adverse side effects it induces. The C₃A will react with water, producing a C-A-S-H gel as long as gypsum is present, as depicted in simplified reaction 2.5. However, once the initial gypsum content in OPC is depleted, the reaction of C₃A with water will yield a C-A-H gel instead, as illustrated in reaction 2.6. (Boel, 2006)



The C_4AF reacts with a reaction product of one of the previous reactions, resulting in the forming of C-A-H gel and C-F-H gel as shown in reaction 2.7.(Boel, 2006)



These reactions all contribute to what is known as the hydration process of cement. Physically the cement will first have a high workability but after a while the cement paste will start to harden until it becomes a solid consistency. The hardening of the concrete will continue until the concrete reaches a curing time of approximately 28 days. (Boel, 2006)

Because Portland cement causes up to seven percent of the global CO_2 emissions, it is necessary to find alternatives for this binder (Abhishek et al., 2022).

2.2 Supplementary cementitious materials

Cement can partially be replaced by Supplementary cementitious materials to produce low-carbon concrete. SCMs are typically by-products of industrial processes (Nandhini & Ponmalar, 2018). Various types of SCMs are known and new types are still being tested today. The most commonly known types of SCMs are FA, GGBFS, and MS/ SF (Ralli & Pantazopoulou, 2021). However, natural pozzolans can also be used as SCMs (Papadakis et al., 2002). The term "supplementary cementitious material" typically refers to materials that either have pozzolanic activity or can react with the hydration products of cement to enhance the properties of concrete. (Ralli & Pantazopoulou, 2021)

As previously mentioned there are two types of binders, being the hydraulic and the pozzolanic binder. Pozzolanic binders will react in the presence of water and calcium hydroxide ($Ca(OH)_2$) (Pacewska & Wilinska, 2015). The formation of $Ca(OH)_2$ is a consequence of the hydration reaction triggered by OPC, as detailed in section 2.1. When a combination of OPC and FA is used as a binder, the hydraulic reaction will occur first. The calcium hydroxide that is then formed will subsequently react with the FA as a result of the pozzolanic reaction. This reaction results in the formation of C-A-S-H or C-A-H gel. However, certain varieties of FA have high concentrations of calcium compounds, enabling them to exhibit self-cementing characteristics. This implies that they can harden in the presence of water without the need for additional $Ca(OH)_2$. (Pacewska & Wilinska, 2015) OPC is a hydraulic binder, while FA and VPI can be categorized as pozzolanic binders.

2.2.1 Fly ash

Fly ash, a by-product of power plants generating pulverized coal is the most dominantly used SCM when making low-carbon concrete (Ralli & Pantazopoulou, 2021). It is a pozzolanic binder which means that it reacts chemically with calcium hydroxide in the presence of water. (Shania Zehra Naqvi 2022)

When powdered coal is burned in thermo-electric power plants, fine dust particles will be transported with the gasses that are released during the burning process. In the chimney, there are electrostatic or mechanical dust removers present. These dust removers will catch the dust particles which are then quenched in water to achieve the fly ash that can be used as a SCM. (Boel, 2006)

There are two categories in which fly ash can be classified. These are class C fly ash and class F fly ash. Class C stands for high calcium fly ash that contains more than 20% limestone, whilst class F is low calcium fly ash that contains less than 7 % limestone. (Ralli & Pantazopoulou, 2021) Class F fly ash is typically produced by burning high-quality coals, such as anthracite and bituminous coals. These ashes possess pozzolanic properties, which means they react with calcium hydroxide ($\text{Ca}(\text{OH})_2$) and water to form compounds that contribute to the hardening of concrete. However, Class F fly ash lacks inherent cementitious characteristics and thus requires mixing with either Portland cement (OPC) or limestone powder (LP) to create concrete. On the other hand, Class C fly ash is generated from the combustion of lower-quality coals, including lignite and sub-bituminous coal. This class of FA not only exhibits pozzolanic properties but also possesses cementitious properties. As a result, Class C fly ash may not necessarily require the addition of OPC or LP to initiate the hydraulic reactions necessary for concrete formation. (Shania Zehra Naqvi 2022) Class F fly ash is used the most to produce LCC since it is easier to find and has a slower hardening process than class C. (Ralli & Pantazopoulou, 2021).

By partially replacing cement with fly ash, a reduction of CO_2 emissions is made. By partially substituting cement with fly ash there is a small risk of getting cracking at an early age due to the reductions of hydration heat (Shania Zehra Naqvi 2022). A study done by Khan et al. (2017) similarly states that drying shrinkage reduces. However, this reduction is relatively small and therefore the shrinkage-induced stress development in FA-concrete and OPC-concrete were similar. Substituting OPC with FA does not negatively affect the concrete properties in terms of shrinkage-induced stress development. Moreover, the use of FA results in a concrete mix that requires less water for achieving the desired workability. Consequently, this contributes to

greater long-term strength of the concrete (lynx, 2023). However, it's crucial to acknowledge that an excessively high substitution ratio can lead to a reduction in initial strength, as FA concrete necessitates a longer curing period to reach its optimal strength. (Bouzoubaâ et al., 2011)

According to a study conducted by Wang et al.(2017) incorporating FA and SF into concrete leads to a notable enhancement in its resistance against a combined F-T and sulfate attack, particularly when the substitution level of fly ash reaches 25%. A later study conducted by Wang et al. (2022) confirms this by stating that concrete containing FA can lead to improved F-T durability when an appropriate dosage is used. The study stated that a substitution percentage of 5-20% is recommended. The pozzolanic reaction and filling effect of FA particles enhance cementation, thereby limiting external water infiltration. FA-concrete possesses a denser internal structure with fewer pores and fine cracks compared to non-FA concrete. However, a study done by Bouzoubaâ et al. (2011) states that a very high fly ash substitution ratio (>50%) may exhibit decreased durability against freeze-thaw cycles or carbonation at an early age. Wang et al. (2022) confirms this by stating that due to the slower pozzolanic reaction of FA in the early stages compared to cement, concrete with very high FA content (> 50%) is not recommended for use in salt freezing conditions.

The substitution percentage of FA lies within the range of 15-33wt% but can go up to 70wt% for different types of concrete structures. (Shania Zehra Naqvi 2022) The Norwegian standard NS-EN 206 ("NS-EN 206," 2022) however, recommends not exceeding a substitution percentage of 35% of the total binder mass. The standard also states that frost-resistant concrete consisting of a FA percentage over 20% needs to be submitted to freeze-thaw testing.

2.2.2 Limestone powder

Limestone powder does not contain hydraulic or pozzolanic properties. This binder will enhance some properties that cement has, leading to good processability. (Boel, 2006) LP can be used as a filler material to improve properties such as workability and density. Literature may classify it as an SCM but it's crucial to distinguish that it doesn't fall under the same classification as materials like FA, which actively engage in chemical reactions within concrete.

LP is almost inert but it does partially react with aluminates, producing carbo-aluminate and carbo-silicate hydrates. LP will also dilute the binder phase in concrete which contributes to a higher porosity. This negatively impacts durability properties associated with porosity, such as resistance to carbonation.(Marinkovic et al., 2023)

Celik et al.(2019) found that incorporating FA as a partial substitute for OPC increases early-age strength in concrete when LP is added to the mix. Similar observations were made when natural pozzolans were used as a partial substitute in the concrete instead of FA. This observation is supported by Marinkovic et al. (2023), who highlight that LP usage in concrete leads to higher early-age strength due to the early formation of carbo-aluminates. However, this phenomenon does not necessarily extend to the concrete's strength over time.

LP also attributes to improved particle packing within the concrete due to the filler effect. This means that LP can fill the space between cement particles, subsequently improving the packing density (Marinkovic et al., 2023)

2.2.3 Natural pozzolans

Natural pozzolans (NP) can serve as substitutes for cement in concrete manufacturing. The utilization of natural pozzolans in concrete dates back over 3000 years when they were initially combined with lime to create concrete and mortars. Historical evidence reveals that Romans utilized volcanic tuffs and pumice in their concrete. The Greeks also used natural pozzolans, as evidenced by the discovery of a concrete-lined water storage tank in the city of Kamiros on the island of Rhodes. (gcca, 2023) However, with the rapid expansion of the construction industry and the widespread adoption of cement, natural pozzolans fell out of favor. In light of contemporary climate concerns, there is a renewed interest in reintegrating these pozzolans into construction practices.

NP needs to have pozzolanic activity for them to be considered as a SCM to use in concrete. Several methods exist for assessing the pozzolanic activity of a material, with two prominent ones being the chemical test and the strength activity index (SAI) outlined in ASTM C618 ("ASTM C618," 2023). The chemical test mandates that the combined oxides of silicon, iron, and aluminum (SiO_2 , Fe_2O_3 , and Al_2O_3) should comprise at least 70% of a natural pozzolan's composition to meet concrete usage criteria. The SAI test evaluates the ratio of compressive strength between mortar containing 20% natural pozzolan as a supplementary cementitious material (SCM) and control mortar. The water-to-binder ratio of the control mortar remains fixed at 0.484, while that of the SCM-mortar is adjusted to achieve a flow within ± 5 of the control mortar. The compressive strengths of SCM-mortars must reach at least 75% of the control mortar's strength at either 7 or 28 days. (Parhizkar et al., 2010; Wang et al., 2023)

However, several studies have begun questioning whether the tests stated by ASTM C618 are accurate in defining the pozzolanic reactivity of the materials. Kalina et al. (2019) states that these tests may result in false positives, indicating that inert natural pozzolans could wrongly be categorized as pozzolanic materials based on the standard. Hence, it is crucial to explore alternative testing methods. Parhizkar et al. (2010) made a similar statement and highlighted the importance of incorporating multiple test procedures when determining the suitability of a material to be used as a SCM.

Another renowned method for assessing pozzolanic activity in materials is the Frattini test, outlined in EN 196-5 ("EN 196-5," 2011). In this procedure, samples are prepared by blending cement and natural pozzolan with distilled water. These samples are subsequently enclosed in a sealed plastic container and kept in an oven at 40°C for at least 8 days. Afterward, the samples

undergo vacuum filtration through filter paper and are allowed to cool in sealed Buchner funnels until reaching ambient temperature. The filtrate is then subjected to titration to determine the presence of OH^- and Ca^{2+} . The obtained results are plotted on a graph featuring a predefined curve, which delineates pozzolanic and non-pozzolanic regions. The analyzed material is then positioned on this graph. Materials falling on or above the curve are classified as non-pozzolanic, while those falling below are deemed pozzolanic. (Parhizkar et al., 2010; Wang et al., 2023)

Pozzolanic activity can also be assessed using thermo-gravimetric analysis (TGA). Pozzolanic materials contain crystalline calcium hydroxide, which decomposes when subjected to temperatures between 400-500°C. In TGA, the material undergoes this temperature treatment, causing the calcium hydroxide to decompose and resulting water to evaporate. The decrease in weight is then measured. Effective pozzolans exhibit minimal weight loss, whereas weaker ones show greater weight reduction. It's important to note however, that this method is not standardized. (Parhizkar et al., 2010)

Another test to determine the pozzolanic reactivity of VP is the chemical pozzolanicity test (CPT) according to EN-196-5 ("EN 196-5," 2011). This test compares the amount of calcium ions in a solution that's in contact with hydrated cement to the amount of calcium ions that saturate a solution made of a mixture of OPC and VA. (Presa et al., 2023)

The final test under consideration is the electrical conductivity method (ECM). This test measures the conductivity shift in the cement-NP slurry as the pozzolanic reaction unfolds. As the consumption of $\text{Ca}(\text{OH})_2$ due to the pozzolanic reaction intensifies, the conductivity diminishes. Hence, reduced conductivity signifies heightened pozzolanic activity. While this method serves well for comparing various types of NP, quantifying activity proves challenging. Consequently, it is typically employed alongside other techniques. (Wang et al., 2023)

NP can be classified into two categories. The first category consists of those with a sedimentary origin, commonly known as sedimentary clays and shales. However, these sedimentary pozzolans typically exhibit minimal pozzolanic reactivity. Consequently, heat treatments are often employed to enhance their reactivity. (Yuan & Ma, 2021) Since sedimentary pozzolans such as clays and shales are not relevant to this thesis, they will not be further discussed. Instead, the focus will be on the second category. These are the natural pozzolans of volcanic origin, also referred to as volcanic pozzolans (VP).

2.2.3.1 How are volcanic pozzolans formed?

First, it's crucial to understand the distinction between lava, magma, and tephra. Magma refers to molten rock beneath the Earth's surface, while lava is the molten rock that emerges onto the surface during a volcanic eruption (USGS, 2023). Tephra represents the ejected materials during eruptions and consists of rock fragments, ash, and volcanic glass (Thordarson & Larsen, 2007).

Volcano eruptions are typically categorized based on their eruption style, either as effusive or explosive. Effusive eruptions involve the gradual movement of lava onto the Earth's surface, whereas explosive eruptions result in the sudden release of gas and tephra. The behavior of these eruptions is largely influenced by the amount of gas trapped within the magma. If there is a significant buildup of gas pressure, it can trigger an explosion. Conversely, magma with low viscosity allows gas to escape more easily, resulting in slower and more steady lava flows during volcanic eruptions, as the magma slowly ascends through the volcano's vent. (BGS, 2024). Subsequently, the majority of ejected material will consist of tephra for explosive eruptions and lava for the effusive eruptions (Thordarson & Larsen, 2007).

Volcanic materials (VM) can be classified based on their geological properties, which relate to their formation process. The primary categories include volcanic rocks (VR), volcanic glass (VG), and volcanic ash (VA). (Waikado, 2010) Additionally, these materials can undergo pozzolanic classification, where their pozzolanic properties are assessed independently of their geological classification. This classification determines whether the materials exhibit pozzolanic activity, regardless of their geological origin. This second classification is the most relevant for the usage of VM in concrete. However, to avoid confusion a clarification will first be made on the geological classification.

VG forms when lava or magma cools rapidly, preventing the formation of crystalline structures resulting in the glassy texture characteristic of VG (Britannica, 2024). Another consequence of volcanic eruptions is volcanic ash (VA). During explosive eruptions, magma undergoes fragmentation, producing small particles that are ejected into the air, forming VA. As these particles are propelled into the atmosphere, they cool rapidly due to the lower temperatures, inhibiting the formation of large crystals. VA can be transported over long distances by wind and eventually settles onto the Earth's surface. (USGS, 2024)

When a volcano erupts, volcanic rocks (VR) are formed as a result of magma cooling (Jubera-Pérez et al., 2024). The type of VR that is formed is highly dependent on the type of magma it originates from and the respective cooling process. There are three types of magma: basaltic, andesitic, and rhyolitic. Basaltic magma is characterized by its high iron and magnesium content and low silica content, with temperatures reaching approximately 1200°C. Andesitic magma contains less iron, more silica, and typically has temperatures ranging from 800 to 1000°C. Rhyolitic magma, rich in silica and low in iron and magnesium, has lower temperatures between 750 and 850°C. (Waikado, 2010) On the other hand, the cooling process is also important to differentiate different volcanic rocks types. Basalt and hyaloclastite for example both originate from basaltic magma but they have a different cooling process which ultimately distinguishes the two. The most known types of volcanic rocks and their respective abbreviations are shown in table 2.

Table 2: types of volcanic rocks

Type of VR	Abbreviation
Rhyolite	R
Basalt	B
Hyaloclastite	H
Pumice	P

2.2.3.2 Volcanic pozzolans in concrete

Materials of a volcanic origin do not automatically possess pozzolanic activity, which is a requirement for their consideration as a SCM. Therefore, only the volcanic materials that have been tested for pozzolanic activity are classified as VP and can be used as a SCM. (Jubera-Pérez et al., 2024).

Over time, diverse varieties of VP have been gathered from locations across the globe and subjected to different pozzolanic activity tests. Table 3 displays different types of VP collected around the world, the conducted tests, and their respective outcomes. Results are categorized as "good" if the pozzolanic activity meets concrete usage standards set by the performed test, and as "low" if it falls below qualification criteria.

Table 3: Pozzolanic activity of various types of VP according to literature

Source	Type of VP	Location/origin	Test performed	Pozzolanic activity
(Jubera-Pérez et al., 2024)	VA	La palma (canary Islands, Spain)	Chemical test	Good
			SAI	Good
(Sierra et al., 2022)	VA	Tecpan town (Guatemala)	Chemical test	Good
			ECM	Low
			Frattini	Good
			TGA	Good
(Sierra et al., 2022)	VA	El Rancho town (Guatemala)	Chemical test	Good
			ECM	Low
			Frattini	Good
			TGA	Good
(Rahhal & Talero, 2010)	NM*	Olot, Gerona (Spain)	Frattini	Good
"	NM*	Almagro, Ciudad Real (Spain)	Frattini	Good
"	NM*	Canary Islands (Spain)	Frattini	Good
(Presa et al., 2023)	VA	La palma (canary Islands, Spain)	CPT	Good
(Danner et al., 2023)	P	Iceland	TGA	Good
"	R	"	TGA	Good
"	B	"	TGA	Good
"	H	"	TGA	Good

*NM= Not mentioned

A study conducted by Hamada et al. (2023) states that volcanic pozzolans vary in chemical composition depending on their origin. Consequently, outcomes obtained with one type of volcanic pozzolan may diverge from those obtained with another type. The main components of all volcanic pozzolans, regardless of their geological classification, are silicon dioxide (SiO₂), alumina oxide (Al₂O₃) and ferric oxide (Fe₂O₃). Additionally, notable constituents include calcium oxide (CaO), magnesium oxide (MgO), sodium oxide (Na₂O), potassium oxide

(K₂O) and sulfur trioxide (SO₃). The components can be determined using either x-ray fluorescence (XRF), x-ray diffraction (XRD) or other suitable techniques. Table 4 presents the chemical compositions of various VP, used as SCMs, documented in the literature. It offers insight into the range within which the chemical composition of VP may fall.

Table 4: chemical composition of volcanic pozzolans according to literature [wt-%]

Source	SiO ₂	Al ₂ O ₃	Fe ₂ O ₃	CaO	MgO	Na ₂ O	K ₂ O	SO ₃	Others
(Jubera-Pérez et al., 2024)	38.20	14.10	18.60	11.20	6.50	3.00	1.50	0.20	6.30
(Sierra et al., 2022)	70.49	13.57	1.83	1.82	0.50	3.35	4.02	0.11	0.94
"	72.06	12.67	1.14	1.14	0.40	3.68	4.45	0.19	0.69
(Rahhal & Talero, 2010)	45.12	13.84	13.82	10.48	9.54	3.18	2.40	0.46	0.00
"	41.38	19.36	12.05	11.11	10.58	1.24	0.44	0.00	0.00
"	54.18	20.10	3.12	2.38	2.04	5.64	5.17	0.00	0.00
(Siddique, 2012)	59.32	17.5	7.06	6.10	3.80	2.55	2.03	0.71	0.00
(Pougnong et al., 2022)	39.83	17.74	14.27	8.72	7.65	1.68	0.88	0.02	4.92
"	45.15	16.93	11.44	8.14	5.41	2.90	1.83	0.06	3.8
(Presa et al., 2023)	43.40	13.40	13.50	10.90	8.10	3.77	1.47	0.00	4.56
(Taniguchi et al., 2018)	72.60	15.30	2.30	0.10	0.10	2.80	6.30	0.00	0.50
"	67.80	16.50	6.80	1.80	0.80	2.70	2.20	0.00	1.40
"	74.60	13.60	23.00	0.80	0.20	2.10	6.20	0.00	0.30
"	73.30	14.00	2.80	1.10	0.30	2.60	5.50	0.00	0.30
(Danner et al., 2023)	65.8	14.80	6.50	3.30	0.50	4.60	2.00	0.00	0.00
"	60.40	13.80	8.00	4.80	2.30	2.70	1.60	0.00	0.00
"	47.90	14.70	11.90	12.10	8.60	1.80	0.30	0.01	0.00
"	47.80	14.40	11.90	11.80	9.20	1.80	0.30	0.01	0.00
Minimum	38.20	12.67	1.14	0.1	1.24	0.30	0.00	0.00	0.00
Maximum	74.60	20.10	23.00	12.10	10.58	5.64	6.30	0.71	6.30
Median	56.75	14.55	9.72	5.45	3.05	2.75	2.02	0.01	0.30
Mean	56.63	15.35	9.45	5.99	4.25	2.89	2.70	0.10	1.32

A study done by Siddique (2012) additionally says that the particle size of the volcanic pozzolans varies based on the distance from the volcano. This study specifically talks about volcanic ash (VA), a type of volcanic pozzolan, that is generated when solid rock shatters and magma separates into very small particles during explosive volcanic activity. These fine particles of ash settle across the landscape and their particle size decreases with an increased distance to the volcano it originated from. In a study done by Celik et al. (2019) it is stated that volcanic ash with a smaller particle size enhances microstructural development of the matrix when used in concrete. This occurs through the generation of secondary C-S-H gel and calcite, resulting in increased compressive strength. Similarly, Kupwade-Patil et al. (2018) found that using VA of smaller particle size in concrete increases strength through the formation of secondary C-S-H gels compared to concrete with VA that has a bigger particle size.

Generally speaking, the substitution of OPC with VP in concrete will initially decrease its early compressive strength, which can lead to the extension of construction durations. Nevertheless, the strength will keep increasing due to the additional pozzolanic reaction that occurs later in time. (gcca, 2023). When LP is added to the mix the early-age strength can increase (Celik et al., 2019). The substitution percentage of NP also has an important effect on durability and compressive strength. According to Hossain & Lachemi (2007) the compressive strength of concrete with VA will decrease with the increase of the VA substitution percentage compared to concrete with only OPC. A similar study that was conducted by Aziz et al. (2021) concludes the same thing.

Yuan & Ma (2021) state that the use of NP in concrete can lead to workability loss, resulting in a higher need for superplasticizer (SP) or water. Similarly, Liu et al. (2023) states that utilizing VA in concrete diminishes its workability, requiring a greater amount of superplasticizer than regular Portland cement concrete to achieve the same slump. However, replacing some VA with LP can improve concrete workability, thus decreasing the need for superplasticizer to attain desired workability levels (Liu et al., 2023).

The use of NP in concrete can also improve resistance to chemically aggressive surroundings such as an improved resistance to carbonation. This generally improves durability and therefore leads to concrete buildings that have prolonged service lives and require less maintenance. (gcca, 2023) Taniguchi et al. (2018) similarly states that concrete with a partial substitution of VA can result in an improved carbonation resistance, but that it severely depends on the reaction

ratio and fine particle quantity. Yuan & Ma (2021) state that the use of NP leads to lower chloride migration and improved sulfate resistance.

2.2.3.3 Volcanic pozzolan Iceland

VPI is a SCM that is planned to be introduced by “Heidelberg Materials Sement Norge”. It is made by using volcanic pozzolans that originates from “Lambafell” in Iceland. Lambafell is a volcanic mountain that is located in the south-west region of Iceland as shown in Figure 2. The volcanic pozzolan found at Lambafell originates from nearby volcanic activity. (Norge, 2023) Since Iceland resides on top of a tectonic boundary where the North American and Eurasian plates are diverging, it is subject to many volcanic eruptions (Sigmundsson et al., 2020).

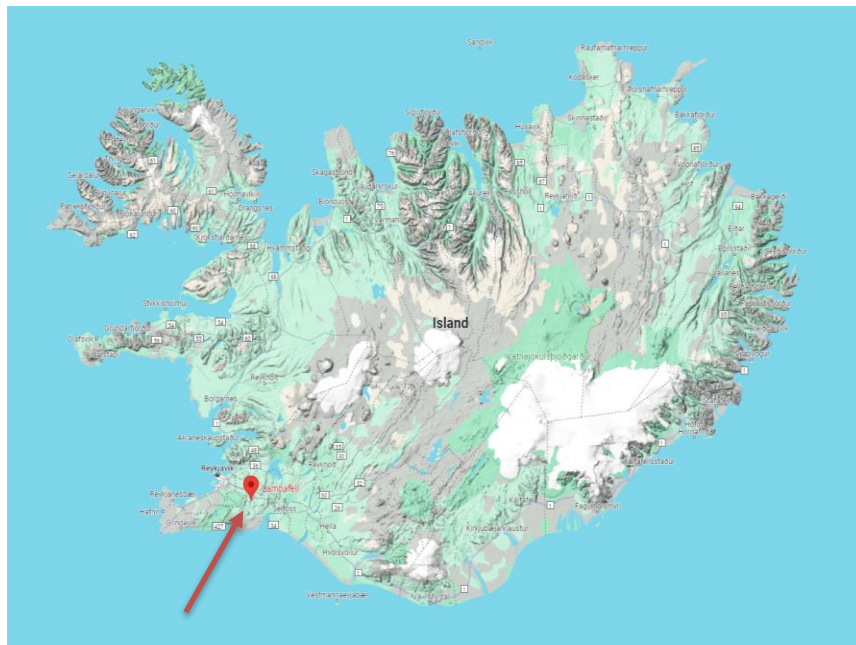


Figure 2: Lambafell Iceland (Norge, 2023)

The volcanic pozzolans found at Lambafell are known as hyaloclastites, which are typically associated with explosive eruptions. Hyaloclastites are created during volcanic eruptions that take place underwater, beneath ice, or when lava flows on land meet the sea or other bodies of water. The lava and rock fragments that are created due to the explosive eruption will mix with the water or ice, forming hyaloclastites through rapid cooling and solidification. (Norge, 2023)

These volcanic pozzolans have a lot of good properties to be considered as a supplement for cement. According to research done by “Heidelberg Sement Norge”, VPI is highly resistant to damaging alkali reactions, chloride intrusion, and carbonatation (Norge, 2023)

The chemical composition of VPI is given in Table 5. This chemical composition was achieved by an XRF analysis done by “Heidelberg Sement Norge”.

Table 5: Chemical composition of VPI

Full name	Chemical abbreviation	Percentage (%)
Silica Oxide	SiO ₂	47.42
Aluminum Oxide	Al ₂ O ₃	13.35
Ferric Oxide	Fe ₂ O ₃	12.32
Calcium Oxide	CaO	10.98
Potassium Oxide	K ₂ O	0.409
Sodium Oxide	Na ₂ O	1.883
Magnesium Oxide	MgO	11.29
Titanium Dioxide	TiO ₂	1.660
Phosphorous Pentoxide	P ₂ O ₅	0.193
Manganic oxide Chloride	Mn ₂ O ₃	0.210
	Cl	0.017
Sodium Oxide Equivalent	Na ₂ O Eq	2.15

As previously mentioned there are many different ways in which the pozzolanic reactivity can be assured. When using the chemical test stated in ASTM C618 ("ASTM C618," 2023) it is clear that VPI can be classified as a NP useable in concrete. VPI contains a high Silica, alumina, and Ferric content with a total of 74.09% as shown in 2.8, which meets the requirements given by the standard.

$$47.42 SiO_2 + 13.35 Al_2O_3 + 12.32 Fe_2O_3 = 74.09 \% \quad (2.8)$$

“Heidelberg sement Norge” also tested the pozzolanic activity using the TGA method and found that the material qualifies as a SCM according to this test. VPI has a specific weight of 2.98 g/cm³ and a specific surface area of 686 m²/kg. Since VPI is still a relatively unknown SCM, it is important to research more of its properties and durability.

2.3 What affects the durability of concrete?

The durability of concrete represents its ability to resist deterioration, thereby ensuring that it can reach its designed service life. It is important to design concrete structures in a way that includes the possible risks concrete structures can have for deteriorating. (Schutter, 2013)

For many years, the durability of concrete structures was often equated solely with their strength. However, with increased research focusing on concrete and its durability, it has become evident that numerous other factors play a significant role. A high compressive strength does not guarantee durable concrete, contrary to previous assumptions. Cracking in reinforced concrete is inevitable, as concrete and steel must collaborate. Therefore, when designing concrete structures, it's crucial to limit crack formation to a specific threshold to prevent structural damage. Nonetheless, even small cracks pose risks to the structure's integrity. These cracks can allow harmful chemicals to penetrate the concrete, potentially damaging both the reinforcement steel and the concrete itself, thus compromising durability. (Schutter, 2013)

As shown in Figure 3 3, damage to concrete structures can either be a result of the deterioration of the reinforcement steel or the concrete itself. However, 60 percent of deterioration cases are a result of the deterioration of reinforcement steel. (Schutter, 2013)

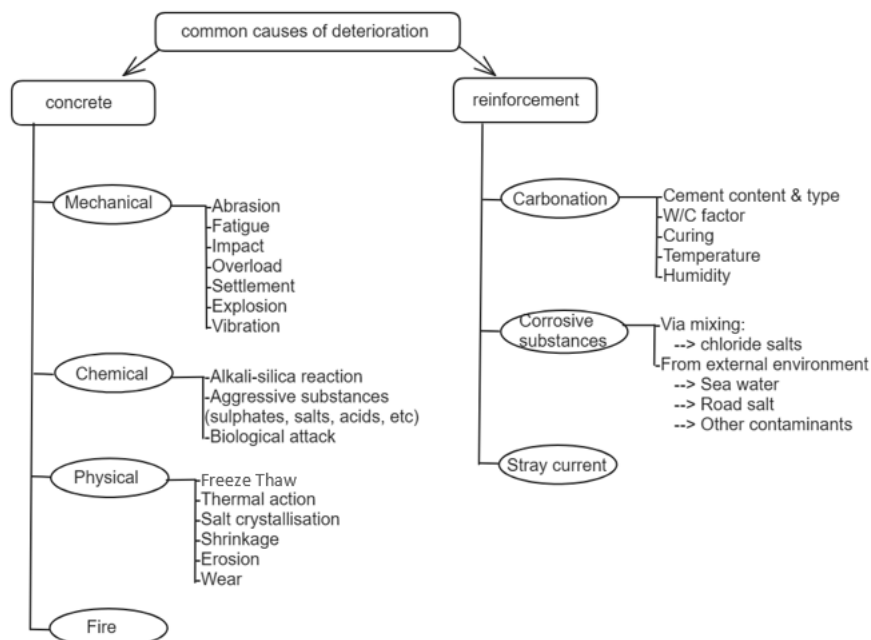


Figure 3: common causes of deterioration ("EN 1504-9," 2008)

The curing conditions are an important factor to consider when making concrete. Inadequate curing may diminish concrete quality by causing premature water loss, thus halting hydration prematurely. This can trigger early shrinkage cracks as water loss reduces volume, providing pathways for corrosive substances to infiltrate, potentially deteriorating reinforcement steel. A similar problem occurs with thermal cracking due to heat exposure. The binder that is used to make the concrete can also have a significant effect on the type of deterioration that occurs. (Schutter, 2013)

2.3.1 Compressive strength

Key factors contributing to the compressive strength of concrete are the binder and aggregates (S. Druart & L. Taerwe, 2018). The ratios of cement, aggregates, and water in the mix design are particularly significant. Additionally, the incorporation of additives like admixtures can exert considerable influence over concrete strength. (lynx, 2023) Although Portland cement remains the most widely used binder, ongoing research has broadened the scope to include SCMs. The utilization of SCMs in concrete can impact its compressive strength, often resulting in lower initial strength due to the delayed onset of the pozzolanic reaction. (S.Druart & L.Taerwe, 2018)

Another important contributing factor to the compressive strength of concrete is the curing conditions. By having proper curing conditions, it can be ensured that the concrete is subdued to adequate moisture and temperature levels. This is necessary to facilitate the hydration process in a proper manner to ensure that the concrete can gain strength efficiently. Concrete will continue to gain strength over time and concrete with OPC will typically achieve its maximum strength at 28 days. However, when SCMs are used in the concrete, it may need more time to reach its final strength.

The European standard EN 206-1 ("EN 206-1," 2001) categorizes the compressive strength of concrete mixes into strength classes. These classes are determined according to specifications outlined in Table 6, which are based on cylindrical specimens with a diameter of 150 mm and a height of 300 mm, or cubic specimens with dimensions of 150 mm.

Table 6: compressive strength classes according to EN 206-1

Compressive strength class	Minimal cylinder strength [N/mm ²]	Minimal cube strength [N/mm ²]
C8/10	8	10
C12/15	12	15
C16/20	16	20
C20/25	20	25
C25/30	25	30
C30/37	30	37
C35/45	35	45
C40/50	40	50
C45/55	45	55
C50/60	50	60
C55/67	55	67
C60/75	60	75
C70/85	70	85
C80/95	80	95
C90/105	90	105
C100/115	100	115

2.3.2 Freeze-thaw

One of the common physical causes of deterioration for concrete structures in colder climates is freeze-thaw (F-T). The concrete structures that reside in these climates will undergo various cycles of freezing and thawing. This can occur due to the different temperatures during winter and summer or sometimes even during day and night. (Nili et al., 2017) F-T can lead to the development of uneven cracks resulting in internal damage of the structure thereby shortening their structural life. (R. J. Wang et al., 2022)

2.3.2.1 Principle

Concrete is a porous material consisting of pores that are typically at least partially filled with water. This means that internal frost damage can occur when the water inside these pores starts to freeze. The damage that occurs is a result of the rising pressure within the concrete as the water inside starts to freeze and therefore undergoes a volume expansion. (Schutter, 2013) In the thawing phase, pressure is released, allowing for either a redistribution or absorption of moisture from the surroundings. This alternating cycle of freezing and thawing results in the development of microcracks and surface scaling. Over time, through repeated freeze-thaw cycles, these microcracks accumulate, ultimately causing the formation of macrocracks and

consequent structural deterioration.(Nili et al., 2017) Freeze-thaw cycles therefore pose a dual risk: not only do they threaten the concrete's integrity, but they also increase the likelihood of steel bar corrosion due to the formation of cracks (Guo et al., 2022).

Deterioration of concrete due to F-T consists of three main phases as shown in Figure 4. These phases are water absorption, water freezing, and structural failure. The concrete starts out in the initial phase, which includes two types of cracks: cracks from initial damage and cracks caused by air bubbles in the concrete. The initial damage cracks allow external water to penetrate and fill the internal pores. The next phase is triggered by a temperature drop, causing the water inside the concrete to freeze and expand. This can happen naturally when concrete is exposed to the environment or be simulated using F-T chambers for testing. As the water freezes, it expands by approximately 9%, creating pressure within the concrete and leading to the final stage of the deterioration process. (R. J. Wang et al., 2022)



Figure 4: phases of F-T mechanism (R. J. Wang et al., 2022)

Many different theories exist, explaining what happens during the final phase of the F-T mechanism. The most used theories to explain the deterioration process of concrete as a result of freeze-thaw cycles are the hydraulic pressure theory, the crystallization pressure theory, and the osmotic pressure theory. (Schutter, 2013)

The hydraulic pressure theory explains internal frost damage based on the mechanism that occurs as shown in Figure 5. The water in parts of the capillary pores will start to freeze which leads to an expansion in volume. Because of this there will not be enough room for the non-frozen water to stay inside the pores. Therefore the non-frozen water is pushed away into the air voids. If there are enough air voids present within a short distance, then the hydraulic pressure can be released and the concrete will not be damaged. When this is not the case the hydraulic pressure will lead to crack formation within the concrete. Because of this theory, it was assumed that making the spaces between air voids smaller would help the water escape more easily and therefore reduce the formation of cracks. However, this also caused the concrete to shrink more when it got cold. When the concrete warms up again the pressure inside the concrete doesn't decrease as was assumed with this theory. To conclude, this theory does not suffice as an explanation for freeze-thaw deterioration anymore. (Schutter, 2013)

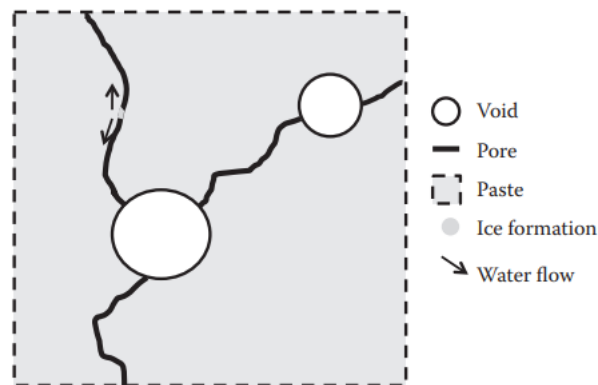


Figure 5: hydraulic pressure theory (Schutter, 2013)

Another theory to explain this concept is the crystallization theory as shown in Figure 6. Depending on the size of the pores, the freezing point of water in concrete changes. Tiny ice crystals have more surface area compared to their volume, which means the water in the smaller pores will take longer to freeze because the freezing point is lower. The bigger pores will freeze first and after that the smaller pores will freeze. When there is no more room for the ice, the

pressure will build up leading to cracks in the concrete. This theory is based on the fact that ice grows and causes pressure which is different to the idea that the pressure builds up like water in a pipe does, as stated in the hydraulic pressure theory. The water in the smaller pores stays liquid and therefore a thermodynamical equilibrium arises, which works as the driving force to move the water in the smaller pores to the bigger pores. The crystallization theory is assumed to be the best explanation for the mechanism that occurs in concrete under the influence of freeze-thaw cycles. (Schutter, 2013)

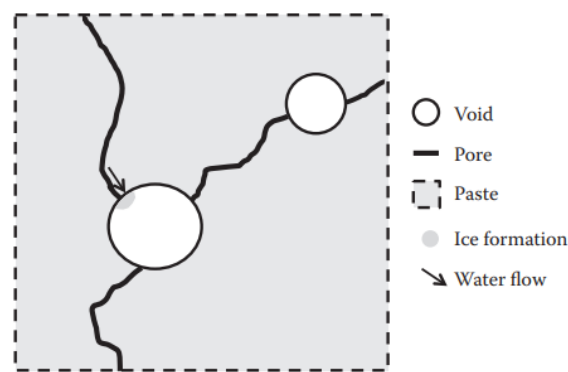


Figure 6: crystallization theory (Schutter, 2013)

The last theory that provides an explanation for the freeze-thaw mechanism is the osmotic pressure theory. This theory says that ice will first form in the larger pores, as was also stated in the crystallization theory. However, this theory adds that the alkalinity of the remaining non-frozen water within the larger pores will increase. Since a thermodynamic equilibrium has to occur, the pore water with a lower alkalinity will move from the smaller pores to the larger pores. This in itself results in further formation of ice in the larger pores due to an alkalinity drop of the fluid around the already existing ice. Another effect that occurs is osmotic pressure. This is the pressure difference between the areas with a higher alkalinity and a lower alkalinity. After further research it was concluded that the osmotic pressure itself does not contribute to concrete damage but can be viewed as an additionally occurring phenomenon. (Schutter, 2013)

2.3.2.2 Influencing factors

There are different factors that influence the behavior of concrete when it undergoes freeze-thaw cycles. Those factors can be split into two main categories, being the environmental and the material characteristics. Environmental characteristics include the cooling rate, minimum freezing temperature and water saturation. The material characteristics encompass W/B ratio, aggregates used, the air void system and mineral additives. (R. J. Wang et al., 2022)

The most obvious influence factor is the saturation degree that is shown in formula 2.9

$$sat\ degree = \frac{\text{amount of free water in pores}}{\text{max amount of water if all pores are filled}} \quad (2.9)$$

When concrete contains no water inside the pores and therefore has a saturation degree of zero then there will be no damage as a result of freeze-thaw. When the concrete has partially filled pores, there will be some room for the ice to expand resulting in a relief of pressure. Since there is a 9% volume increase during ice formation, a saturation degree below 90% will not result in damage to the concrete. When the saturation degree is below a certain percentage of around 85 or 90% there will be no significant damage to the concrete. This value is called the critical saturation value. (Schutter, 2013)

The cooling rate can also influence the freeze-thaw deterioration. A slow cooling rate will be more destructive than a fast cooling rate. The minimum temperature is also an important environmental factor since it affects the phase transformation and the migration of pore water in the concrete. Many simulation tests for freeze-thaw will have a minimum temperature of -20°C. However, the areas in which these concrete structures reside will very rarely reach this temperature. (R. J. Wang et al., 2022)

Another important factor is the air void system. As previously said there is less chance of damage when the ice has room to expand. However, it is also important that the available expansion volume is easily accessible for pressurized water or expanding ice. (Schutter, 2013) An air entrainer can be used to create air bubbles in the concrete. This provides room for the water to expand when freezing leading to a reduction of internal pressure. When there is not enough air present inside the concrete this will lead to an uneven distribution and a large spacing between the pores. The freeze-thaw durability of concrete is considered bad when the pore spacing factor exceeds 300 µm. To withstand internal cracking in rapid freezing and thawing it is necessary to have an air void spacing factor of approximately 0.20 mm or less and an air

content within the range of 3-6%. The smaller air spacing factor results in less distance for the water to enter an air void during freezing which can reduce the internal pressure. (R. J. Wang et al., 2022) Pore size distribution is also a crucial factor in F-T resistance (Taylor et al., 2021). It refers to the distribution of different pores within the concrete, which include capillary pores, gel pores, and air voids shown in figure 7. (Honorio et al., 2018) Another important factor is the specific surface which refers to the total surface area of air voids per unit volume of concrete, indicating the fineness or coarseness of the air-void system. A specific surface value greater than 25 mm^{-1} is considered beneficial for freeze-thaw performance, as it suggests a well-distributed air-void system that can effectively resist damage caused by freeze-thaw cycles. ("ASTM C457/457M-16," 2024)

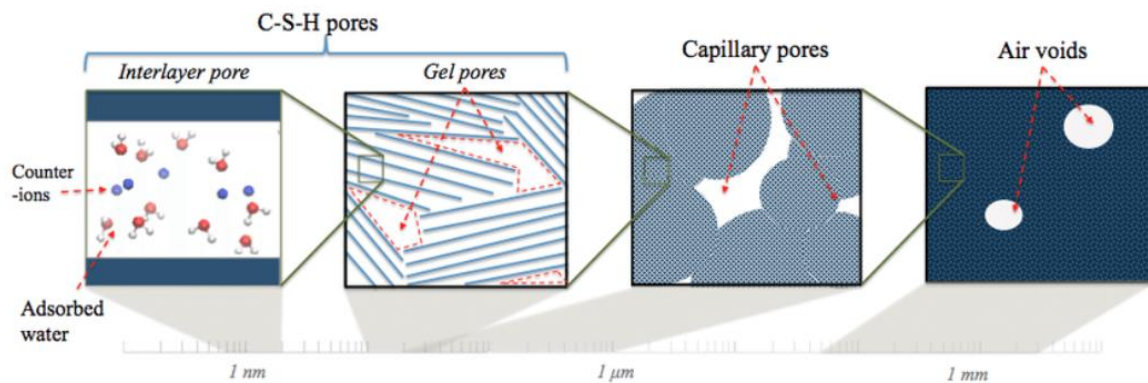


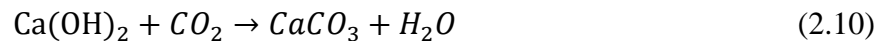
Figure 7: different types of pores (Honorio et al., 2018)

Air voids, created by using an air-entraining agent, improve F-T resistance by providing space for water to expand upon freezing. Gel pores are tiny pores located within the structure of the hydrated cement gel. In contrast, capillary pores are larger pores formed from the spaces between hydrated cement particles. These larger pores facilitate the transport of water and other liquids through the concrete, which can negatively impact F-T resistance if too abundant. More water can enter through these pores, leading to worse F-T performance. An overview of the different pores and their effects on F-T are shown in table 7. (Taylor et al., 2021)

Table 7: different pore types and their effect on F-T (Taylor et al., 2021)

Pore Type	Diameter	Location	Effects on F-T
Gel pores	Intra-gel < 0.6 mm	Inside C-S-H	Water in gel pores may travel into capillary pores to reduce solution concentration due to osmotic pressure
	Inter-hydrate 0.1nm-100nm	Space between C-S-H and CH	
Capillary pores	Small 2nm-50nm	Between cement grains and products of hydration	Ice crystals form in capillary pores (>50 nm) and may generate stresses that damage the paste
	Large 1 μ m- 10 μ m		
Air voids	Entrained 10 μ m- 1000 μ m	Between cement grains and products of hydration	Provide boundaries for water to be forced out in capillary pores due to ice formation: limit hydraulic pressure
	Entrapped 1 mm		No effect

Reducing the size and connectivity of the capillary pores enhances F-T durability, which can be achieved through CO₂-curing. This method involves exposing the test pieces to CO₂ which results in the formation of calcium carbonate (CaCO₃) as shown in reaction 2.10. If the CaCO₃ fills up the capillary pores, less water will be able to enter the concrete leading to improved F-T resistance.



However, not only the capillary pores can be filled. If smaller pores are filled while capillary pores remain open, it can adversely affect the F-T performance of the sample. (Taylor et al., 2021) Therefore, CO₂- curing can have either a positive or negative impact on the freeze-thaw resistance of concrete samples depending on the type of pores that are filled.

The W/B ratio can also influence the damage mechanism of freeze-thaw. When the this ratio is low the concrete has a reduced permeability resulting in a higher resistance to freeze-thaw. Because of the lower permeability, the critical value of saturation will almost never be reached. Other than that, the pore volume will also be smaller which means there will be less water inside the pores that can be frozen. (Schutter, 2013) Conversely, if the W/B ratio is high then more capillary pores will be present in the concrete which leads to more water absorption and a bigger risk for F-T damage. (Taylor et al., 2021) A high W/B ratio also results in reduced density and therefore a larger vulnerability to damage from freeze-thaw cycles (R. J. Wang et al., 2022).

The type of binder that is used also plays a significant role in freeze-thaw damage. The binder influences the microstructure development and thus the pore system. (Schutter, 2013) As previously mentioned in section 2.2.1 the use of FA and SF can improve F-T resistance with the ideal substitution range being 5-20%. A substitution percentage of FA higher than 50% will however reduce F-T resistance. Therefore it is important to experiment with the mix design for different SCMs to see which substitution percentages are optimal.

2.3.2.3 Freeze-thaw with deicing salts

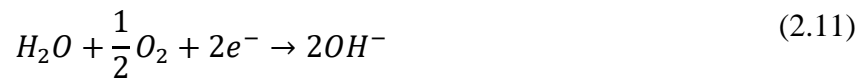
Often chemicals, like salts, are used for deicing especially on roads or bridges to make it safer for traffic to drive on. Additionally, chloride ions and sulfates can be present in groundwater or soil. These salts can increase the likelihood of freeze-thaw damage by promoting the penetration of water into the concrete. When concrete structures suffer from the combination of freeze-thaw and salt erosion, it can lead to structural failure far before its designed lifetime is achieved. Ice crystals will be formed when water that contains salt freezes. When this water resides inside the concrete, the ice crystals that are formed will expand and put pressure on the concrete. This will cause the concrete surface to break, flake or peel, in turn exposing the aggregates. This is called scaling and will weaken the concrete structure, making it more susceptible to additional damage such as the corrosion of reinforcement steel. Scaling may occur even without the presence of salts. Many factors such as deficient mix design or insufficient curing can lead to scaling. However, it will occur more frequently in the presence of salts. (Li et al., 2021)

2.3.3 Chloride induced corrosion

Rebar corrosion is responsible for approximately 60 percent of damage to concrete structures. Therefore it is important to find ways to reduce this type of damage. The process of creating reinforcement steel involves heating iron ore (Fe_2O_3) in a blast furnace, transforming it into steel (Fe) with the infusion of a considerable amount of energy. It is crucial to recognize that materials inherently strive to revert to their lowest energy state, which is why the corrosion reaction happens. (Belleghem, 2023)

There are two main reactions involved in the corrosion process, the first being the anodic reaction (2.10) and the second being the cathodic reaction (2.11).





The anodic reaction results in iron giving off free electrons. When the steel comes in contact with water and oxygen these free electrons will react, resulting in hydroxide-ions. As shown in reaction (2.13) the iron ions produced at the anode will react with the hydroxide ions that were formed at the cathode. This reaction results in the formation of rust ($Fe(OH)_2$). The rust will settle on the rebar as shown in Figure 8. This is known as the corrosion process and leads to rebar deteriorations which ultimately results in a loss of reinforcement strength. The rust that settles on the concrete has a bigger volume than the original rebars resulting in a volume expansion within the concrete. This creates a tension that will ultimately lead to cracks when it exceeds the tensile strength of the concrete.

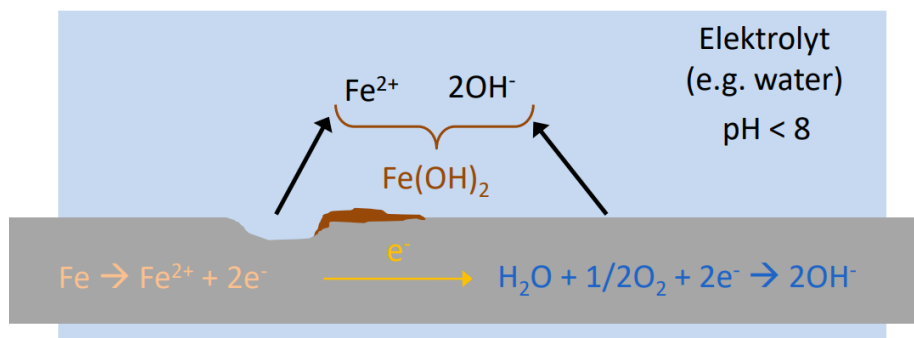


Figure 8: chloride induced corrosion (Bellegheem, 2023)

However, when rebar steel is imbedded in concrete, a protective passivation layer forms around the steel. This layer consists of oxides that form on the surface of the steel preventing the corrosion reaction to continue. Nevertheless, this does not mean that the steel is not viable for corrosion anymore. The passivation layer can be compromised under the influence of either carbon dioxide or the infiltration of chlorides, initiating a renewed corrosion process. If depassivation occurs due to carbon dioxide, it is termed carbonation, a topic beyond the scope of this thesis and therefore not delved into further. Nevertheless, it's essential to highlight that depassivation can also transpire as a consequence of chlorides infiltrating the concrete, marking a noteworthy consideration in this thesis. (Bellegheem, 2023)

Chlorides can enter concrete either through its mixing process or infiltration from external sources. For instance, chlorides may naturally exist in raw materials like sand or water utilized in concrete production. In the years between 1960 and 1980, calcium chloride served as a frequently used concrete accelerator. However, it has since been recognized that the use of these chlorides can lead to corrosion, prompting the end of their widespread application in concrete production practices. Additionally, chlorides from external sources, such as marine environments, de-icing salts, or industrial process wastewater can enter the concrete. (Bellegheem, 2023)

Regardless of the source of the chlorides, their effect on concrete remains the same. Chlorides will migrate through the concrete until they reach the steel rebar as shown in Figure 9. The iron ions will then react with water and the chlorides, resulting in the reaction products that are shown in reaction 2.14. (Bellegheem, 2023)

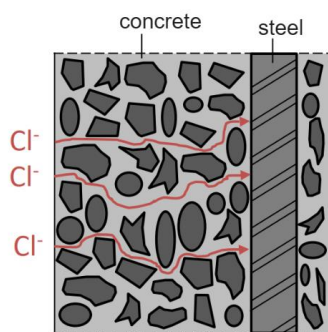
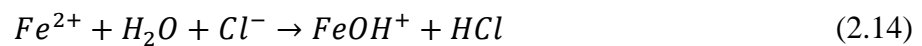


Figure 9: chloride intrusion
(Bellegheem, 2023)

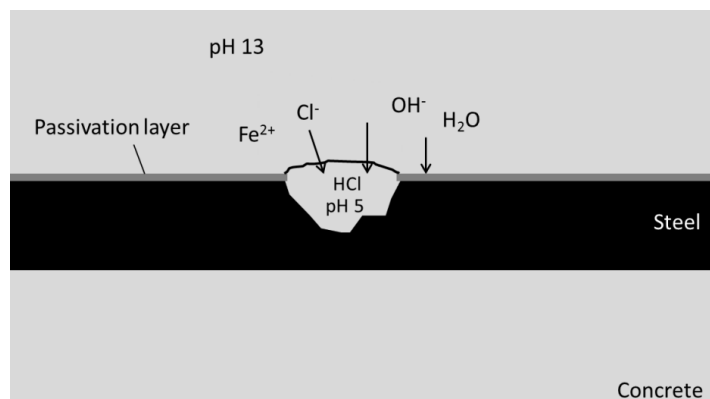


Figure 10: PH reduction due to chloride migration
(Bellegheem, 2023)

As shown in Figure 10 this will result in a locally low PH value because of the HCl that forms. The corrosion process will start when the chloride degree surpasses a critical value. The critical value is usually estimated to be between 0,2-2 m%. Chloride induced corrosion is often called macrocel corrosion since it leads to the formation of a macroscopical anode resulting in pitting corrosion. Chloride induced corrosion is usually very local. It is important to get a general

picture of chloride migration within concrete in order to protect concrete structures from this phenomenon. (Schutter, 2013)

The porosity of concrete greatly influences transport properties within the concrete, thus influencing its permeability. The migration of chlorides is therefore highly dependent on the pore structure and consequently the permeability of the concrete. (Szweda, 2019) When concrete is made with SCMs it often reduces the permeability due to the filling effect and the pozzolanic activity. This leads to an improved durability performance such as a high resistance to chloride migration. (Borosnyói, 2016). A study done by Kubissa (2016) similarly concludes that the use of SCMs in concrete can lower the intrusion of chloride ions into the concrete.

2.4 Durability improvement

When working with concrete containing SCMs it is important to conduct research on its durability. As outlined in section 2.2, various factors influence concrete durability. By adjusting these factors it is possible to improve durability.

First and foremost it is generally known that concrete made with OPC will have generated most of its strength ability after a curing period of 28 days. However, when concrete is made with SCMs, there may be a need for a longer curing period. It is therefore important to consider prolonged curing before submitting the test pieces to harsh tests such as freeze-thaw.

When concrete is submitted to freeze-thaw cycles, the water in the pores will expand, as previously established in section 2.2.2. Since many of the influencing factors for freeze-thaw encompass material characteristics it can be beneficial to test different mix designs to see which ones are more resistant to the freeze-thaw damage. (Li et al., 2021) The same is true for chloride migration testing.

Part II
Research

3

Test procedures

This chapter will provide a short explanation of the tests that were performed during the research proportion of this thesis. Additionally, the necessary equations for the calculations are given and explained.

3.1 Fresh concrete tests

The hardened concrete tests that have been explained in earlier subchapters were necessary to research the durability of the concrete. However, it was also important to conduct some tests on the freshly made concrete to ensure that it had the desired properties.

First, a slump test was conducted according to NS-EN 12350-2 ("NS-EN 12350-2," 2019). This is a test that determines the workability of concrete by filling up a standard cone-shaped mold with fresh concrete and then lifting it vertically. The slump is then defined as the distance between the top of the cone and the top point of the concrete that has settled. The slump can be classified in different slump classes. For this thesis it was important that the slump class of all the concrete mixes was S4. This is a slump of approximately 200-220 mm. However, when measuring a slump it is only valid when a true slump occurs. This means that the concrete slumps evenly and maintains a symmetrical, uniform shape after the cone mold is removed.

Secondly, an air percentage test was performed according to NS-EN 12350-7 ("NS-EN 12350-7," 2019). A container as shown in Figure 11 is filled with concrete and then the main air valve is closed. Valve A and B are opened and water is injected through these valves. The air bleeder valve is then closed and subsequently air is pumped into the chamber. Valves A and B are then closed and the main air valve is opened, the pressure gauge will then show a value indicating the air percentage that is present in the concrete. The desired air percentage of the concrete was 4-6% for this thesis.

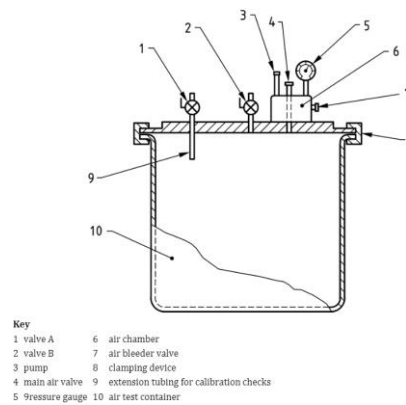


Figure 11: air pressure gauge ("NS-EN 12350-7," 2019)

3.2 Compressive Strength

The compressive strength tests were conducted according to EN 12390-3 ("EN 12390-3," 2019). Each mix was tested at 2 days, 28 days and 56 days. For each age, three cubes were tested per mix. The average of the test results from these three cubes was then utilized.

The determination of compressive strength involves placing the cube specimen in the machine depicted in Figure 12 and applying a force to it. It is assumed that the load is uniformly distributed over the cube. This force is steadily increased until the cube fractures, at which point the cracks are examined to assess the acceptability of the breaking pattern.



Figure 12: compressive strength machine

The compressive strength is then determined by using equation 6.1.

$$f_c = \frac{F}{A_c} \quad (6.1)$$

With:

f_c	Compressive strength [MPa]
F	Maximum load at failure [N]
A_c	Cross-sectional area of the specimen on which the compressive force acts

3.3 Chloride Migration

The chloride migration test was conducted according to NT-build-492 ("NT-build-492," 2018). Each mix underwent testing at both 28 and 56 days. To perform this test, cylinders were initially created with a radius of 50 mm and a height of 200 mm. Subsequently, each cylinder was segmented into three pieces, each approximately 50 mm in height by using a diamond saw. Henceforth, these segmented portions will be referred to as the test pieces. The test pieces were always cut one day before the testing day.

After the cutting process, the test pieces were placed inside a vacuum pump for three hours. Following this, the pump was filled with water and operated for an additional hour. Upon completion of the four-hour treatment, the pump was deactivated, and the test pieces remained inside for approximately 18 additional hours before testing commenced. The vacuum pump apparatus is shown in Figure 13.



Figure 13: vacuum pump

The testing procedure involves placing the test pieces between a chloride-free and a chloride-containing alkaline solution. Subsequently, an electric voltage is applied between two external electrodes to facilitate the migration of chloride ions into the concrete specimen. The experimental setup is illustrated in Figure 14.

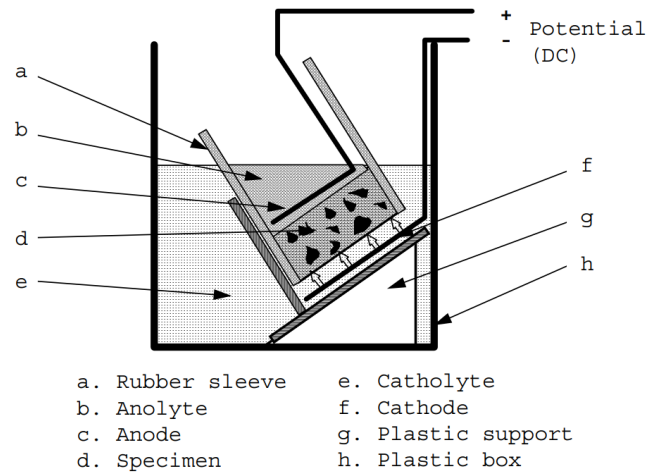


Figure 14: chloride migration test set-up

After a specified test duration, the samples are broken in half as depicted in Figure 15 and 16, and a silver nitrate solution is sprayed onto them. This process allows the visualization and subsequent measurement of the chloride penetration depth.



Figure 15: test piece split in half



Figure 16: test piece side profile

The chloride migration coefficient can be determined using Equation 6.2. This offers a broad indication of the concrete's resistance to chloride penetration and, consequently, its

susceptibility to chloride-induced corrosion when employed alongside steel in construction projects.

$$D_{\text{nssm}} = \frac{0,0239(273 + T)L}{(U - 2)t} \left(x_d - 0,0238 \sqrt{\frac{(273 + T)Lx_d}{U - 2}} \right) \quad (6.2)$$

With:

D_{nssm}	Non-steady state migration coefficient [m ² /s]
U	Absolute value of the applied voltage [V]
T	Average value of initial and final temperatures in the anolyte solution [°C]
L	Thickness of the specimen [mm]
x_d	Average value of the penetration depths [mm]
t	Test duration [h]

3.4 Freeze-thaw testing

Freeze-thaw testing was conducted according to SN-EN12390-9 ("SN-EN 12390-9," 2016). During this test, the samples are placed in a F-T chamber where temperature fluctuations induce both freezing and thawing. Each day in the chamber equals one complete cycle of freezing and thawing. As a result, this chamber accelerates the effects of F-T cycles on concrete.

The freeze-thaw tests were conducted with the use de-icing salts. For this test, cubes of 150 mm were made and eventually samples with a thickness of 50 ± 2 mm were cut. Subsequently, the samples underwent curing using three distinct methods, as detailed in section 4.3. To waterproof the samples, they were affixed to a plastic box. They were then insulated by positioning them within Styrofoam boxes, as depicted in Figure 17, thereby exposing only the top surface to the freeze-thaw chamber conditions. On top of the samples a layer of water with de-icing salts is placed. Prior to placement in the F-T chamber shown in Figure 18, the samples were then covered with a plastic sheet. The samples were marked in two different spots so they could not be mistaken for one another.

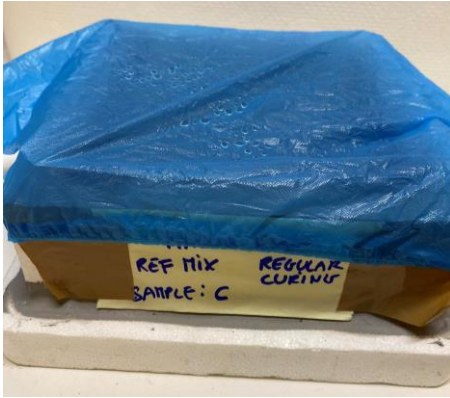


Figure 17: F-T test piece



Figure 18: samples in F-T chamber

The temperature of the freeze-thaw chamber was closely monitored and the chamber was always filled to its full capacity. Given that not all samples were introduced into the F-T chamber simultaneously due to varying mixing dates and curing conditions, old samples were utilized to occupy vacant slots. This guaranteed the maintenance of constant conditions within the chamber.

The scaled material is cumulatively added together after each cycle according to formula 6.3.

$$m_{s,n} = m_{s,before} + (m_{v+s(+f)} - m_{v(+f)}) \quad (6.3)$$

With:

$m_{s,n}$	Cumulative mass of dried scaled material after n F-T cycles rounded to the nearest 0,1g [g]
$m_{s,before}$	Cumulative mass of dried scaled material calculated at previous measuring occasion [g]
$m_{v+s(+f)}$	Mass of the vessel containing the dried scaled material rounded to the nearest 0,1g [g]
$m_{v(+f)}$	Mass of the empty vessel rounded to the nearest 0,1g [g]

The cumulative amount of scaled material per unit area after n cycles can then be calculated using formula 6.4 for each measurement and each specimen.

$$S_n = \frac{m_{s,n}}{A} * 10^3 \quad (6.4)$$

With:

S_n	Mass of scaled material related to the test surface after the n-th cycle [kg/m ²]
$m_{s,n}$	Cumulative mass of dried scaled material after n F-T cycles[g]
A	Effective area of the testing surface, calculated from the length measurements after the glue string is applied and rounded to the nearest 100 mm ² [mm ²]

4

Research Characteristics

This section provides more information about the specifics of the test samples, mix design and curing methods. Characteristics such as their chemical properties can have a huge impact on test results.

4.1 Terminology for the mixes

Four concrete mixes were formulated following the mix design provided by Iveta Nováková, researcher at UiT. Table 8 lists the official names assigned to these blends, along with their corresponding code names, for easier reference during result analysis. The mixes with VPI get the code names M 18/6-360, M 18/6-300 and M 25/10-360 where the M stands for mix and the number correspond to the percentages of VPI and LP that is used in each mix. The top mix gets the code name REF as it is the reference mix. The full mix design and further details about the mixes is shown in section 4.2.

Table 8: code names given to the concrete mixes

Official name mix	Code name
C25XF1 w/c<0.55	REF-360
VPI+LP 18+6(tot360)	M 18/6-360
VPI+LP 18+6(tot300)	M 18/6-300
VPI+LP 25+10(tot360)	M 25/10-360

In Table 9 the codes are given for the different curing methods for the freeze-thaw tests. The details of these curing methods are further specified in section 4.3.

Table 9: code names given to the curing conditions

Curing condition F-T test	Code name
Normal curing	N
CO ₂ curing	CO2
Prolonged CO ₂ curing	CO2P

4.2 Mix design and details about the used materials

The objective of this thesis was to assess the durability of these varied concrete compositions with VPI. Among these mixes, three incorporate VPI, while the fourth serves as a reference mix, made with FA-cement. FA-cement was chosen as FA is a well-established Supplementary Cementitious Material (SCM) with numerous test results from various researchers. Additionally, all mixes incorporate limestone powder as a constituent. Table 10 shows the mix design for 1 m³ of binder for all the mixes. The full mix design including the aggregates, admixtures and free water can be found in appendix C.

Table 10: mix design of binder for 1 m³ of concrete

	REF-360		M18/6-360		M18/6-300		M25/10-360	
W/B ratio	0.40		0.40		0.47		0.42	
W/C ratio	0.48		0.47		0.55		0.54	
	[kg/m ³]	[w%]	[kg/m ³]	[w%]	[kg/m ³]	[w%]	[kg/m ³]	[w%]
CEM II***	360	100	0	0	0	0	0	0
C+G*	273.6	76	0	0	0	0	0	0
LP	21.6	6	0	0	0	0	0	0
FA	64.8	18	0	0	0	0	0	0
CEM I**	0	0	287	79.8	239	79.8	246	68.2
C+G*	0	0	273.5	76	227.8	76	234.4	65
LP	0	0	13.5	3.8	11.2	3.8	11.6	3.2
LP	0	0	8	2.2	7	2.2	24	6.8
Sum of LP	21.6	6	21.5	6	18.2	6	35.6	10
VPI	0	0	65	18	54	18	90	25
	[kg/m ³]	[w%]	[kg/m ³]	[w%]	[kg/m ³]	[w%]	[kg/m ³]	[w%]
Total SCM content	86.4	24	86.5	24	72.2	24	125.6	35
Total binder materials	360	100	360	100	300	100	360	100

*C+G= Clinker + gypsum

**contains 4.7% LP

***contains 18% FA and 6% LP

When concrete is made using supplementary materials alongside cement it is important to determine both the water/binder (W/B ratio) and the water/cement (W/C ratio). The W/B ratio allows the additional binder to be incorporated into the ratio. This is done by using the principle of k-values. The k-values for every type of additional binder are specified in EN-206 ("NS-EN 206," 2022) and are shown in Table 11.

Table 11: k-values of binders

Name of binder	k-value
Norcem CEM I	1.0
Norcem CEM II	1.0
LP	0.3
VPI	0.7

The formula to determine the W/B ratio is given in 7.1. The calculations of the W/C ratio and W/B ratio are shown in appendix D for all the mixes.

$$wbr = \frac{W}{(C + k * A)} \tag{7.1}$$

With:

wbr	Water/binder ratio
W	Free water [kg/m ³]
C	Cement [kg/m ³]
k	k-value
A	Additional binder [kg/m ³]

To make the concrete mixes two types of cement were available: CEM I and CEM II. Both were produced by “Heidelberg Sement Norge” and their specifications are respectively shown in Figure 19 19 and Figure 20. To get the desired ratios as shown in Table 10, it was important to see how much limestone powder was already present in the two cement types. Based on this, additional LP could be added to get to desired amount for each mix. For three of the mixes VPI was also added. The full technical information sheets of the binders can be found in appendix B.

Product specification

Portland cement

Materials	Value	Unit
Klinker	88,4	%
Gips	6,9	%
Kalksteinsfiller	4,7	%

Technical data:

CEM I 52,5 R Further information is available at www.norcem.no

Product specification

Portland-composite cement.

Materials	Value	Unit
Klinker	70,1	%
Gips	5,9	%
Flygeaske	18	%
Kalksteinsfiller	6	%

Technical data:

CEM II/B-M (V-L) 42,5 R Further information is available at www.norcem.no

Figure 19: CEM I product specification

Figure 20: CEM II product specification

The aggregates that were used were the same for all the mixes and originated from northern parts of Norway. The used aggregates and some specifications about them are shown in Table 12.

Table 12: aggregates

Material	Density [kg/m ³]	Water absorption [%]	Aggregate percentage used per mix [%]
Sand 0-8mm	2580	0.8	49
Coarse 8-22mm	2770	0.5	43
Crushed 4-8 mm	2700	0.5	8

Additionally, two types of admixtures were used in all the concrete mixes. The superplasticizer (SP) that was used came from Mapei and is called DYNOMON SX-23. The air entrainer that was used, came from the same company and was named MAPEAIR 25. The technical information sheets for these admixtures can be found in appendix B.4 and B.5. Lastly, the water that was used in the concrete was normal tap water at room temperature, derived from “NarvikVann” water company.

4.3 Curing conditions

The curing conditions that were implemented are shown in Table 13. For freeze-thaw, the samples were divided into three groups based on their curing conditions. The normal curing conditions are based on the reference method according to the standard SN-EN12390-9 ("SN-EN 12390-9," 2016). For the CO₂ curing with a CO₂ percentage of 1% the Swedish standard SS137003 ("SS137003," 2004) was used. Additionally, prolonged curing with a CO₂ percentage of 1% was also conducted. For this last curing method, the samples were placed in

the CO₂ chamber for an additional period of 1 week. These curing methods were discussed and agreed upon with Magdalena Rajczakowska (PhD) from Sweden who is also a part of the Ar2CorD project. Magdalena enforced similar curing methods so results can be compared in the Ar2CorD project. Introducing CO₂ during the curing phase can enhance the precision of testing procedures. As concrete exposed to the environment naturally faces CO₂ infiltration, samples subjected to freeze-thaw testing with CO₂ exposure yield results more closely aligned with real-world conditions compared to those without CO₂ exposure.

Table 13: curing conditions per test

Test	Curing conditions		
Chloride migration	Placed in 100% RH (water bath, 20°C) up until testing		
Compressive Strength	Placed in 100% RH (water bath, 20°C) up until testing		
Freeze-thaw	Normal	1 day	Place in 100% RH (water bath, 20°C)
		7 days	Place in 65% RH (20°C)
		21 days	Specimens are sawn and returned to 65% RH
		25 days	Specimens are insulated and placed in forms + 65% RH
		28 days	Water saturation (de-ionizing water)
		31 days	Move to freeze-thaw chamber= start F-T cycles
	CO ₂ (1%)	1 day	Place in 100% RH (water bath 20°C)
		7 days	Place in 65% RH (20°C)
		21 days	Specimens are sawn and returned to 65% RH
		25 days	Specimens are insulated and placed in forms + 65% RH
		28 days	Place in 1% CO ₂ for 7 days
		35 days	Water saturation (de-ionizing water)
	Prolonged + CO ₂ (1%)	38 days	Move to freeze-thaw chamber = start F-T cycles
		1 day	Place in 100% RH (water bath 20°C)
		7 days	Place in 65% RH (20°C)
		21 days	Specimens are sawn and returned to 65% RH
		25 days	Specimens are insulated and placed in forms + 65% RH
		28 days	Place in 1% CO ₂ for 14 days
	42 days	Water saturation (de-ionizing water)	
	45 days	Move to freeze-thaw chamber = start F-T cycles	

4.4 Test pieces

As previously stated, various tests were conducted on the hardened concrete samples, utilizing three types of test specimens. Detailed specifications for these test pieces are shown in Table 14.

According to the standards that were mentioned in section 3.2, four cubes per curing method and per mix should be tested for freeze-thaw. However, due to the limited capacity of the laboratory and its freeze-thaw chambers, the choice was made to have three samples per curing method for every mix instead.

Table 14: test pieces

Name test piece	Used for	Dimensions (mm)	V (l)	Total pieces per mix
small cylinder	Chloride migration testing	200*50	1,6	6
Small cube	Compressive strength testing	100*100*100	1,0	9
Big cube	Freeze-thaw testing	150*150*150	3,4	9

An overview of the distribution of the test pieces per test is given in Table 15. For the F-T test the test pieces were divided over the three different curing conditions. Per mix and per curing condition a total of three test pieces were tested. For the CS test the test pieces were divided into three groups based on the testing ages. Per testing age and mix a total of three test pieces were tested. For the CM testing only one test piece was necessary per mix and testing age. This is because the test piece was cut into three even pieces with a height of approximately 50 mm to be tested. Hence, the test results per mix and testing age were derived from three concrete pieces subjected to the chloride migration test, all originating from the same cylinder.

Table 15: overview number of test pieces per test

Mix name	F-T test (150x150x150mm)			CS test (100x100x100 mm)			CM test (φ50 X 200 mm)	
	N	CO2	CO2P	2d	28d	56d	28 d	56 d
REF MIX	3	3	3	3	3	3	1	1
MIX 1	3	3	3	3	3	3	1	1
MIX 2	3	3	3	3	3	3	1	1
MIX 3	3	3	3	3	3	3	1	1

Part III

Results and Discussion

5

Results

In this section the results are presented and compared to each other. It's important to compare the different mixes with each other and with the reference mix. The test results of different tests can also be linked to each other. This section thoroughly researches the results found in this thesis of both fresh and hardened concrete and explains them through knowledge collected in the literature study.

5.1 Fresh concrete properties

The mixes required a slump ranging from approximately 200 to 220 mm, categorizing them under slump class S4. The targeted air content fell within the range of 4-6%. Slump (NS-EN 12350-2) and air content (NS-EN 12350-7) were determined using the methods outlined in section 4.3. The results of these tests are presented in Table 16. Additionally, it was essential to record the quantities of air entrainer (Mapair) and superplasticizer (SP) added to the mix to attain the desired fresh concrete characteristics. The slump results were rounded to increments of 5 mm.

Table 16: fresh concrete properties

Mix name	Slump [mm]	Air* [%]	Mapair [kg/m ³]	SP [kg/m ³]
REF-360	220	4.5	0.14	4.32
M 18/6-360	220	4.8	0.14	4.80
M 18/6-300	220	5.4	0.16	3.60
M 25/10-360	220	6.0	0.14	4.32

*not the actual air content, reason explained in text

Due to a malfunction of the standardized air pressure gauge typically used to measure the air content in concrete, a smaller, less precise version was utilized. This led to concerns about the accuracy of the air content measurements. Upon reviewing some of the test results achieved in this thesis, it became evident that the measured air contents were likely inaccurate. After

visually inspecting samples and consulting with Iveta Nováková, a researcher at UiT, it was concluded that the actual air content in REF-360, for example, was likely higher than reported. This conclusion was based on visual comparisons between samples M25/10-360, which had a recorded air content of 6%, and REF-360. Preliminary visual examination revealed similar quantities of air bubbles in both sets of samples (see Figures 21 and 22).



Figure 21: surface of REF-360

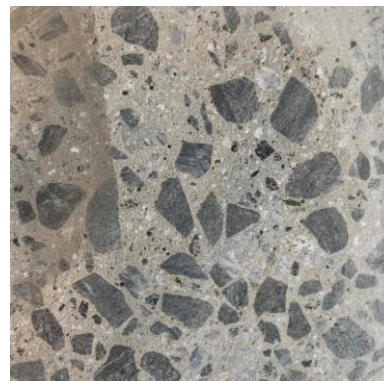


Figure 22: surface of M 25/10-360

Consequently, it was decided to send four samples, one per mix, to a lab in Iceland for air content and spacing factor analysis. This test was conducted by Kjartan Björgvin Kristjánsson, a lab researcher, following ASTM C457/457M-16 Procedure B. The results are presented in Table 17. As expected, the initial air percentage measurements were found to be inaccurate. The air percentages shown in Table 17 are the only values that will be used for further analysis and discussion of the results.

Table 17: results of test performed according to ASTM C457/457M-16

Mix name	Air* [%]	Spacing factor [mm]	Specific surface [mm ⁻¹]
REF-360	5.3	0.14	33
M 18/6-360	3.8	0.26	22
M 18/6-300	4.0	0.25	22
M 25/10-360	6.0	0.16	28

*measured on hardened concrete according to ASTM C457/457M-16 Procedure B

The amount of SP used in the mixes is also an important factor to discuss. It is evident that the quantities of SP required to attain the targeted workability were relatively consistent across all the mixes, ranging between 3.60 and 4.80. However, it's notable that the W/B ratio significantly

influences the necessary amount of SP to achieve the desired workability. A lower W/B ratio indicates less free water in the mix relative to the binder leading to a reduced workability. However, it is worth noting that the W/B ratios are calculated using the k-values as mentioned in section 4.2. When two types of binders are compared, and the first one has a k-value of 0.7 while the second has a k-value of 1, using the same amount of water will result in a higher W/B ratio for the first binder. For this reason, it is important to not only include the W/B ratio and amount of SP but also the amount of free water used for each of the mixes.

Both the REF-360 and M 18/6-360 had a W/B ratio of 0.4, yet M 18/6-360 required more SP to achieve the desired workability. M 18/6-360 partially uses VPI as a binder, indicating that its use leads to inferior workability compared to the mix containing CEM II, which partially consists of FA (REF-360), thereby necessitating a higher dosage of SP. However, M 18/6-360 had a lower amount of free water compared to REF-360, indicating that the use of more SP could also be a result of the need to compensate for the lower amount of free water in the mix. REF-360 had a k-value of 1 whereas M 18/6-360 partially consisted of VPI which had a k-value of 0.7. Because of this, a different amount of free water translated into the same W/B ratio. Despite the similar W/B ratios, the difference in free water content suggests that FA (REF-360) might have a slightly higher water demand or water retention properties compared to VPI (M 18/6-360). Conversely, M 18/6-300 required less SP compared to REF-360, but its higher W/B ratio of 0.47 and total binder mass of 300 instead of 360 contributed to this variation.

Equal amounts of SP were applied to both M 25/10-360 and REF-360. M 25/10-360 has a higher substitution percentage of OPC compared to REF-360. Since the use of VPI reduces workability, a higher amount of SP of water would typically be required. However, despite M 25/10-360 having a higher W/B ratio, the actual amount of free water is lower than in REF-360 due to the use of k-values in determining these ratios. Additionally, the amount of SP used in M 25/10-360 is the same as REF-360.

When VPI reduces workability, more water or more SP is generally needed, as supported by other results and statements in the literature review. An explanation could be related to the particle size or shape of the materials used. The particle size and shape of the substituted materials in M 25/10-360 could affect the mix's workability and the effectiveness of the SP. Finer particles or particles with a more angular shape can increase the surface area, requiring more water or SP to achieve the desired workability. Conversely, spherical particles or larger particles might reduce the water or SP demand. Therefore, the differences in particle

characteristics between M 25/10-360 and REF-360 might have led to the unexpected workability results, independent of the recorded SP amounts. However, this theory can't be checked as long as there is no known knowledge of the particle shape and size for both VPI and FA. Another explanation for the contradictory results could be a recording error in the actual amount of SP added.

Table 18: comparison of amount of SP and free water

MIX name	W/B	SP [kg/m ³]	Δ REF	Free water [kg/m ³]
REF-360	0.40	4.32	-	143
M 18/6-360	0.40	4.80	+0.11%	136
M 18/6-300	0.47	3.60	-0.17%	132
M 25/10-360	0.42	4.32	+0.00 %	132

5.2 Density evaluation

The density of the hard concrete was determined after 2 days, 28 days and 56 days. These results are shown in Table 19. All density results were rounded to the nearest 5kg/m³.

Table 19: density results for fresh concrete and hard concrete (2d,28d,56d)

Mix name	Density 2 days [kg/m ³]	Density 28 days [kg/m ³]	Density 56 days [kg/m ³]
REF-360	2340	2345	2345
M 18/6-360	2385	2390	2395
M 18/6-300	2385	2400	2400
M 25/10-360	2355	2360	2365

A visual representation of the density evaluation is shown in Figure 23. This graph illustrates that the densities of REF-360 and M 25/10-360 consistently remain lower throughout the entire process compared to the other two mixes. This is likely due to the higher air content in the concrete, as increased air content results in lower density. Specifically, M 25/10-360 had an air percentage of 6%, while REF-360 had an air percentage of 5.3%, contributing to their lower densities. However, it is noteworthy that REF-360 had an even lower density than M 25/10-360. This can be attributed to the slightly lower air percentage in REF-360 or the lower density

of FA compared to VPI. The density of the VPI used in the mixes was 2.98 g/cm^3 , whereas the density of the FA was 2.3 g/cm^3 .

M 18/6-360 and M 18/6-300 exhibit very similar densities throughout the entire curing period, which can be attributed to their similar air percentages of 3.8% and 4%, respectively. The lower air percentages result in higher concrete densities. At 28 days, M 18/6-300 has a slightly higher density, which is due to a higher proportion of aggregates and a lower proportion of binder, as binders typically have lower densities compared to aggregates.

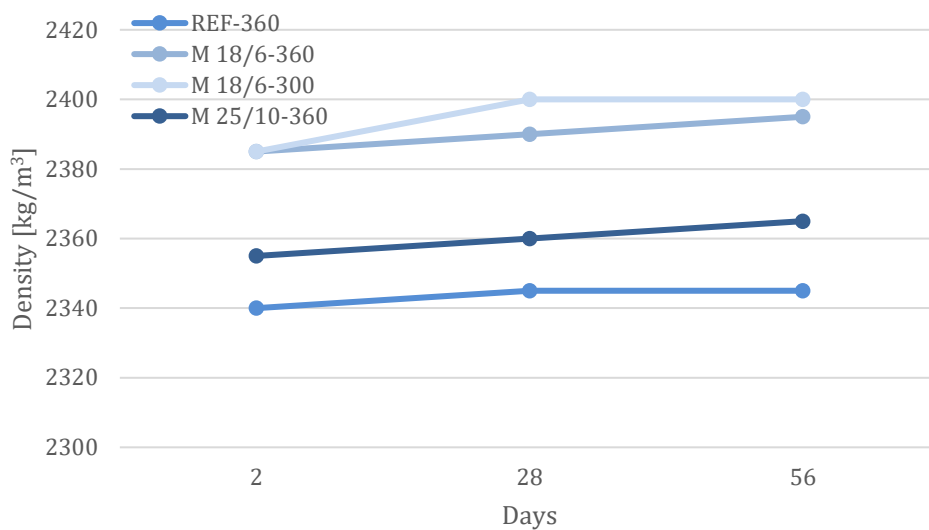


Figure 23: density progress of concrete samples

5.3 Compressive strength

The compressive strength results for all the mixes are displayed in Table 20. However, it's important to note that the compressive strength test was conducted on $100 \times 100 \times 100 \text{ mm}$ cubes, following common practice in Norway, whereas EN 206-1 ("EN 206-1," 2001) specifies strength classes for cubes of $150 \times 150 \times 150 \text{ mm}$, as explained in section 2.3.1. Although a conversion factor is often applied to results obtained from cubes with dimensions differing from the standard, the variance in compressive strength post-conversion is negligible. Therefore, it is customary in Norway to utilize results obtained from 100 mm cubes without converting them. Given that the research portion of this thesis was conducted at UiT Narvik, the Norwegian guidelines will be followed to discuss the results.

Table 20: compressive strength results for cubes 100x100x100mm

	2 days [MPa]	28 days [MPa]	56 days [MPa]
REF-360	35.77	55.31	61.88
M 18/6-360	42.25	66.40	75.14
M 18/6-300	34.45	54.00	61.70
M 25/10-360	35.91	58.50	68.62

A visual representation of the results is given in Figure 24. The compressive strength classes for concrete given in EN 206-1 are based on samples that were tested after 28 days of curing. When looking at the test results of the samples used in this thesis it is noticeable that all the mixes can reach a strength class of C40/50 which required a strength of 50 MPa for cubes. However, the strength of all the mixes is relatively high after only two days as well. This phenomenon can be attributed to the types of cement used to make the mixes. REF used CEM II/B-M (V-L) 42.5R, a type of FA-cement, whereas the three other mixes used CEM I 52.5R in combination with VPI to make the concrete. In the name of these cement types “42.5R” and “52.5R” are mentioned. The number refers to the compressive strength the mortar prisms made with this cement should reach after 28 days according to EN-196-1. Additionally, the “R” stands for “Rapid” which refers to the ability of the cement type to develop strength quite quickly. However, by partially replacing CEM I with VPI, the original strength class of 52.5R will be reduced. According to Iveta Nováková, researcher at UiT, the strength class should be degraded to 42.5 by using VPI.

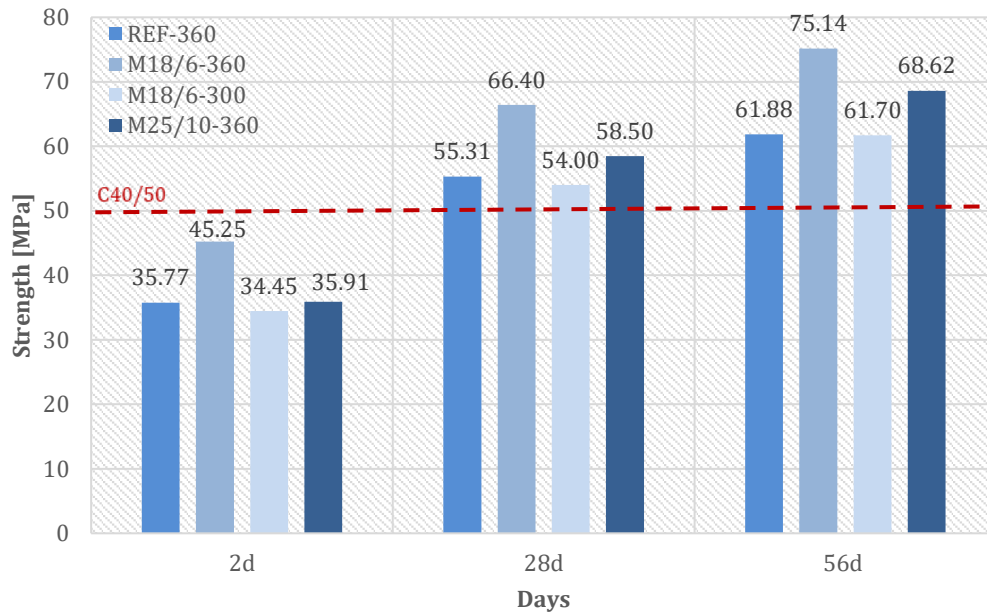


Figure 24: compressive strength for cubes 100x100x100mm (2d,28d,56d)

M 18/6-360 and M25/10-360 had a higher compressive strength than REF-360 at all the testing ages, whereas M 18/6-300 had a lower compressive strength. Since M 18/6-300 has less binder than the other mixes, it is normal for the compressive strength to be lower.

Assuming that at 28 days all the concrete samples reach the desired strength, a comparison can be made of the strength gain throughout the curing. Table 21 gives this strength gain in percentages compared to 28 days of curing. This table shows that a higher amount of VPI gives a more delayed strength gain at two days. Additionally, the mixes with VPI have a slightly lower strength gain compared to REF-360 with FA-cement at two days. However, when looking at 56 days it is worth noting that the mixes with VPI have a bigger strength gain than the reference mix containing FA-cement. This will be further discussed in the discussion part of this thesis.

Table 21: strength gain at different curing times [%]

	2 days	28 days	56 days
REF-360	64.7	100.0	110.5
M 18/6-360	63.6	100.0	113.2
M 18/6-300	63.8	100.0	114.3
M 25/10-360	61.4	100.0	117.3

Table 22 gives the strength of the samples compared to the strength of the reference mix. The W/C and air percentage are also given. Cement is the primary binding agent in concrete and contributes significantly to its strength. SCMs like VP can enhance strength due to the pozzolanic reaction but their contribution is not as significant as that of cement. Therefore the actual W/C-ratio will be used to make conclusions instead of the W/B ratio. A higher W/C ratio equals more free water and therefore a lower compressive strength. The air content also significantly affects the compressive strength results, as a higher air percentage results in lower compressive strength.

Table 22: compressive strength comparison

MIX name	W/C	Air [%]	2 days [MPa]	Δ REF	28 days [MPa]	Δ REF	56 days [MPa]	Δ REF
REF-360	0.48	5.3	35.77	-	55.31	-	61.88	-
M 18/6-360	0.47	3.8	45.25	+27%	66.40	+20%	75.14	+21%
M 18/6-300	0.55	4.0	34.45	-3.8%	54.00	-2.4%	61.70	-0.29%
MIX 25/10-360	0.54	6.0	35.91	+0.4%	58.50	+5.77%	68.62	+10.89%

First, the three mixes containing VPI will be compared to each other since they all utilize the same cement type. M 18/6-360 has the lowest W/C ratio at 0.47 among the trio, correlating with its highest compressive strength among the VPI-containing mixes. Conversely, M 18/6-300 and M 25/10-360 have a W/C ratio of 0.55 and 0.54 respectively with the former showing slightly lower strength than the latter. The air percentages for these mixes correlate with their strength results, as M 18/6-360, which has the lowest air percentage, also exhibits the highest compressive strength.

The reference mix has a W/C ratio of 0.48 and an air percentage of 5.3% , explaining why its compressive strength is lower than M 18/6-360. However, it is notable that REF-360 has a slightly higher strength at all ages compared to M 18/6-300, though the difference is minimal. This result is remarkable considering M 18/6-300 contains 60 kg/m³ less binder than REF-360, yet their compressive strengths are very similar. This suggests that VPI might contribute more to strength development through the pozzolanic reaction than FA does.

5.4 Freeze-thaw

This section is divided into two parts, each presenting the same results in a different format. The first part features three separate graphs for each curing condition, allowing for a

comparison of the mix design effects under each specific condition. In contrast, the second part includes four graphs for each mix, enabling a comparison of the curing condition effects on each individual mix. Each graph will be accompanied by a brief explanation of the results, informed by insights from the literature review.

To avoid confusion, the basics regarding F-T performance are briefly explained again. A higher air content leads to better F-T performance because it provides space for the water inside the pores to expand, thereby releasing pressure. The spacing factor refers to the average distance between the added air voids and is optimal for F-T when it is lower than 0.20 mm. The specific surface refers to the total surface area of air voids per unit volume of concrete, indicating the fineness or coarseness of the air-void system. A specific surface value greater than 25 mm^{-1} is considered beneficial for F-T performance. A higher W/B ratio leads to the formation of more capillary pores, which is not beneficial for F-T performance since these pores can absorb water. The pore size distribution refers to the distribution of different sizes of pores within the concrete. This distribution can change when the pores get filled and their sizes reduce, which can occur, for example, through CO_2 curing. These different terms will be used to explain the results found in the subsequent chapters. A more detailed explanation of these factors was provided in the literature review in paragraph 2.3.2.

According to EN12390-9 the limit for scaling when doing F-T testing for a concrete slab is 1 kg/m^2 . NS-EN 206 says that the scaling cannot surpass 0.50 kg/m^2 for concrete slabs. The primary requirement for determining freeze-thaw resistance will be the 0.50 kg/m^2 limit, although the 1 kg/m^2 limit will also be considered. Additionally, photos are provided of the samples after enduring the F-T-test in appendix H.

5.4.1 Results: graphs by curing condition

For the F-T tests three samples per mix were used for each of the curing methods. The graphs and tables for these individual test results are given in appendix G. The graphs presented in the following subchapters display the average values derived from the three test samples.

5.4.1.1 Regular curing

The results found for the mixes enduring regular curing are shown in Figure 25. This graph shows the mean value line for each of the mixes as well as both the limits for scaling.

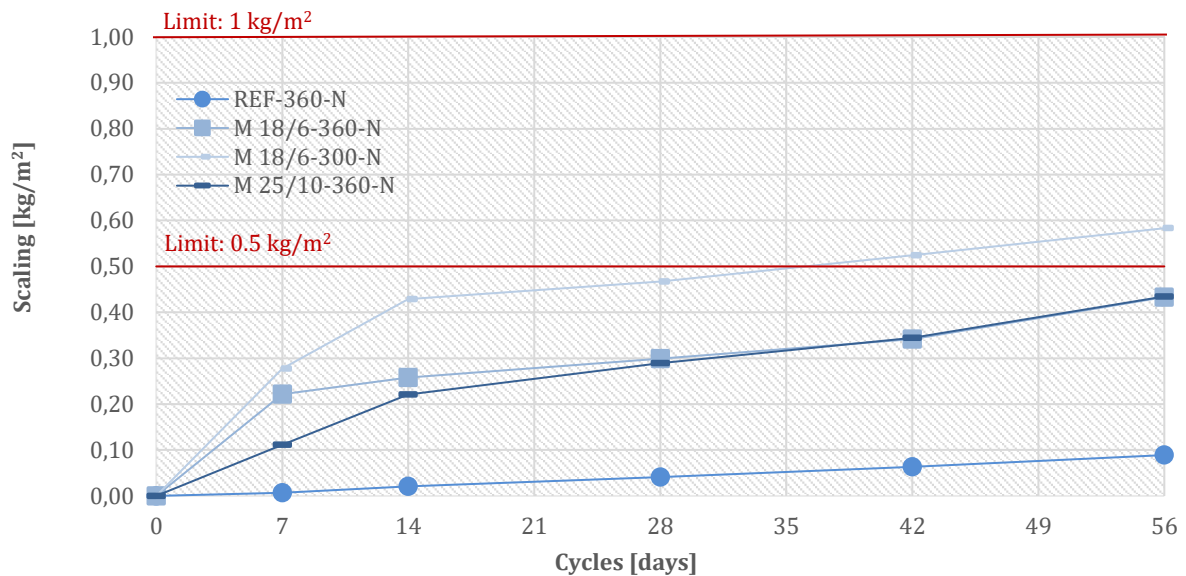


Figure 25: F-T results for regular curing

REF-360 has the lowest scaling out of all the mixes and stays well below the limit for all the cycles. Both M 18/6-360 and M 25/10-360 also stay below the limit for all the cycles. M 18/6-300 is the only mix that surpasses the limit of 0.5 kg/m^2 . The fact that this mix performs worse than the other three mixes can be attributed to the fact that less binder was used. Due to the lower binder volume, the air entrained in the mix is not evenly distributed, which is confirmed by the spacing factor of 0.25 mm . Additionally, the higher W/B ratio in this mix could lead to the formation of capillary pores which also negatively affects the F-T resistance.

However, since an air percentage close to 6% is what was strived towards while making these mixes there were more air bubbles present in the concrete which provides room for the freezing water to expand. This is most likely the reason that M 18/6-300 does not surpass the limit before 28 cycles. Additionally, both M 25/10-360 and REF-360 have a spacing factor $< 0.20 \text{ mm}$ which might explain why these two mixes perform the best. M 18/6-360 had a spacing factor greater than 0.20 and the lowest air percentage among the samples. Despite this, it remained below the limit at all cycles. This performance can be attributed to the lower W/B ratio of 0.4 , which results in the formation of fewer capillary pores. It is also worth noting that all the mixes stay below the limit of 1 kg/m^2 set by EN12390-9.

The mixes containing VPI have higher scaling than the reference mix containing FA implying that concrete with VPI is less F-T resistant than concrete with FA. This will be further discussed in the discussion part of the thesis where the results will be compared to results previously established in the literature.

5.4.1.2 CO₂ curing

An overview graph for CO₂ curing is given in Figure 26. This graph shows the mean value line for each of the mixes as well as the limit for scaled material.

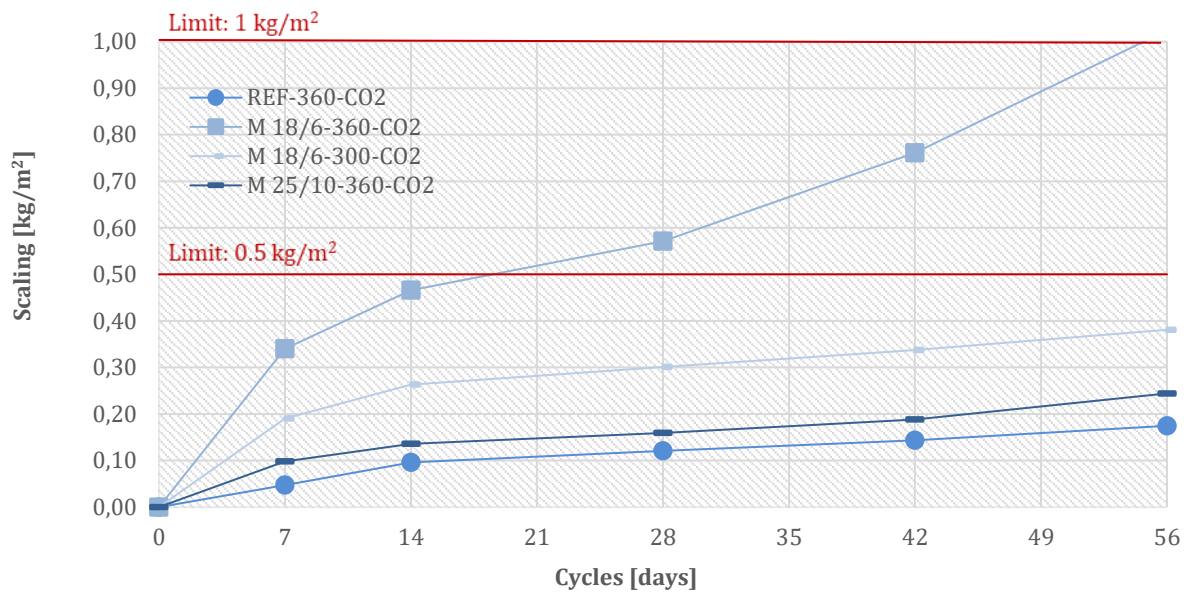


Figure 26: F-T results for CO₂ curing

The only mix surpassing the limit is M 18/6-360. This mix surpasses the scaling limit of 0.5 kg/m² between the testing of 14 and 28 cycles. The mix also exceeds the scaling limit of 1 kg/m² after 56 cycles. The other mixes perform very well, staying below both established limits. The reference mix containing FA once again has the lowest scaling compared to the other mixes.

The CO₂ curing simulates the effects that would occur for real life samples that are subjected to CO₂ intrusion, thus it can be stipulated that these results are more accurate than the ones found with normal curing.

5.4.1.3 Prolonged CO₂ curing

An overview graph for prolonged CO₂ curing is given in Figure 27. This graph shows the mean value line for each of the mixes as well as the limit for scaled material. Only M 18/6-300 goes below the limit of 0.5 kg/m². However, all the mixes stay below the limit of 1 kg/m². It should be noted that there is no data for scaling at 56 days for M 18/6-300 and M 25/10-360.

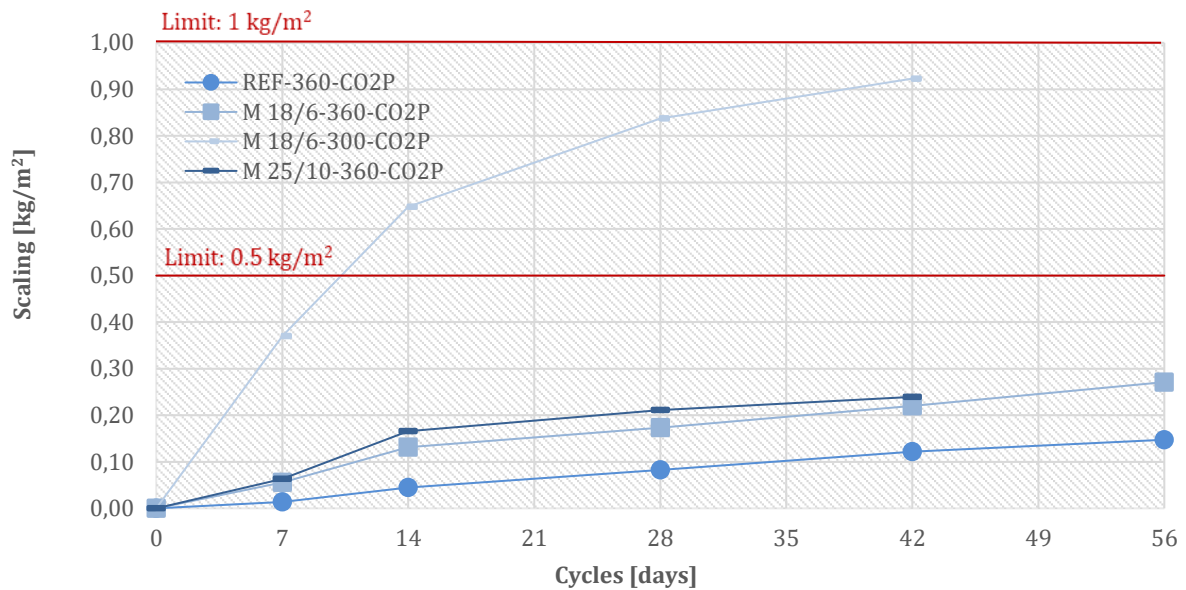


Figure 27: results for prolonged CO₂ curing

5.4.2 Results: graphs by concrete mix

This section showcases the previously established results in a different way by splitting the results up in four graphs. Each graph represents one of the mixes and the results found for the curing conditions that were implemented on this mix. Explanations are given as to why these curing conditions might have led to the results found. These explanations are based on the knowledge gathered in the literature study. The reason why certain mixes behave differently for certain curing conditions is discussed in the discussion part of this thesis.

5.4.2.1 REF-360

The graph comparing the F-T results of REF-360 for the different curing conditions is given in Figure 28. The F-T results for this mix are relatively similar for all the curing conditions and stay below both of the limits (0.5 kg/m² and 1 kg/m²) at all times.

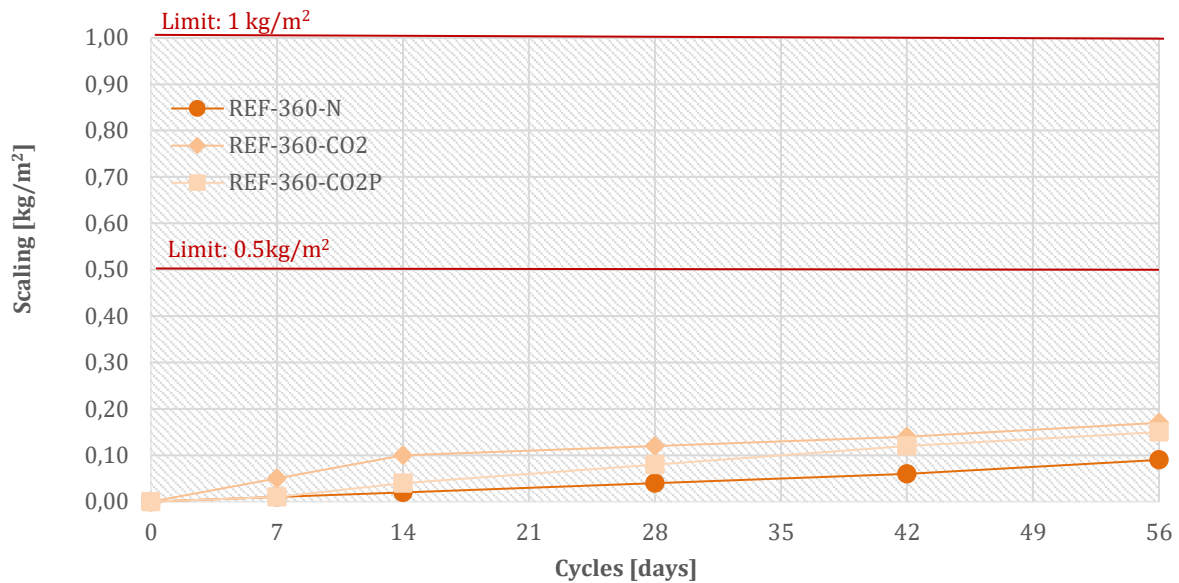


Figure 28: F-T results for REF-360

This mix had a W/B ratio of 0.4, which is relatively low and therefore results in the formation of fewer capillary pores. This positively influences the F-T resistance. The air percentage in this mix was 5.3% which is also very beneficial for F-T performance. Additionally, the spacing factor was 0.14 mm, below the optimal threshold of 0.22 mm, and the specific surface area was 33 mm^{-1} , exceeding the ideal minimum of 25 mm^{-1} . The pore size distribution was likely very good as well due to the low W/B ratio.

Although normal curing performs slightly better than the other two curing conditions, the difference is negligible. In other words, the scaling with CO_2 and prolonged CO_2 curing is worse but still within acceptable limits. The slightly worse performance of CO_2 curing is likely because more gel pores than capillary pores were filled with CaCO_3 , resulting in an uneven pore size distribution and thus worse F-T results. The F-T performance improves slightly with prolonged CO_2 curing. This improvement could be attributed to the fact that the CO_2 had more time to fully penetrate the concrete, leading to an overall better pore size distribution.

5.4.2.2 M 18/6-360

The graph comparing the F-T results of M 18/6-360 for the different curing conditions is given in Figure 29. This graph shows that M 18/6-360 surpasses the limit of 0.5 kg/m^2 at 28 cycles

for CO₂ curing and the limit of 1 kg/m² at 56 cycles. In contrast, the results for normal curing and prolonged CO₂ curing remain below these limits.

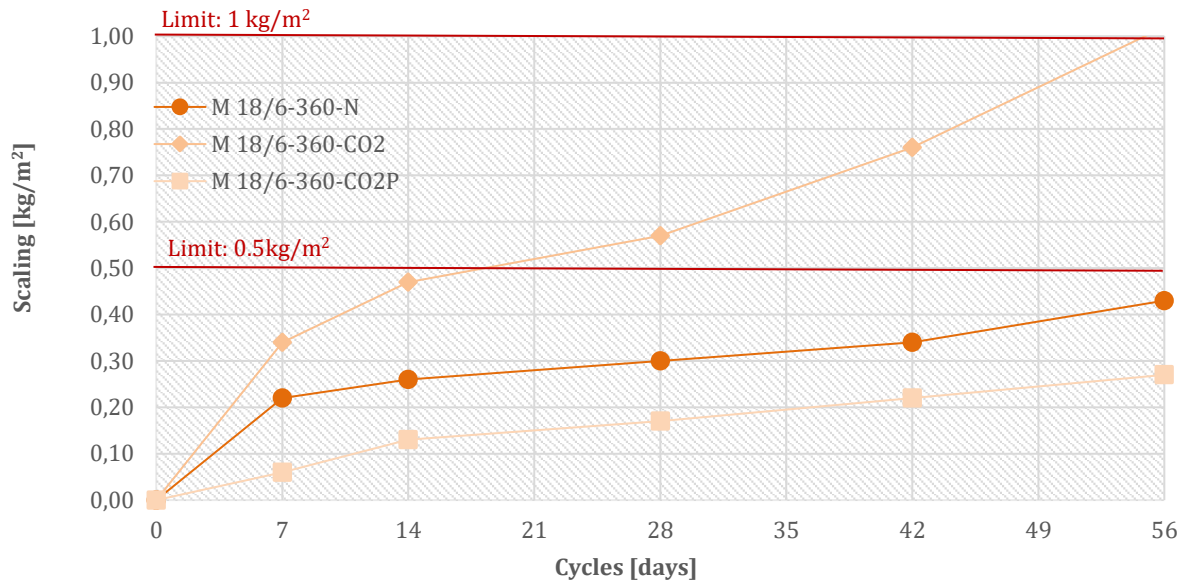


Figure 29: F-T results for M 18/6-360

This mix had a W/B ratio of 0.4, an air content of 3.8% and a spacing factor of 0.26 mm. The relatively low W/B ratio suggests that fewer capillary pores were formed, which is beneficial for F-T performance. However, the low air content and spacing factor higher than 0.20 mm contributes to worse F-T results. Additionally, the specific surface area was 22 mm⁻¹ which is lower than ideal minimum of 25 mm⁻¹ and therefore also contributes worse F-T resistance.

The standard CO₂ curing leads to the formation of CaCO₃, which fills the pores. The poor F-T performance under standard CO₂ curing suggests that more gel pores, rather than capillary pores, were filled, or that the filling of pores was unevenly distributed. However, prolonged CO₂ curing performs better, staying below the limits. This improvement is likely because the extended time in the CO₂ chamber allows for more thorough and uniform penetration of CO₂, resulting in better F-T resistance.

5.4.2.3 M 18/6-300

The graph comparing the F-T results of M 18/6-300 for the different curing conditions is given in Figure 30. It should be noted that there is no data for scaling at 56 days for the prolonged CO₂ curing due to time constraints for this thesis.

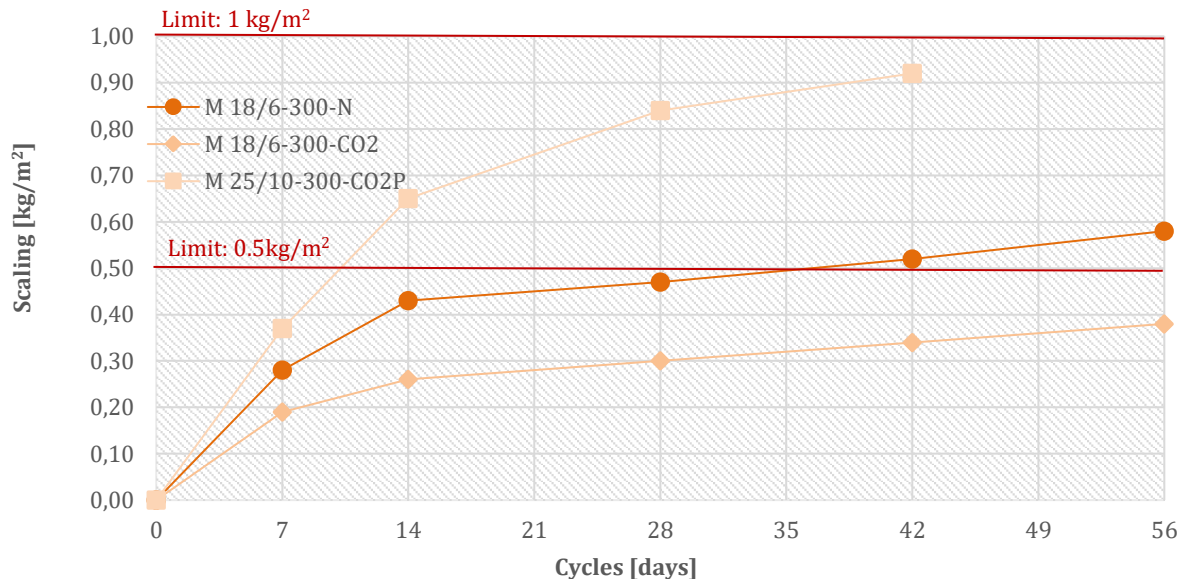


Figure 30: F-T results for M 18/6-300

This graph shows that the results for both normal curing and prolonged curing surpass the limit of 0.5 kg/m². The results for CO₂ curing however, stay below the limits for all the cycles. In this case the CO₂ curing most likely filled the capillary pores, resulting in less water absorption and thus better F-T results. The normal curing performs well up until 42 cycles, when it eventually exceeds the limit of 0.5 kg/m². However, it does not exceed the limit of 1 kg/m² at any time. The worst performance is this of the prolonged CO₂ curing, which exceeds the limit of 0.5 kg/m² relatively quick.

This mix had an air percentage of 4% which is not very high but can still contribute to better F-T performance. However, the mix does have a relatively high W/B ratio (0.47) which can lead to the formation of more capillary pores. The air percentage might explain why the concrete doesn't exceed the limit for normal curing at first despite the fact that there are probably more capillary pores present in the concrete. However, this mix does have a spacing factor of 0.25

mm and a specific surface of 22 mm^{-1} . Both of these values are not optimal and also contribute to worse F-T performance.

CO_2 curing likely produced the best results because the capillary pores were partially filled with CaCO_3 , improving the F-T performance by reducing the pore size. However, the fact that prolonged CO_2 curing resulted in the worst performance suggests that the extended time in the CO_2 chamber led to excessive carbonation, which may have filled both gel and capillary pores unevenly. This uneven pore structure might have led to poorer F-T performance.

5.4.2.4 M 25/10-360

The graph comparing the F-T results of M 25/10-360 for the different curing conditions is given in Figure 31. It should be noted that there is no data for scaling at 56 days for the prolonged CO_2 curing due to time constraints for this thesis. For this mix, all three curing conditions resulted in scaling that remained below both limits (0.5 kg/m^2 and 1 kg/m^2) throughout all testing cycles.

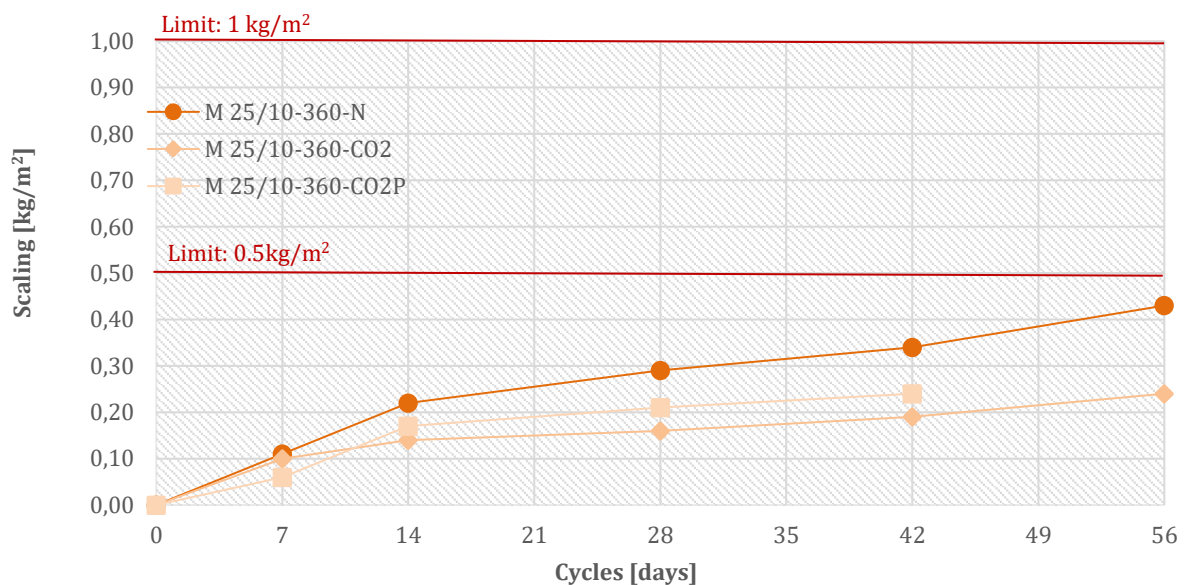


Figure 31: F-T results for M 25/10-360

This mix contained a relatively high substitution percentage of 25% VPI. The VPI reacts with $\text{Ca}(\text{OH})_2$ to form additional compounds that fill the capillary pores, resulting in consistently excellent F-T performance that remains below the limit at all times. Additionally, the mix had

a measured air content of 6%, which is relatively high and contributes to a good spacing factor (0.16 mm) and thus to the good F-T results. The W/B ratio was 0.42, which could lead to the formation of more capillary pores but the higher VPI content effectively fills these pores. Generally speaking, this mix likely had an optimal pore size distribution.

It is noticeable that normal curing resulted in the poorest performance among the three methods, whereas the standard CO₂ curing performed the best. CO₂ curing results in the creation of CaCO₃ which ideally fills up the capillary pores, which is likely the case for this mix. The high VPI percentage and the high air percentage already contribute to really good F-T performance, but the extra filling of the capillary pores due to the CO₂ curing added to this even more. The prolonged CO₂ curing performs slightly worse than the standard CO₂ curing. This could be attributed to over carbonization which lead to an uneven pore distribution.

5.5 Chloride migration

The chloride migration coefficient can be categorized based on Table 23 outlined in the NT-BUILD-492 standard. This table provides the ranges within which chloride migration can be classified, varying from low resistance to very high resistance.

Table 23: resistance to chloride migration according to NT BUILD-492

Resistance to chloride migration	
Dnssm	28 days test
>15	Low
10-15	Moderate
5-10	High
2,5-5	Very high
<2,5	Extremely high

The results for the chloride migration test are given in Figure 32. All the mixes were tested at both 28 days and 56 days.

When looking at the results it is noticeable that M 25/10-360 was highly chloride resistant at 28 days and could be classified as very high resistant at 56 days. The three other mixes were classified as moderate resistant to chloride migration at 28 days and high resistant after 56 days.

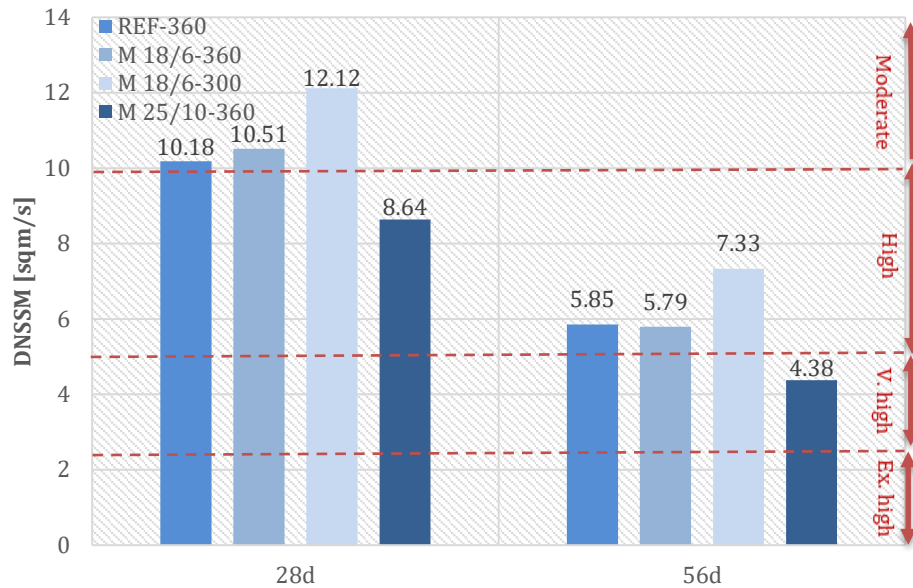


Figure 32: chloride migration at 28d and 56d

It is noticeable that M 18/6-360 and M 18/6-300 are both in the same chloride resistance category as the reference mix. Meaning, the reference mix which contains fly-ash cement does not necessarily perform better than the mixes with VPI. M 25/10-360 even surpasses the reference mix in terms of chloride migration resistance.

The reduction rate of the chloride migration tests at different curing times is given in Table 24. This shows the reduction rate is higher for samples with more VPI. This becomes evident when looking at M 18/6-360 and M 25/10-360, both containing the same binder mass, with the latter having the highest substitution percentage of VPI. REF-360, M 18/6-360 and M 25/10-360 also show that for mixes with the same binder mass, the reduction rate is higher for mixes with VPI than FA. M 18/6-300 has the lowest reduction rate, meaning the resistance to chloride migration does not improve that much compared to the other mixes. This fact is most likely related to the lower mass of binder that can densify over time.

Table 24: chloride migration reduction percentages

	28d	56d	Reduction: 28d-56d	Reduction [%]
REF-360	10.18	5.85	4.33	42.5
M 18/6-360	10.51	5.79	4.72	44.9
M 18/6-300	12.12	7.33	4.79	39.5
M 25/10-360	8.64	4.38	4.26	49.3

6

Discussion

This section compares the findings presented in section 5 with those documented in the existing literature. Those results can be correlated with the test results conducted in this thesis to determine their alignment. The discussion of the results is divided in subsections correlating to different variables based on the research questions asked in section 1.3.

6.1 Effect of mix design on workability

In section 5.1 a comparison was made between the different mixes regarding their workability and the need for SP. One of the observations was that the mix with VPI needed more SP compared to the mix with FA-cement with the same W/B ratio. Meaning, VPI generally lead to a loss of workability. This aligns with the results found by Yuan & Ma (2021) and , Liu et al. (2023) who both state that using VP will lead to workability loss.

6.2 Effect of mix design on F-T resistance

When looking at the F-T-test results in section 5.4.1, it is noticeable that the mixes with VPI generally have higher scaling than the mix with FA for all of the curing conditions. This implies that concrete made with VPI is less F-T-resistant than concrete made with FA. This is similar to the finding stated in a study conducted by Mousavinezhad et al. (2023) which stated that concrete made with pumicite, a type of VP, performed worse in F-T testing compared to concrete made with FA. A study conducted by Peng et al. (2017) similarly stated that F-T performance for concrete made with volcanic tuff was worse than concrete made with FA.

Nevertheless, all mixes tested in this thesis performed well in general. Zhang & Shao (2018) state that concrete with a strength exceeding 40 MPa is very resistant to surface scaling when exposed to F-T cycles. The results found in this thesis align with this statement since all of the

mixes perform very well under F-T exposure and they all have a compressive strength exceeding 40 MPa at the age of 28 days.

6.3 Effect of mix design on compressive strength

According to Hossain & Lachemi (2007) the compressive strength of concrete with VA will decrease with the increase of the VA substitution percentage compared to concrete with only OPC. A similar study that was conducted by Aziz et al. (2021) concludes the same thing. The results from this thesis also find a similar trend. The compressive strength of M 25/10-360 is lower than the compressive strength of M 18/6-360 which both have the same amount of binder but a different substitution percentage of OPC.

Another statement made in section 5.3 is that VPI has a higher strength gain after a long curing period (56 days) but FA has a higher strength gain in the beginning (2 days), based on the results that were found. A study conducted by Mohsen et al. (2023) states that the particle size of the binder can influence the speed of the pozzolanic reaction. Finer particles usually have a larger surface area to volume ratio which allows for a quicker reaction with calcium hydroxide, leading to faster strength gains in the initial stages of curing. Assuming that the VPI had larger particles than the FA, this could explain why the strength gain of FA is bigger at first whereas VPI has a bigger strength gain after a longer curing period.

6.4 Effect of mix design on chloride migration

As mentioned in section 2.2.3 a high resistance to chloride migration is associated with a lower permeability and porosity. Concrete made with SCMs usually have a lower permeability and porosity due to the filling effect and the pozzolanic reaction that occurs. Based on the results that were found it can be concluded that M 25/10-360 has a lower porosity than the three other mixes who are more likely to have a similar porosity since they are all in the same chloride migration class. This result corresponds to what can be found in the literature since M 25/10-360 has the highest substitution percentage of volcanic pozzolan. A study conducted by Borosnyói (2016) stated that concrete made with SCMs leads to a higher resistance to chloride migration.

Celik et al. (2014) found that concrete samples using a combination of natural pozzolan (NP) and limestone powder (LP) performed better than those made with only ordinary Portland

cement (OPC). In this thesis, there were no samples made with only OPC, so this finding cannot be directly confirmed or denied. However, the mixes in this study that included both NP and LP showed very good performance in chloride migration tests. Celik et al. (2014) attributed the improved resistance to the lower porosity of concrete with SCMs, meaning it has fewer gel pores for chloride to penetrate. Additionally, adding LP can form carbo-aluminates, further reducing pore size and blocking chloride entry. These results are clearly supported by the findings in this thesis.

6.5 Impact of curing conditions on F-T resistance

CO₂ curing of concrete reduces the volume of capillary pores accessible to water, meaning there is less water available to freeze, which generally improves the concrete's performance in F-T tests (Zhang & Shao, 2018). A study by Zhang and Shao (2018) examined concrete with 20% FA replacement, cured in the open air for 5.5 hours to reduce free water and facilitate CO₂ diffusion. The samples were then CO₂ cured, reducing the pore size, followed by water curing. These samples absorbed less water and performed better in F-T tests compared to samples cured without CO₂.

Conversely, Hasholt et al. (2022) found that CO₂ curing can also make concrete perform worse in F-T tests, depending on the water content before CO₂ exposure. Their study used a RH of 65% and a CO₂ concentration of 1%, resulting in increased scaling. This suggests that if the water content is not adequately reduced before CO₂ curing, the smaller pores can lead to higher internal tension when water freezes, worsening F-T resistance. Thus, the relative humidity of the CO₂ chamber and the initial water content are crucial factors in determining the outcome.

Similarly, the results of this study were achieved by curing in a CO₂-chamber with a RH of 65% and a CO₂-percentage of 1%. However the results differed immensely between the mixes even though all the mixes were cured in the same way according to each of the curing conditions. Table 25 shows the scaling ratio of CO₂-curing over the normal curing. If the ratio > 0 , the CO₂ sample performed worse and if the ratio < 0 than the sample performed better. Each of the ratios were rounded to 0.1. Both REF-360 and M 18/6-360 performed worse when CO₂-curing was performed similar to what was found in the study by Hasholt et al. (Hasholt et al., 2022). Conversely, M 18/6-300 and M 25/10-360 performed better when CO₂-curing was performed.

The impact of CO₂- curing relies on the presence of Ca(OH)₂, which is a byproduct of cement hydration. The reaction that forms CaCO₃ from CO₂ and Ca(OH)₂ fills the pores in the concrete, reducing space for ice formation during freeze-thaw cycles. Higher substitution percentages of SCMs typically result in less Ca(OH)₂ being available for this reaction, which could lead to worse freeze-thaw results with CO₂- curing. However, the addition of LP can enhance the carbonation process by providing additional sources of carbonate, compensating for the reduced Ca(OH)₂. (Y. C. Wang et al., 2022)

Additionally, SCMs contribute to the formation of more C-S-H gel through pozzolanic reactions, which densifies the concrete matrix and improves F-T performance (Su et al., 2022). This could explain why M 25/10-360 performs better for curing with CO₂ compared to the normal curing as the higher SCM content already densifies the concrete and the CO₂-curing adds to that. The reason why M 18/6-300 performs better with CO₂- curing compared to normal curing was previously explained in section 5.4.2

Table 25: comparison of normal curing to CO₂-curing

	REF-360			M 18/6-360			M 18/6-300			M 25/10-360		
	N	CO2	Ratio	N	CO2	Ratio	N	CO2	Ratio	N	CO2	Ratio
	[kg/m ²]			[kg/m ²]			[kg/m ²]			[kg/m ²]		
7d	0.01	0.05	5.0	0.22	0.34	1.5	0.28	0.19	0.7	0.11	0.10	0.9
14d	0.02	0.10	5.0	0.26	0.47	1.8	0.43	0.26	0.6	0.22	0.14	0.6
28d	0.04	0.12	3.0	0.30	0.57	1.9	0.47	0.30	0.6	0.29	0.16	0.6
42d	0.06	0.14	2.3	0.34	0.76	2.2	0.52	0.34	0.7	0.34	0.19	0.6
56d	0.09	0.17	1.9	0.43	1.02	2.4	0.58	0.38	0.7	0.43	0.24	0.6

The same comparison was made for the prolonged CO₂-curing samples. A ratio was made to easily compare the amount of scaling found with normal curing compared to the amount found with prolonged CO₂-curing. For REF-360 and M 18/6-300 the samples performed worse with prolonged CO₂-curing as shown in Table 26. M 18/6-360 and M 25/10-360 performed better with prolonged CO₂-curing.

Table 26: comparison of normal curing and prolonged CO₂ curing

	REF-360			M 18/6-360			M 18/6-300			M 25/10-360		
	N	CO2P	Ratio	N	CO2P	Ratio	N	CO2P	Ratio	N	CO2P	Ratio
	[kg/m ²]			[kg/m ²]			[kg/m ²]			[kg/m ²]		
7d	0.01	0.01	1.0	0.22	0.06	0.3	0.28	0.37	1.3	0.11	0.06	0.6
14d	0.02	0.04	2.0	0.26	0.13	0.5	0.43	0.65	1.5	0.22	0.17	0.8
28d	0.04	0.08	2.0	0.30	0.17	0.6	0.47	0.84	1.8	0.29	0.21	0.7
42d	0.06	0.12	2.0	0.34	0.22	0.7	0.52	0.92	1.8	0.34	0.24	0.7
56d	0.09	0.15	1.7	0.43	0.27	0.6	0.58	ND*	-	0.43	ND*	-

*ND=NO DATA

Lastly, a table was made to compare CO₂ curing to prolonged CO₂ curing. A ratio was made to easily compare the amount of scaling found with CO₂ curing compared to the amount found with prolonged CO₂ curing. Table 27 shows that prolonged CO₂ curing performed better than regular CO₂ curing for REF-360 and M 18/6-360, but worse for M 18/6-300 and M 25/10-360.

Table 27: comparison of CO₂ curing and prolonged CO₂ curing

	REF-360			M 18/6-360			M 18/6-300			M 25/10-360		
	CO2	CO2P	Ratio	CO2	CO2P	Ratio	CO2	CO2P	Ratio	CO2	CO2P	Ratio
	[kg/m ²]			[kg/m ²]			[kg/m ²]			[kg/m ²]		
7d	0.05	0.01	5.0	0.34	0.06	5.7	0.19	0.37	0.5	0.10	0.06	1.7
14d	0.10	0.04	2.5	0.47	0.13	3.6	0.26	0.65	0.4	0.14	0.17	0.8
28d	0.12	0.08	1.5	0.57	0.17	3.4	0.30	0.84	0.4	0.16	0.21	0.8
42d	0.14	0.12	1.2	0.76	0.22	3.5	0.34	0.92	2.8	0.19	0.24	1.3
56d	0.17	0.15	0.9	1.02	0.27	0.3	0.38	ND*	-	0.24	ND*	-

*ND=NO DATA

To give visual representation of the scaling for the different curing methods a graph was made of the amount of cumulative scaling measured at 28 days for all the mixes and the different curing methods. This graph is shown in Figure 33. This graph shows that REF-360 performs the best with normal curing, it has the worst scaling when implementing CO₂ curing but the scaling lowers a little bit when prolonged CO₂ curing is used. M 18/6-360 has the best scaling for prolonged CO₂ curing and the worst for standard CO₂ curing. M18/6-300 performs the best in standard CO₂ curing and performs the worst in prolonged CO₂ curing. M 25/10-360 however, performs best in CO₂ curing and worst in normal curing.

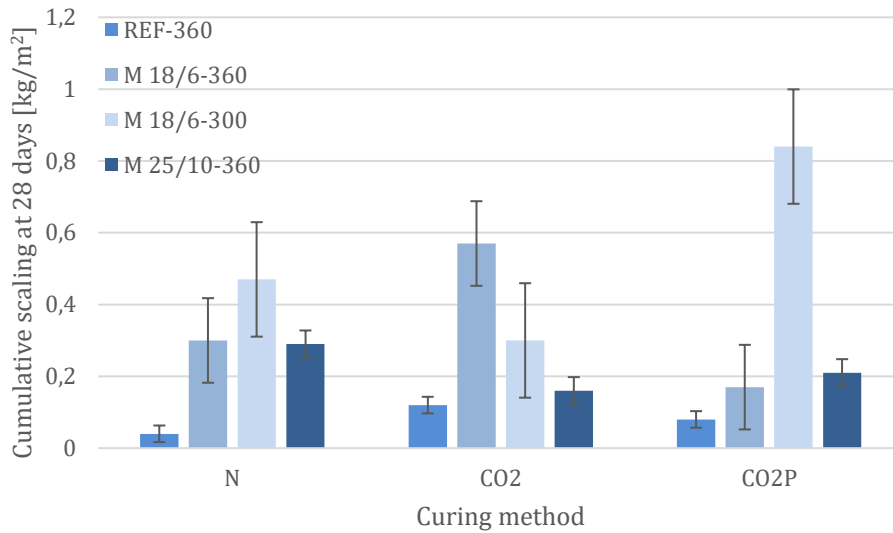


Figure 33: visual representation of scaling for different curing conditions

Table 28 gives an overview of the curing method that performed best and the one that performed worst for all of the mixes. Hereby W= worst, B= Best and M= middle. The absence of a visible pattern in these results is evident, making it worthwhile to discuss several potential factors that could have contributed to this lack of pattern.

Table 28: best and worst curing method for each mix

	REF-360	M 18/6-360	M 18/6-300	M 25/10-360
N	B	M	M	W
CO2	W	W	B	B
CO2P	M	B	W	M

One possible reason for these results is the placement of the samples in the F-T chamber, as shown in Appendix J. Although the F-T conditions should be uniform throughout the chamber, it is worth considering if the placement might have influenced the results, given that the temperature regulation mechanism is located at the top. This suggests that samples positioned higher in the chamber might have experienced the full effect of the F-T cycles, while those lower down might not have fully frozen. For instance, sample M 18/6-360, which was placed at the bottom of the chamber, should have shown better performance for CO₂ curing but worse for normal curing, given its position. However, the results show the opposite trend for this and other samples, indicating that the F-T chamber functioned correctly and the sample placement did not affect the results.

It is possible to explain the individual results based on factors such as air percentage, spacing factor, W/B ratio, and pore size distribution, as discussed in Chapter 5.4. However, this does not account for why certain mixes behave differently. The key question remains: Why did REF-360 and M 18/6-360, both performing poorly with standard CO₂ curing, show better results with prolonged CO₂ curing, while M 18/6-300 and M 25/10-360, initially showing the best results with CO₂ curing, experienced worse outcomes with prolonged CO₂ curing? One explanation previously proposed is that M 18/6-300 and M 25/10-360 suffered from over carbonation, whereas REF-360 and M 18/6-360 benefited from prolonged CO₂ curing due to a more even filling of the pores. But why does prolonged CO₂ curing lead to over carbonation in some mixes and more even pore filling in others? As Su et al. (2022) explains there are many factors influencing CO₂ penetration in concrete. This makes it difficult to pinpoint a specific reason for the behavior of these mixes.

There is no universal curing condition that suits all concrete mixes, even those made with the same type of binder. This variability is evident in Table 24, which shows that the optimal curing conditions differ significantly across the three mixes made with VPI. Each mix responds differently, highlighting the complexity of the F-T mechanism. More research is needed to obtain additional test results that can help form explanations, especially concerning curing conditions performed according to Swedish standards, as these results do not show a clear pattern.

Part IV
Conclusions

Conclusion

In this master's thesis, the durability performance of concrete incorporating VPI was investigated, with a primary focus on F-T resistance. This research was conducted as part of the larger collaborative project Ar2CorD, aiming to optimize LCC through the utilization of various SCMs, including VPI.

The findings revealed that the inclusion of VPI in concrete led to a loss of workability, necessitating adjustments such as a higher W/B ratio or increased SP dosage. Moreover, compressive strength decreased with higher substitution percentages of OPC. Notably, concrete containing VPI exhibited greater strength gain at later ages compared to concrete with FA. Even with a lower binder content, mixes with VPI showed comparable compressive strength to those with higher binder content, suggesting a significant contribution of VPI to strength development through pozzolanic reactions.

Furthermore, the chloride resistance of concrete mixes varied, with M 25/10-360 demonstrating high resistance at 28 days and very high resistance at 56 days, while the other mixes exhibited moderate to high resistance over time. Generally, the inclusion of VPI resulted in good chloride resistance, with higher resistance observed at higher VPI substitution percentages.

Regarding F-T resistance, all tested mixes performed relatively well, with VPI mixes showing higher scaling compared to FA mixes under all curing conditions. However, the choice of curing condition significantly influenced F-T performance. While some mixes surpassed scaling limits under certain conditions, they remained within acceptable limits for others.

In conclusion, concrete incorporating VPI demonstrated good durability performance overall, affirming its suitability as an SCM in concrete applications. However, the complexity of F-T mechanisms and the variability of mix responses highlight the need for further research, particularly regarding curing conditions according to Swedish standards. Additional studies in this area can provide valuable insights for optimizing concrete performance and informing future construction practices.

Sustainability reflection

Sustainability has become a critical concern in many industries, including the concrete sector. The concrete industry has made efforts to reduce its carbon footprint by incorporating SCMs, yet there remains significant potential for further improvement.

Use of natural pozzolans and transportation impact

In the current study, volcanic pozzolans sourced from Iceland were transported to Norway. While these pozzolans effectively reduce carbon emissions when used in concrete, their transportation contributes additional CO₂ emissions. Future research should explore the viability of locally sourced natural pozzolans in Norway, such as sedimentary clays, to minimize transportation-related emissions and enhance sustainability. Another option could be to conduct a study regarding the environmental impact of different types of SCMs and their transportation methods. This way it can be assessed if the use of certain materials would still result in less CO₂ emissions compared to just using OPC. It could also give insights into which SCMs are the best options for certain regions.

F-T testing standards and SCM performance

The standards for F-T testing are strict, particularly regarding permissible scaling. The testing chambers typically range from -25°C to +25°C. However, temperatures as low as -25°C are infrequent even in Northern Norway, raising questions about the applicability of these limits. Some SCMs might fail under these strict conditions despite performing adequately in real-world scenarios. Historical evidence shows that structures made with sedimentary clays and volcanic ashes have endured well before the advent of Portland clinker. Reevaluating and potentially lowering these standards could increase SCM usage, thereby further reducing CO₂ emissions. However, research would have to point out the best limit for the F-T tests.

Waste reduction and sample reuse

Efforts to minimize waste were evident during this research. Scrap pieces from sample preparation were allocated for other research projects, which is a sustainable practice. If these scraps were not repurposed in this manner, they could have been reused as aggregates in new

concrete mixes. Additionally, these scraps could be turned into art pieces or crushed for alternative uses.

In Northern Norway, where snow and ice cover the ground for extended periods, preventing slips and falls is crucial. Currently, small stones are sprinkled on roads to create more grip. An innovative solution could involve shaping scrap concrete into smaller particles to replace these stones. This not only provides a practical use for waste material but also contributes to road safety.

Laboratory practices and personal contributions

Several personal efforts were made to contribute to sustainability. Reusable gloves and dust masks were used for concrete production. To reduce CO₂ loss when opening the chamber, a plastic sheet was hung inside. This significantly decreased CO₂ consumption, allowing the CO₂ tank to be replaced only once instead of multiple times. A piece of scrap paper displayed the exact positions of samples in the CO₂ chamber, reducing the time and CO₂ loss associated with grabbing certain samples. Additionally, the CO₂ and humidity chambers were turned off immediately when not in use to save electricity. Lastly, the plastic sheets used for sealing the F-T samples and the Styrofoam boxes for insulation were reused.

Future perspectives

In this study, one type of volcanic pozzolan was investigated and subjected to F-T testing. However, to understand the effects of volcanic pozzolans on concrete performance, it is important to expand the scope of research by exploring various types of volcanic pozzolans and subjecting them to F-T testing. In this thesis the prolonged CO₂ curing only lasted one week longer than the normal one due to limited time. However, it might be interesting to see the results of the samples when they are cured for an even longer period before being submitted to F-T testing.

Since the number of samples and the implementation of curing methods were limited in this research it is important to conduct more tests with a broader range of samples. Future research could consist of testing different mix designs, exploring the effects of alternative curing methods such as prolonged curing or heat treatment, and comparing concrete containing volcanic pozzolans with those made with other NP or SCMs. Such comparative studies could shed light on the unique advantages of volcanic pozzolans and their suitability for various applications.

Expanding the database of test results with volcanic pozzolans can provide a comprehensive understanding of their application capabilities and optimal mix designs. Moreover, conducting research on mix designs with volcanic pozzolans while varying other crucial factors such as aggregates or admixtures can further enhance our understanding of this material and its potential benefits.

In summary, future research endeavors should focus on exploring different types of volcanic pozzolans, investigating the influence of various curing methods, conducting comparative studies with other SCMs, and expanding the database of test results to optimize the application of volcanic pozzolans in concrete construction.

References

- Abhishek, H. S., Prashant, S., Kamath, M. V., & Kumar, M. (2022). Fresh mechanical and durability properties of alkali-activated fly ash-slag concrete: a review [Review]. *Innovative Infrastructure Solutions*, 7(1), 14, Article 116. <https://doi.org/10.1007/s41062-021-00711-w>
- ASTM C457/457M-16. (2024). In.
- ASTM C618. (2023). In.
- Aziz, M. M., Moundi, A., Dawai, D., Ntieche, B., Koungang, B. M. G., & Michel, F. (2021). Effect of the use of volcanic pozzolan from Mbepit Massif (West-Cameroon) on the mechanical properties of mortar and composite cements production [Article]. *Engineering Research Express*, 3(1), 8. <https://doi.org/10.1088/2631-8695/abe954>
- Belleghem, B. V. (2023). *schadediagnose en betonherstelling*, Sanacon UGent.
- BGS. (2024). *Eruption styles*. In.
- Boel, V. (2006). *Microstructuur van zelfverdichtend beton in relatie met de gaspermeabiliteit en duurzaamheidsaspecten Ghent*. <http://hdl.handle.net/1854/LU-4271638>
- Borosnyói, A. (2016). Long term durability performance and mechanical properties of high performance concretes with combined use of supplementary cementing materials [Article]. *Construction and Building Materials*, 112, 307-324. <https://doi.org/10.1016/j.conbuildmat.2016.02.224>
- Bouzoubaâ, N., Bilodeau, A., Fournier, B., Hooton, R. D., Gagné, R., & Jolin, M. (2011). Deicing salt scaling resistance of concrete incorporating fly ash and (or) silica fume: laboratory and field sidewalk test data [Article]. *Canadian Journal of Civil Engineering*, 38(4), 373-382. <https://doi.org/10.1139/111-008>
- Britannica. (2024). *volcanic glass*. <https://www.britannica.com/science/obsidian>
- Celik, K., Hay, R., Hargis, C. W., & Moon, J. (2019). Effect of volcanic ash pozzolan or limestone replacement on hydration of Portland cement [Article]. *Construction and Building Materials*, 197, 803-812. <https://doi.org/10.1016/j.conbuildmat.2018.11.193>
- Danner, T., Justnes, H., & Kjellsen, K. O. (2023). Reactivity of alternative SCMs from Nordic Countries – Input for the R3 test. https://www.researchgate.net/publication/374169680_Reactivity_of_alternative_SCMs_from_Nordic_Countries_-_Input_for_the_R3_test
- Durastanti, C., & Moretti, L. (2020). Environmental Impacts of Cement Production: A Statistical Analysis [Article]. *Applied Sciences-Basel*, 10(22), 25, Article 8212. <https://doi.org/10.3390/app10228212>
- EN 196-5. (2011). In.

- EN 206-1. (2001). In.
- EN 1504-9. (2008). In.
- EN 12390-3. (2019). In.
- gcca. (2023). natural pozzolans: GCCA. <https://gccassociation.org/cement-and-concrete-innovation/clinker-substitutes/natural-pozzolans/>
- Guo, J. J., Sun, W. Q., Xu, Y. Q., Lin, W. Q., & Jing, W. D. (2022). Damage Mechanism and Modeling of Concrete in Freeze-Thaw Cycles: A Review [Review]. *Buildings*, 12(9), 36, Article 1317. <https://doi.org/10.3390/buildings12091317>
- Hamada, H. M., Abed, F., Beddu, S., Humada, A. M., & Majdi, A. (2023). Effect of Volcanic Ash and Natural Pozzolana on mechanical properties of sustainable cement concrete: A comprehensive review [Review; Early Access]. *Case Studies in Construction Materials*, 19, 14, Article e02425. <https://doi.org/10.1016/j.cscm.2023.e02425>
- Hasholt, M. T., Frid, K., Spörel, F., Lahdensivu, J., Helsing, E., Müller, M., . . . Jacobsen, S. (2022). Nordic Concrete Research workshop: "Accelerated freeze-thaw testing of concrete", Lyngby, 20th April 2022 [Article]. *Nordic Concrete Research*, 66(1), 113-133. <https://doi.org/10.2478/ncr-2022-0007>
- Honorio, T., Bary, B., & Benboudjema, F. (2018). Thermal properties of cement-based materials: Multiscale estimations at early-age. *Cement & Concrete Composites*, 87, 205-219. <https://doi.org/10.1016/j.cemconcomp.2018.01.003>
- Hossain, K. M. A., & Lachemi, M. (2007). Strength, durability and micro-structural aspects of high performance volcanic ash concrete [Article]. *Cement and Concrete Research*, 37(5), 759-766. <https://doi.org/10.1016/j.cemconres.2007.02.014>
- Jubera-Pérez, F. J., Jaizme-Vega, E., Rosa-Orihuela, R., Damas-Montesdeoca, R., Hernández-Díaz, C., Rodríguez-Díaz, J., & Gonzalez-Diaz, E. (2024). Pozzolanic activity of volcanic ashes produced by the eruption of the Tajogaite Volcano in La Palma, Canary Islands [Article]. *Construction and Building Materials*, 419, 11, Article 135498. <https://doi.org/10.1016/j.conbuildmat.2024.135498>
- Kalina, R. D., Al-Shmaisani, S., Ferron, R. D., & Juenger, M. C. G. (2019). False Positives in ASTM C618 Specifications for Natural Pozzolans [Article]. *Aci Materials Journal*, 116(1), 165-172. <https://doi.org/10.14359/51712243>
- Khan, I., Castel, A., & Gilbert, R. I. (2017). Effects of Fly Ash on Early-Age Properties and Cracking of Concrete [Article]. *Aci Materials Journal*, 114(4), 673-681. <https://doi.org/10.14359/51689898>
- Kubissa, W., Jaskulski, R., & Brodnan, M. (2016). Influence of SCM on the Permeability of Concrete with Recycled Aggregate [Article]. *Periodica Polytechnica-Civil Engineering*, 60(4), 583-590. <https://doi.org/10.3311/PPci.8614>

- Kupwade-Patil, K., Chin, S. H., Johnston, M. L., Maragh, J., Masic, A., & Büyüköztürk, O. (2018). Particle Size Effect of Volcanic Ash towards Developing Engineered Portland Cements [Article]. *Journal of Materials in Civil Engineering*, 30(8), 14, Article 04018190. [https://doi.org/10.1061/\(asce\)mt.1943-5533.0002348](https://doi.org/10.1061/(asce)mt.1943-5533.0002348)
- Li, H., Zhang, Y., & Guo, H. L. (2021). Numerical Simulation of the Effect of Freeze-Thaw Cycles on the Durability of Concrete in a Salt Frost Environment [Article]. *Coatings*, 11(10), 12, Article 1198. <https://doi.org/10.3390/coatings11101198>
- Liu, J. C., Hossain, M. U., Xuan, D. X., Ali, H. A., Ng, S. T., & Ye, H. L. (2023). Mechanical and durability performance of sustainable concretes containing conventional and emerging supplementary cementitious materials [Article]. *Developments in the Built Environment*, 15, 12, Article 100197. <https://doi.org/10.1016/j.dibe.2023.100197>
- lynx, b. (2023). why use fly ash and slag in concrete. <https://bay-lynx.com/education/why-use-fly-ash-and-slag-in-concrete/>
- Marinkovic, M., Radovic, A., & Carevic, V. (2023). Carbonation of limestone powder concrete: state-of-the-art overview [Review]. *Gradevnski Materijali I Konstrukcije-Building Materials and Structures*, 66(2), 13, Article 2300005m. <https://doi.org/10.5937/grmk2300005m>
- Mohsen, M. O., Aburumman, M. O., Al Diseet, M. M., Taha, R., Abdel-Jaber, M., Senouci, A., & Taqa, A. A. (2023). Fly Ash and Natural Pozzolana Impacts on Sustainable Concrete Permeability and Mechanical Properties. *Buildings*, 13(8), 19, Article 1927. <https://doi.org/10.3390/buildings13081927>
- Mousavinezhad, S., Garcia, J. M., Toledo, W. K., & Newton, C. M. (2023). A Locally Available Natural Pozzolan as a Supplementary Cementitious Material in Portland Cement Concrete. *Buildings*, 13(9), 24, Article 2364. <https://doi.org/10.3390/buildings13092364>
- Nandhini, K., & Ponmalar, V. (2018). PASSING ABILITY, WATER AND CHLORIDE PENETRATION OF SELF-COMPACTING CONCRETE USING MICRO-SILICA AS CEMENTITIOUS REPLACEMENT MATERIAL [Article]. *Revista Romana De Materiale-Romanian Journal of Materials*, 48(3), 362-368.
- Nidheesh, P. V., & Kumar, M. S. (2019). An overview of environmental sustainability in cement and steel production [Review]. *Journal of Cleaner Production*, 231, 856-871. <https://doi.org/10.1016/j.jclepro.2019.05.251>
- Nili, M., Azarioon, A., & Hosseinian, S. M. (2017). Novel Internal-Deterioration Model of Concrete Exposed to Freeze-Thaw Cycles [Article]. *Journal of Materials in Civil Engineering*, 29(9), 11, Article 04017132. [https://doi.org/10.1061/\(asce\)mt.1943-5533.0001978](https://doi.org/10.1061/(asce)mt.1943-5533.0001978)
- Norge, H. m. (2023). vulkansk pozzolan aske fra island i fremtidens sementer? https://www.sement.heidelbergmaterials.no/no/vulkansk_aske
- NS-EN 206. (2022). In.

NS-EN 12350-2. (2019). In.

NS-EN 12350-7. (2019). In.

NT-build-492. (2018). In.

Pacewska, B., & Wilinska, I. (2015). Comparative investigations of influence of chemical admixtures on pozzolanic and hydraulic activities of fly ash with the use of thermal analysis and infrared spectroscopy [Article]. *Journal of Thermal Analysis and Calorimetry*, 120(1), 119-127. <https://doi.org/10.1007/s10973-014-4334-x>

Papadakis, V. G., Antiohos, S., & Tsimas, S. (2002). Supplementary cementing materials in concrete - Part II: A fundamental estimation of the efficiency factor [Article]. *Cement and Concrete Research*, 32(10), 1533-1538, Article Pii s0008-8846(02)00829-3. [https://doi.org/10.1016/s0008-8846\(02\)00829-3](https://doi.org/10.1016/s0008-8846(02)00829-3)

Parhizkar, T., Najimi, M., Pourkhorshidi, A. R., Jafarpour, F., Hillemeier, B., & Herr, R. (2010). Proposing a New Approach for Qualification of Natural Pozzolans [Article]. *Scientia Iranica Transaction a-Civil Engineering*, 17(6), 450-456.

Peng, S. T., Li, X., Wu, Z. Y., Chen, J. K., & Lu, X. (2017). Study of the key technologies of application of tuff powder concrete at the Daigo hydropower station in Tibet. *Construction and Building Materials*, 156, 1-8. <https://doi.org/10.1016/j.conbuildmat.2017.08.138>

Pougnong, T. E., Belibi, P. D. B., Baenla, J., Thamer, A., Tiffo, E., & Elimbi, A. (2022). Effects of chemical composition of amorphous phase on the reactivity of phosphoric acid activation of volcanic ashes [Article]. *Journal of Non-Crystalline Solids*, 575, 11, Article 121213. <https://doi.org/10.1016/j.jnoncrysol.2021.121213>

Presa, L., Rosado, S., Peña, C., Martín, D. A., Costafreda, J. L., Astudillo, B., & Parra, J. L. (2023). Volcanic Ash from the Island of La Palma, Spain: An Experimental Study to Establish Their Properties as Pozzolans [Article]. *Processes*, 11(3), 13, Article 657. <https://doi.org/10.3390/pr11030657>

Rahhal, V., & Talero, R. (2010). Fast physics-chemical and calorimetric characterization of natural pozzolans and other aspects [Article]. *Journal of Thermal Analysis and Calorimetry*, 99(2), 479-486. <https://doi.org/10.1007/s10973-009-0016-5>

Ralli, Z. G., & Pantazopoulou, S. J. (2021). State of the art on geopolymer concrete [Article]. *International Journal of Structural Integrity*, 12(4), 511-533. <https://doi.org/10.1108/ijsi-05-2020-0050>

S.Druart, & L.Taerwe. (2018). *betontechnologie* (6th ed.). Belgische betongroepering.

Schutter, G. D. (2013). *damage to concrete structures*. <https://doi.org/10.1201/b12914>

Shania Zehra Naqvi , J. R., and Kamal K. Kar. (2022). coal-based fly ash. <https://www.sciencedirect.com/topics/earth-and-planetary-sciences/pozzolan>

- Siddique, R. (2012). Properties of concrete made with volcanic ash [Review]. *Resources Conservation and Recycling*, 66, 40-44. <https://doi.org/10.1016/j.resconrec.2012.06.010>
- Sierra, O. M., Payá, J., Monzó, J., Borrachero, M. V., Soriano, L., & Quiñonez, J. (2022). Characterization and Reactivity of Natural Pozzolans from Guatemala [Article]. *Applied Sciences-Basel*, 12(21), 20, Article 11145. <https://doi.org/10.3390/app122111145>
- Sigmundsson, F., Einarsson, P., Hjartardóttir, A. R., Drouin, V., Jónsdóttir, K., Arnadóttir, T., . . . Ofeigsson, B. G. (2020). Geodynamics of Iceland and the signatures of plate spreading [Review]. *Journal of Volcanology and Geothermal Research*, 391, 16, Article 106436. <https://doi.org/10.1016/j.jvolgeores.2018.08.014>
- Singh, N. B., Kumar, M., & Rai, S. (2020). Geopolymer cement and concrete: Properties [Proceedings Paper]. *Materials Today-Proceedings*, 29, 743-748. <https://doi.org/10.1016/j.matpr.2020.04.513>
- SN-EN 12390-9. (2016). In.
- SS137003. (2004). In.
- Su, A. S., Chen, T. F., Gao, X. J., Li, Q. Y., & Qin, L. (2022). Effect of carbonation curing on durability of cement mortar incorporating carbonated fly ash subjected to Freeze-Thaw and sulfate attack [Article]. *Construction and Building Materials*, 341, 10, Article 127920. <https://doi.org/10.1016/j.conbuildmat.2022.127920>
- Szweda, Z. (2019). Chloride diffusion and migration coefficients in concretes with CEM I 42.5 R; CEMII/B-V 32.5 R; CEM I 42.5N/SR3/NA cement determined by standard methods and thermodynamic migration model [Article]. *Ochrona Przed Korozja*, 62(5), 162-169. <https://doi.org/10.15199/40.2019.5.1>
- Taniguchi, M., Takahashi, T., & Sagawa, T. (2018). Effect of Pozzolanic Reactivity of Volcanic Ash in Hokkaido on the Durability of Volcanic Ash Concrete [Proceedings Paper]. *High Tech Concrete: Where Technology and Engineering Meet*, 2177-2184. https://doi.org/10.1007/978-3-319-59471-2_249
- Taylor, P., Sadati, S., Wang, K., Ling, Y., Wang, X., Sun, W., . . . Ryazi, S. (2021). *Entrained air-void systems for durable highway concrete* (n. a. press, Ed.)
- Thordarson, T., & Larsen, G. (2007). Volcanism in Iceland in historical time: Volcano types, eruption styles and eruptive history [Article; Proceedings Paper]. *Journal of Geodynamics*, 43(1), 118-152. <https://doi.org/10.1016/j.jog.2006.09.005>
- UIT. (2023). Ar2CorD project. <https://en.uit.no/project/ar2cord>
- USGS. (2023). what is the difference between "magma" and "lava". In.
- USGS. (2024). Questions about volcanic ash and other tephra from Kilauea. In.

- Waikado, u. o. (2010). types of volcanic rock. <https://www.sciencelearn.org.nz/resources/650-types-of-volcanic-rock>
- Wang, D. Z., Zhou, X. M., Meng, Y. F., & Chen, Z. (2017). Durability of concrete containing fly ash and silica fume against combined freezing-thawing and sulfate attack [Article]. *Construction and Building Materials*, 147, 398-406. <https://doi.org/10.1016/j.conbuildmat.2017.04.172>
- Wang, H. M., Liu, X. M., & Zhang, Z. Q. (2023). Pozzolanic activity evaluation methods of solid waste: A review [Review]. *Journal of Cleaner Production*, 402, 14, Article 136783. <https://doi.org/10.1016/j.jclepro.2023.136783>
- Wang, R. J., Hu, Z. Y., Li, Y., Wang, K., & Zhang, H. (2022). Review on the deterioration and approaches to enhance the durability of concrete in the freeze-thaw environment [Review]. *Construction and Building Materials*, 321, 24, Article 126371. <https://doi.org/10.1016/j.conbuildmat.2022.126371>
- Wang, Y. C., Lee, M. G., Wang, W. C., Kan, Y. C., Kao, S. H., & Chang, H. W. (2022). CO₂ Curing on the Mechanical Properties of Portland Cement Concrete. *Buildings*, 12(6), 17, Article 817. <https://doi.org/10.3390/buildings12060817>
- Yuan, Q., & Ma, C. (2021). natural pozzolans. <https://www.sciencedirect.com/topics/engineering/natural-pozzolans>
- Zhang, D., & Shao, Y. X. (2018). Surface scaling of CO₂-cured concrete exposed to freeze-thaw cycles. *Journal of Co2 Utilization*, 27, 137-144. <https://doi.org/10.1016/j.jcou.2018.07.012>

Appendices

A Detailed planning of lab work

Timeline F-T testing in combination with :

Normal curing (N)

2 F-T chambers can be used

DAY 0	Make concrete + perform fresh concrete tests + make testing molds
DAY 1	Demold after 24 h + place in 100% RH chamber
DAY 7	Move to 65 % RH chamber
DAY 21	Cut cube in three slices (50 mm) , clean surface with water and brush, mark samples + return to 65 % RH chamber
DAY 25	Fit samples in plastic boxes + insulate with glue + return to 65 % RH chamber
DAY 28	Move samples to room with laboratory condition + deionized water + cover with plastic + load by a wooden board
DAY 31	Check if samples are water tight (no leakages trough edges) → in case there is leakage, fix it and then return to the 65% RH chamber and after three days move the samples again and repeat the process When there is no leakage: Pour away deionized water + dry surface + place sample in polystyrene insulation box + cut overlapping plastic box frame with scissors (little bit shorter than polystyrene box) + mark sample in different places + pour freezing medium + cover with plastic cover + place in freezing chamber (freeze chamber always has to be full so place some old samples with new samples which are about to be tested) + prepare test report sheet
Testing period starts (testing after 7, 14, 28, 42, 56 cycles)	
DAY 38 (7 cycles)	Take samples out during the period when freezing temp is above 10°C (most convenient between 15-24°C) For chamber 1 : best time is in the morning hours For chamber 2: best time is in the afternoon hours → But check the computer screen for the actual temp Prepare small aluminum bowls + give them same mark as sample name + record the weight of the bowls Wash off scaled material in bigger bowl + collect scale material in smaller bowl Dry surface of sample (if any scales are on the towel, add them to small bowl) Place bowl in dryer + when dry pour new freezing medium with thickness of 3 mm on testing surface + cover with plastic Return sample to freezing chamber Check if ref the two reference samples in each chamber (one with freezing medium and one with pure water) do not lack liquids + the free samples = ones not being tested (old ones) have to be maintained the same as the tested ones, check if they do not lack freezing medium + check the recording of temperature changes
DAY 39/40	Weigh aluminum bowl with scaled material (record weight to nearest 0,1 g + place in card box file under next testing date)

DAY 45	Check if ref the two reference samples in each chamber (one with freezing medium and one with pure water) do not lack liquids + the free samples = ones not being tested (old ones) have to be maintained the same as the tested ones, check if they do not lack freezing medium + check the recording of temperature changes
DAY 52 (14 cycles)	Take samples out during the period when freezing temp is above 10°C (most convenient between 15-24°C) For chamber 1 : best time is in the morning hours For chamber 2: best time is in the afternoon hours → But check the computer screen for the actual temp Prepare small aluminum bowls + give them same mark as sample name + record the weight of the bowls Wash off scaled material in bigger bowl + collect scale material in smaller bowl Dry surface of sample (if any scales are on the towel, add them to small bowl) Place bowl in dryer + when dry pour new freezing medium with thickness of 3 mm on testing surface + cover with plastic Return sample to freezing chamber Check if ref the two reference samples in each chamber (one with freezing medium and one with pure water) do not lack liquids + the free samples = ones not being tested (old ones) have to be maintained the same as the tested ones, check if they do not lack freezing medium + check the recording of temperature changes
DAY 53/54	Weigh aluminum bowl with scaled material (record weight to nearest 0,1 g + place in card box file under next testing date)
DAY 59	Check if ref the two reference samples in each chamber (one with freezing medium and one with pure water) do not lack liquids + the free samples = ones not being tested (old ones) have to be maintained the same as the tested ones, check if they do not lack freezing medium + check the recording of temperature changes
DAY 66 (28 cycles)	Take samples out during the period when freezing temp is above 10°C (most convenient between 15-24°C) For chamber 1 : best time is in the morning hours For chamber 2: best time is in the afternoon hours → But check the computer screen for the actual temp Prepare small aluminum bowls + give them same mark as sample name + record the weight of the bowls Wash off scaled material in bigger bowl + collect scale material in smaller bowl Dry surface of sample (if any scales are on the towel, add them to small bowl) Place bowl in dryer + when dry pour new freezing medium with thickness of 3 mm on testing surface + cover with plastic Return sample to freezing chamber Check if ref the two reference samples in each chamber (one with freezing medium and one with pure water) do not lack liquids + the free samples = ones not being tested (old ones) have to be maintained the same as the tested ones, check if they do not lack freezing medium + check the recording of temperature changes
DAY 67/68	Weigh aluminum bowl with scaled material (record weight to nearest 0,1 g + place in card box file under next testing date)

DAY 73	Check if ref the two reference samples in each chamber (one with freezing medium and one with pure water) do not lack liquids + the free samples = ones not being tested (old ones) have to be maintained the same as the tested ones, check if they do not lack freezing medium + check the recording of temperature changes
DAY 80 (42 cycles)	Take samples out during the period when freezing temp is above 10°C (most convenient between 15-24°C) For chamber 1 : best time is in the morning hours For chamber 2: best time is in the afternoon hours → But check the computer screen for the actual temp Prepare small aluminum bowls + give them same mark as sample name + record the weight of the bowls Wash off scaled material in bigger bowl + collect scale material in smaller bowl Dry surface of sample (if any scales are on the towel, add them to small bowl) Place bowl in dryer + when dry pour new freezing medium with thickness of 3 mm on testing surface + cover with plastic Return sample to freezing chamber Check if ref the two reference samples in each chamber (one with freezing medium and one with pure water) do not lack liquids + the free samples = ones not being tested (old ones) have to be maintained the same as the tested ones, check if they do not lack freezing medium + check the recording of temperature changes
DAY 81/82	Weigh aluminum bowl with scaled material (record weight to nearest 0,1 g + place in card box file under next testing date)
DAY 87	Check if ref the two reference samples in each chamber (one with freezing medium and one with pure water) do not lack liquids + the free samples = ones not being tested (old ones) have to be maintained the same as the tested ones, check if they do not lack freezing medium + check the recording of temperature changes
DAY 94 (56 cycles)	Take samples out during the period when freezing temp is above 10°C (most convenient between 15-24°C) For chamber 1 : best time is in the morning hours For chamber 2: best time is in the afternoon hours → But check the computer screen for the actual temp Prepare small aluminum bowls + give them same mark as sample name + record the weight of the bowls Wash off scaled material in bigger bowl + collect scale material in smaller bowl Dry surface of sample (if any scales are on the towel, add them to small bowl) Place bowl in dryer + when dry pour new freezing medium with thickness of 3 mm on testing surface + cover with plastic This was the last collecting of scaled materials: Measure the area of the tested surface from glue to glue (measure each dimension three times and state the average of side A and B) Note if there is any unusual damage (for ex: extensive scaling + leakage under rubber insulation) Leave the samples out of the chamber and replace them with old samples to maintain the same condition in the freezing chamber Check if ref the two reference samples in each chamber (one with freezing medium and one with pure water) do not lack liquids + the free samples = ones not being tested (old ones) have to be maintained the same as the tested ones, check if they do not lack freezing medium

	+ check the recording of temperature changes
DAY 95/96	Weigh aluminum bowl with scaled material (record weight to nearest 0,1 g + place in card box file under next testing date)

CO2 curing (C)

DAY 0	Make concrete + perform fresh concrete tests + make testing molds
DAY 1	Demold after 24 h + place in 100% RH chamber
DAY 7	Move to 65 % RH chamber
DAY 21	Cut cube in three slices (50 mm) , clean surface with water and brush, mark samples + return to 65 % RH chamber
DAY 25	Fit samples in plastic boxes + insulate with glue + return to 65 % RH chamber
DAY 28	Place in 1% CO2 for 7 days
DAY 35	Move samples to room with laboratory condition + deionized water + cover with plastic + load by a wooden board
DAY 38	Check if samples are water tight (no leakages trough edges) → in case there is leakage, fix it and then return to the 65% RH chamber and after three days move the samples again and repeat the process When there is no leakage: Pour away deionized water + dry surface + place sample in polystyrene insulation box + cut overlapping plastic box frame with scissors (little bit shorter than polystyrene box) + mark sample in different places + pour freezing medium + cover with plastic cover + place in freezing chamber (freeze chamber always has to be full so place some old samples with new samples which are about to be tested) + prepare test report sheet
Testing period starts (testing after 7, 14, 28, 42, 56 cycles)	
DAY 45 (7 cycles)	Take samples out during the period when freezing temp is above 10°C (most convenient between 15-24°C) For chamber 1 : best time is in the morning hours For chamber 2: best time is in the afternoon hours → But check the computer screen for the actual temp Prepare small aluminum bowls + give them same mark as sample name + record the weight of the bowls Wash off scaled material in bigger bowl + collect scale material in smaller bowl Dry surface of sample (if any scales are on the towel, add them to small bowl) Place bowl in dryer + when dry pour new freezing medium with thickness of 3 mm on testing surface + cover with plastic Return sample to freezing chamber Check if ref the two reference samples in each chamber (one with freezing medium and one with pure water) do not lack liquids + the free samples = ones not being tested (old ones) have to be maintained the same as the tested ones, check if they do not lack freezing medium + check the recording of temperature changes

DAY 46	Weigh aluminum bowl with scaled material (record weight to nearest 0,1 g + place in card box file under next testing date)
DAY 51	Check if ref the two reference samples in each chamber (one with freezing medium and one with pure water) do not lack liquids + the free samples = ones not being tested (old ones) have to be maintained the same as the tested ones, check if they do not lack freezing medium + check the recording of temperature changes
DAY 59 (14 cycles)	Take samples out during the period when freezing temp is above 10°C (most convenient between 15-24°C) For chamber 1 : best time is in the morning hours For chamber 2: best time is in the afternoon hours → But check the computer screen for the actual temp Prepare small aluminum bowls + give them same mark as sample name + record the weight of the bowls Wash off scaled material in bigger bowl + collect scale material in smaller bowl Dry surface of sample (if any scales are on the towel, add them to small bowl) Place bowl in dryer + when dry pour new freezing medium with thickness of 3 mm on testing surface + cover with plastic Return sample to freezing chamber Check if ref the two reference samples in each chamber (one with freezing medium and one with pure water) do not lack liquids + the free samples = ones not being tested (old ones) have to be maintained the same as the tested ones, check if they do not lack freezing medium + check the recording of temperature changes
DAY 60	Weigh aluminum bowl with scaled material (record weight to nearest 0,1 g + place in card box file under next testing date)
DAY 66	Check if ref the two reference samples in each chamber (one with freezing medium and one with pure water) do not lack liquids + the free samples = ones not being tested (old ones) have to be maintained the same as the tested ones, check if they do not lack freezing medium + check the recording of temperature changes
DAY 73 (28 cycles)	Take samples out during the period when freezing temp is above 10°C (most convenient between 15-24°C) For chamber 1 : best time is in the morning hours For chamber 2: best time is in the afternoon hours → But check the computer screen for the actual temp Prepare small aluminum bowls + give them same mark as sample name + record the weight of the bowls Wash off scaled material in bigger bowl + collect scale material in smaller bowl Dry surface of sample (if any scales are on the towel, add them to small bowl) Place bowl in dryer + when dry pour new freezing medium with thickness of 3 mm on testing surface + cover with plastic Return sample to freezing chamber Check if ref the two reference samples in each chamber (one with freezing medium and one with pure water) do not lack liquids + the free samples = ones not being tested (old ones) have to be maintained the same as the tested ones, check if they do not lack freezing medium + check the recording of temperature changes
DAY 74	Weigh aluminum bowl with scaled material (record weight to nearest 0,1 g + place in card box file under next testing date)

DAY 80	Check if ref the two reference samples in each chamber (one with freezing medium and one with pure water) do not lack liquids + the free samples = ones not being tested (old ones) have to be maintained the same as the tested ones, check if they do not lack freezing medium + check the recording of temperature changes
DAY 87 (42 cycles)	Take samples out during the period when freezing temp is above 10°C (most convenient between 15-24°C) For chamber 1 : best time is in the morning hours For chamber 2: best time is in the afternoon hours → But check the computer screen for the actual temp Prepare small aluminum bowls + give them same mark as sample name + record the weight of the bowls Wash off scaled material in bigger bowl + collect scale material in smaller bowl Dry surface of sample (if any scales are on the towel, add them to small bowl) Place bowl in dryer + when dry pour new freezing medium with thickness of 3 mm on testing surface + cover with plastic Return sample to freezing chamber Check if ref the two reference samples in each chamber (one with freezing medium and one with pure water) do not lack liquids + the free samples = ones not being tested (old ones) have to be maintained the same as the tested ones, check if they do not lack freezing medium + check the recording of temperature changes
DAY 88	Weigh aluminum bowl with scaled material (record weight to nearest 0,1 g + place in card box file under next testing date)
DAY 94	Check if ref the two reference samples in each chamber (one with freezing medium and one with pure water) do not lack liquids + the free samples = ones not being tested (old ones) have to be maintained the same as the tested ones, check if they do not lack freezing medium + check the recording of temperature changes
DAY 101 (56 cycles)	Take samples out during the period when freezing temp is above 10°C (most convenient between 15-24°C) For chamber 1 : best time is in the morning hours For chamber 2: best time is in the afternoon hours → But check the computer screen for the actual temp Prepare small aluminum bowls + give them same mark as sample name + record the weight of the bowls Wash off scaled material in bigger bowl + collect scale material in smaller bowl Dry surface of sample (if any scales are on the towel, add them to small bowl) Place bowl in dryer + when dry pour new freezing medium with thickness of 3 mm on testing surface + cover with plastic This was the last collecting of scaled materials: Measure the area of the tested surface from glue to glue (measure each dimension three times and state the average of side A and B) Note if there is any unusual damage (for ex: extensive scaling + leakage under rubber insulation) Leave the samples out of the chamber and replace them with old samples to maintain the same condition in the freezing chamber Check if ref the two reference samples in each chamber (one with freezing medium and one with pure water) do not lack liquids + the free samples = ones not being tested (old ones) have to be maintained the same as the tested ones, check if they do not lack freezing medium

	+ check the recording of temperature changes
DAY 102	Weigh aluminum bowl with scaled material (record weight to nearest 0,1 g + place in card box file under next testing date)

Extra curing (E)

DAY 0	Make concrete + perform fresh concrete tests + make testing molds
DAY 1	Demold after 24 h + place in 100% RH chamber
DAY 7	Move to 65 % RH chamber
DAY 21	Cut cube in three slices (50 mm) , clean surface with water and brush, mark samples + return to 65 % RH chamber
DAY 25	Fit samples in plastic boxes + insulate with glue + return to 65 % RH chamber
DAY 28	Place in 1% CO2 for 7 days
DAY 42	Move samples to room with laboratory condition + deionized water + cover with plastic + load by a wooden board
DAY 45	Check if samples are water tight (no leakages trough edges) → in case there is leakage, fix it and then return to the 65% RH chamber and after three days move the samples again and repeat the process When there is no leakage: Pour away deionized water + dry surface + place sample in polystyrene insulation box + cut overlapping plastic box frame with scissors (little bit shorter than polystyrene box) + mark sample in different places + pour freezing medium + cover with plastic cover + place in freezing chamber (freeze chamber always has to be full so place some old samples with new samples which are about to be tested) + prepare test report sheet
Testing period starts (testing after 7, 14, 28, 42, 56 cycles)	
DAY 52 (7 cycles)	Take samples out during the period when freezing temp is above 10°C (most convenient between 15-24°C) For chamber 1 : best time is in the morning hours For chamber 2: best time is in the afternoon hours → But check the computer screen for the actual temp Prepare small aluminum bowls + give them same mark as sample name + record the weight of the bowls Wash off scaled material in bigger bowl + collect scale material in smaller bowl Dry surface of sample (if any scales are on the towel, add them to small bowl) Place bowl in dryer + when dry pour new freezing medium with thickness of 3 mm on testing surface + cover with plastic Return sample to freezing chamber Check if ref the two reference samples in each chamber (one with freezing medium and one with pure water) do not lack liquids + the free samples = ones not being tested (old ones) have to be maintained the same as the tested ones, check if they do not lack freezing medium

	+ check the recording of temperature changes
DAY 53	Weigh aluminum bowl with scaled material (record weight to nearest 0,1 g + place in card box file under next testing date)
DAY 59	Check if ref the two reference samples in each chamber (one with freezing medium and one with pure water) do not lack liquids + the free samples = ones not being tested (old ones) have to be maintained the same as the tested ones, check if they do not lack freezing medium + check the recording of temperature changes
DAY 66 (14 cycles)	Take samples out during the period when freezing temp is above 10°C (most convenient between 15-24°C) For chamber 1 : best time is in the morning hours For chamber 2: best time is in the afternoon hours → But check the computer screen for the actual temp Prepare small aluminum bowls + give them same mark as sample name + record the weight of the bowls Wash off scaled material in bigger bowl + collect scale material in smaller bowl Dry surface of sample (if any scales are on the towel, add them to small bowl) Place bowl in dryer + when dry pour new freezing medium with thickness of 3 mm on testing surface + cover with plastic Return sample to freezing chamber Check if ref the two reference samples in each chamber (one with freezing medium and one with pure water) do not lack liquids + the free samples = ones not being tested (old ones) have to be maintained the same as the tested ones, check if they do not lack freezing medium + check the recording of temperature changes
DAY 67	Weigh aluminum bowl with scaled material (record weight to nearest 0,1 g + place in card box file under next testing date)
DAY 73	Check if ref the two reference samples in each chamber (one with freezing medium and one with pure water) do not lack liquids + the free samples = ones not being tested (old ones) have to be maintained the same as the tested ones, check if they do not lack freezing medium + check the recording of temperature changes
DAY 80 (28 cycles)	Take samples out during the period when freezing temp is above 10°C (most convenient between 15-24°C) For chamber 1 : best time is in the morning hours For chamber 2: best time is in the afternoon hours → But check the computer screen for the actual temp Prepare small aluminum bowls + give them same mark as sample name + record the weight of the bowls Wash off scaled material in bigger bowl + collect scale material in smaller bowl Dry surface of sample (if any scales are on the towel, add them to small bowl) Place bowl in dryer + when dry pour new freezing medium with thickness of 3 mm on testing surface + cover with plastic Return sample to freezing chamber Check if ref the two reference samples in each chamber (one with freezing medium and one with pure water) do not lack liquids + the free samples = ones not being tested (old ones) have to be maintained the same as the tested ones, check if they do not lack freezing medium + check the recording of temperature changes

DAY 81	Weigh aluminum bowl with scaled material (record weight to nearest 0,1 g + place in card box file under next testing date)
DAY 87	Check if ref the two reference samples in each chamber (one with freezing medium and one with pure water) do not lack liquids + the free samples = ones not being tested (old ones) have to be maintained the same as the tested ones, check if they do not lack freezing medium + check the recording of temperature changes
DAY 94 (42 cycles)	<p>Take samples out during the period when freezing temp is above 10°C (most convenient between 15-24°C)</p> <p>For chamber 1 : best time is in the morning hours For chamber 2: best time is in the afternoon hours</p> <p>→ But check the computer screen for the actual temp</p> <p>Prepare small aluminum bowls + give them same mark as sample name + record the weight of the bowls</p> <p>Wash off scaled material in bigger bowl + collect scale material in smaller bowl</p> <p>Dry surface of sample (if any scales are on the towel, add them to small bowl)</p> <p>Place bowl in dryer + when dry pour new freezing medium with thickness of 3 mm on testing surface + cover with plastic</p> <p>Return sample to freezing chamber</p> <p>Check if ref the two reference samples in each chamber (one with freezing medium and one with pure water) do not lack liquids + the free samples = ones not being tested (old ones) have to be maintained the same as the tested ones, check if they do not lack freezing medium + check the recording of temperature changes</p>
DAY 95	Weigh aluminum bowl with scaled material (record weight to nearest 0,1 g + place in card box file under next testing date)
DAY 101	Check if ref the two reference samples in each chamber (one with freezing medium and one with pure water) do not lack liquids + the free samples = ones not being tested (old ones) have to be maintained the same as the tested ones, check if they do not lack freezing medium + check the recording of temperature changes
DAY 108 (56 cycles)	<p>Take samples out during the period when freezing temp is above 10°C (most convenient between 15-24°C)</p> <p>For chamber 1 : best time is in the morning hours For chamber 2: best time is in the afternoon hours</p> <p>→ But check the computer screen for the actual temp</p> <p>Prepare small aluminum bowls + give them same mark as sample name + record the weight of the bowls</p> <p>Wash off scaled material in bigger bowl + collect scale material in smaller bowl</p> <p>Dry surface of sample (if any scales are on the towel, add them to small bowl)</p> <p>Place bowl in dryer + when dry pour new freezing medium with thickness of 3 mm on testing surface + cover with plastic</p> <p>This was the last collecting of scaled materials:</p> <p>Measure the area of the tested surface from glue to glue (measure each dimension three times and state the average of side A and B)</p> <p>Note if there is any unusual damage (for ex: extensive scaling + leakage under rubber insulation)</p> <p>Leave the samples out of the chamber and replace them with old samples to maintain the same condition in the freezing chamber</p>

	Check if ref the two reference samples in each chamber (one with freezing medium and one with pure water) do not lack liquids + the free samples = ones not being tested (old ones) have to be maintained the same as the tested ones, check if they do not lack freezing medium + check the recording of temperature changes
DAY 109	Weigh aluminum bowl with scaled material (record weight to nearest 0,1 g + place in card box file under next testing date)

Timeline compressive strength testing

DAY 0	Make concrete + Fresh concrete test
DAY 1	Demold + curing in water 20+-2°C until testing
DAY 2	Test compressive strength at 2 days
DAY 28	Test compressive strength at 28 days
DAY 56	Test compressive strength at 56 days

Timeline chloride migration testing

DAY 0	Make concrete + fresh concrete tests
DAY 28	Place sample between a chloride free and a chloride containing alkaline solution and an electric voltage is applied between two external electrodes to drive the chloride ions into the concrete specimen. After a certain amount of time the specimen is split and then the penetration depth of the chlorides is determined by using a color indicator solution. The chloride migration coefficient is calculated based on the measured depth of penetration, the magnitude of the applied voltage and other parameters.
DAY 56	Place sample between a chloride free and a chloride containing alkaline solution and an electric voltage is applied between two external electrodes to drive the chloride ions into the concrete specimen. After a certain amount of time the specimen is split and then the penetration depth of the chlorides is determined by using a color indicator solution. The chloride migration coefficient is calculated based on the measured depth of penetration, the magnitude of the applied voltage and other parameters.

Appendices

Calendar plan:

Ref mix, M 18/6-360, M 18/6-300, M 25/10-360

Chloride migration: CM, freeze-thaw: FT, compressive strength: CS

Fresh concrete tests: FC

MONDAY 29/01	TUESDAY 30/01	WEDNESDAY 31/01	THURSDAY 1/02	FRIDAY 2/02	SATURDAY 3/02	SUNDAY 4/02
			ARRIVAL	Guided tour of the lab		

MONDAY 5/02	TUESDAY 6/02	WEDNESDAY 7/02	THURSDAY 8/02	FRIDAY 9/02	SATURDAY 10/02	SUNDAY 11/02
Mix 1 made (failed) Too much water	Mix 2 made (failed)	Mix made: air measurement system doesn't work = mix failed	Wait till air measurement system is fixed	Wait till air measurement system is fixed		

MONDAY 12/02	TUESDAY 13/02	WEDNESDAY 14/02	THURSDAY 15/02	FRIDAY 16/02	SATURDAY 17/02	SUNDAY 18/02
Dry the aggregates	MIX REF + FC Dry the aggregates	DAY 1:FT DAY 1: CS MIX 1+FC	DAY 2:CS DAY 1:FT DAY 1:CS	DAY 2:CS		Dry the aggregates

MONDAY 19/02	TUESDAY 20/02	WEDNESDAY 21/02	THURSDAY 22/02	FRIDAY 23/02	SATURDAY 24/02	SUNDAY 25/02
MIX 2+FC	DAY 7: FT DAY 1:FT DAY 1:CS MIX 3+ FC	DAY 7:FT DAY 2:CS DAY 1:FT DAY 1: CS	DAY 2: CS			

MONDAY 26/02	TUESDAY 27/02	WEDNESDAY 28/02	THURSDAY 29/02	FRIDAY 1/03	SATURDAY 2/03	SUNDAY 3/03
DAY 7:FT (N)	DAY 7:FT (N)					

MONDAY 4/03	TUESDAY 5/03	WEDNESDAY 6/03	THURSDAY 7/03	FRIDAY 8/03	SATURDAY 9/03	SUNDAY 10/03
	DAY 21: FT N DAY 21: FT C DAY 21 FT E	DAY 21:FT N DAY 21: FT C DAY 21 FT E			DAY 25: FT N DAY 25: FT C DAY 25 FT E	DAY 25:FT N DAY 25: FT C DAY 25 FT E

Appendices

MONDAY 11/03	TUESDAY 12/03	WEDNESDAY 13/03	THURSDAY 14/03	FRIDAY 15/03	SATURDAY 16/03	SUNDAY 17/03
DAY 21: FT N DAY 21 FT C DAY 21 FT E	DAY 28: FT N DAY 28 FT E DAY 28 FT C DAY 28: CS DAY 28: CM DAY 21: FT N DAY 21 FT C DAY 21 FT E	DAY 28: FT N DAY 28 FT E DAY 28 FT C DAY 28: CS DAY 28: CM		DAY 31: FT N DAY 25 FT C DAY 25 FT E DAY 25 FT N	DAY 31: FT N DAY 25 FT C DAY 25 FT E DAY 25 FT N	

MONDAY 18/03	TUESDAY 19/03	WEDNESDAY 20/03	THURSDAY 21/03	FRIDAY 22/03	SATURDAY 23/03	SUNDAY 24/03
DAY 28: FT N DAY 28 FT C DAY 28: CS DAY 28: CM DAY 28 FT E	DAY 28: FT N DAY 28: FT C DAY 28 FT E DAY 28: CS DAY 28: CM DAY 35 FT C	DAY 35 FT C	DAY 31: FT N	DAY 38: FT N DAY 38 FT C DAY 31: FT N	DAY 39: FT N DAY 38: FT N DAY 38: FT C	DAY 39: FT N

MONDAY 25/03	TUESDAY 26/03	WEDNESDAY 27/03	THURSDAY 28/03	FRIDAY 29/03	SATURDAY 30/03	SUNDAY 31/03
DAY 35 FT C	DAY 35 FT C DAY 42 FT E	DAY 42 FT E	DAY 38: FT N DAY 38 FT C	DAY 45: FT N DAY 45 FT E DAY 45 FT C DAY 39: FT N DAY 38: FT N DAY 38 FT C	DAY 45: FT N DAY 45 FT E DAY 45: FT C DAY 39: FT N DAY 46 FT C	DAY 46 FT C

MONDAY 1/04	TUESDAY 2/04	WEDNESDAY 3/04	THURSDAY 4/04	FRIDAY 5/04	SATURDAY 6/04	SUNDAY 7/04
DAY 42 FT E	DAY 42 FT E		DAY 51 FT C DAY 45: FT N DAY 45 FT C DAY 45 FT E	DAY 51 FT C DAY 52: FT N DAY 52 FT E DAY 45: FT N DAY 45 FT C DAY 45 FT E DAY 46 FT C	DAY 53: FT N DAY 53 FT E DAY 52: FT N DAY 52 FT E DAY 46 FT C	DAY 53: FT N DAY 53 FT E

MONDAY 8/04	TUESDAY 9/04	WEDNESDAY 10/04	THURSDAY 11/04	FRIDAY 12/04	SATURDAY 13/04	SUNDAY 14/04
	DAY 56: CS DAY 56: CM	DAY 56: CS DAY 56: CM DAY 51 FT C	DAY 52: FT N DAY 52 FT E DAY 51 FT C	DAY 59: FT N DAY 59 FT C DAY 59 FT E DAY 53: FT N DAY 53 FT E DAY 52: FT N DAY 52 FT E	DAY 59: FT N DAY 59 FT C DAY 59 FT E DAY 53: FT N DAY 53 FT E DAY 60 FT C	DAY 60: FT C

Appendices

MONDAY 15/04	TUESDAY 16/04	WEDNESDAY 17/04	THURSDAY 18/04	FRIDAY 19/04	SATURDAY 20/04	SUNDAY 21/04
DAY 56:CS DAY 56:CM	DAY 56:CS DAY 56:CM		DAY 59:FT N DAY 59 FT E DAY 59 FT C	DAY 66: FT N DAY 66: FT C DAY 66 FT E DAY 59:FT N DAY 59 FT C DAY 59 FT E DAY 60 FT C	DAY 67: FT N DAY 67 FT E DAY 66:FT N DAY 66 FT C DAY 66 FT E DAY 60 FT C	DAY 67:FT N DAY 67 FT E

MONDAY 22/04	TUESDAY 23/04	WEDNESDAY 24/04	THURSDAY 25/04	FRIDAY 26/04	SATURDAY 27/04	SUNDAY 28/04
			DAY 66:FT N DAY 66 FT C DAY 66 FT E	DAY 73: FT N DAY 73 FT C DAY 73 FT E DAY 67:FT N DAY 67 FT E DAY 66:FT N DAY 66 FT C DAY 66 FT E	DAY 73:FT N DAY 73: FT C DAY 73 FT E DAY 67:FT N DAY 67 FT E DAY 74 FT C	DAY 74:FT C

MONDAY 29/04	TUESDAY 30/04	WEDNESDAY 1/05	THURSDAY 2/05	FRIDAY 3/05	SATURDAY 4/05	SUNDAY 5/05
			DAY 73:FT N DAY 73 FT C DAY 73 FT E	DAY 80: FT N DAY 80 FT E DAY 80 FT C DAY 73:FT N DAY 73 FT C DAY 73 FT E	DAY 81: FT N DAY 81 FT E DAY 80 FT C DAY 80:FT N DAY 80 FT E DAY 74 FT C	DAY 81: FT N DAY 81 FT E

MONDAY 6/05	TUESDAY 7/05	WEDNESDAY 8/05	THURSDAY 9/05	FRIDAY 10/05	SATURDAY 11/05	SUNDAY 12/05
			DAY 80:FT N DAY 80 FT C DAY 80 FT E	DAY 87: FT N DAY 87 FT C DAY 87 FT E DAY 81:FT N DAY 81 FT E DAY 80:FT N DAY 80 FT C DAY 80 FT E	DAY 87:FT N DAY 87 FT C DAY 87 FT E DAY 81:FT N DAY 81 FT E DAY 88 FT C	DAY 88 FT C

MONDAY 13/05	TUESDAY 14/05	WEDNESDAY 15/05	THURSDAY 16/05	FRIDAY 17/05	SATURDAY 18/05	SUNDAY 19/05
			DAY 87:FT N DAY 87 FT C DAY 87 FT E	DAY 94: FT N DAY 94 FT C DAY 94 FT E DAY 87:FT N DAY 87 FT C DAY 87 FT E DAY 88 FT C	DAY 95:FT N DAY 95 FT E DAY 94:FT N DAY 94 FT E DAY 94 FT C DAY 88 FT C	DAY 95:FT N DAY 95 FT E

Appendices



MONDAY 20/05	TUESDAY 21/05	WEDNESDAY 22/05	THURSDAY 23/05	FRIDAY 24/05	SATURDAY 25/05	SUNDAY 26/05
			DAY 94: FT N DAY 94 FT C DAY 94 FT E	DAY 95:FT N DAY 95 FT E DAY 94: FT N DAY 94 FT C DAY 94 FT E DAY 101 FT C DAY 101 FT E	DAY 95:FT N DAY 95 FT E DAY 101 FT C DAY 101 FT E DAY 102 FT C	DAY 102 FT C

MONDAY 27/05	TUESDAY 28/05	WEDNESDAY 29/05	THURSDAY 30/05	FRIDAY 31/05	SATURDAY 1/06	SUNDAY 2/06
			DAY 101 FT C DAY 101 FT E	DAY 101 FT C DAY 101 FT E DAY 102 FT C DAY 108 FT E	DAY 102 FT C DAY 109 FT E DAY 108 FT E	DAY 109 FT E

MONDAY 3/06	TUESDAY 4/06	WEDNESDAY 5/06	THURSDAY 6/06	FRIDAY 7/06	SATURDAY 8/06	SUNDAY 9/06
			DAY 108 FT E	DAY 108 FT E DAY 109 FT E HAND IN THESIS	DAY 109 FT E	

B Technical data sheets

B.1 VPI

				
REPORT ON QUALITY TEST				
Customer:	Johan M Dalene		Your ref.:	3-23
Date received:	10.01.2023		Our ref.:	LZ-2023-0001
Sample Marked:	ZeroCarbCon - Uttak og analyse av VPI, parti 1 Big Bag nr.1 Dunk nr. 1 VPI = 90% D50 6µm 21.11.2022			
Parameter:	Results:			Method:
CHEMICAL COMPOSITION				
Chemical Parameters				
Sulfur Trioxide-IR	SO ₃	0.04	%	PD1752
Loss On Ignition	LOI	0.00	%	EN196-2
XRF Analysis				
Silica Oxide	SiO ₂	47.42	%	EN196-2
Aluminium Oxide	Al ₂ O ₃	13.35	%	EN196-2
Ferric Oxide	Fe ₂ O ₃	12.32	%	EN196-2
Calcium Oxide	CaO	10.98	%	EN196-2
Potassium Oxide	K ₂ O	0.409	%	EN196-2
Sodium Oxide	Na ₂ O	1.883	%	EN196-2
Magnesium Oxide	MgO	11.29	%	EN196-2
Titanium Dioxide	TiO ₂	1.660	%	EN196-2
Phosphorous Pentoxide	P ₂ O ₅	0.193	%	EN196-2
Manganic Oxide	Mn ₂ O ₃	0.210	%	EN196-2
Chloride	Cl	0.017	%	EN196-2
Sodium Oxide Equivalent	Na ₂ O Eq.	2.15	%	EN196-2
TECHNICAL PARAMETERS				
Fineness				
Specific surface, Blaine		686	m ² /kg	EN196-6
Specific Weight		2.98	g/cm ³	PD1777
Particle Size Distribution				
Sieve Passing	<24 µm	95.6	%	PD1749
Sieve Passing	<30 µm	98.7	%	PD1749
Sieve Residue	>64 µm	0.0	%	PD1749
Sieve Residue	>90 µm	0.0	%	PD1749
Quantile d(50)	d(0.50)	7.1	µm	PD1749
Quantile d(95)	d(0.95)	23.4	µm	PD1749
 Laboratory Manager				
Brevik, Cement and Concrete Laboratory,		12.03.2024		

B.2 CEM I

PRODUCT DATA SHEET

Anleggsement

CEM I 52.5 N

Last revision January 2023

The cement satisfies the requirements according to NS-EN 197-1:2011 for Portland cement CEM I 52.5 N.

Properties		Declared values	Requirements according to NS-EN 197-1:2011
Fineness (Blaine m ² /kg)		415	
Specific weight (kg/dm ³)		3.14	
Soundness (mm)		1	≤ 10
Initial setting time (min)		120	≥ 45
Compressive strength (MPa)	1 day	21	
	2 days	33	≥ 20
	7 days	49	
	28 days	63	≥ 52.5
Sulfate (% SO ₃)		≤ 4.0	≤ 4.0
Chloride (% Cl ⁻)		≤ 0.07	≤ 0.10
Water soluble chromium (ppm Cr ⁶⁺)		≤ 2	≤ 2 ¹
Alkalis (% Na ₂ O _{eq})		0.6	
Clinker (%)		96	95-100
Minor additional constituents (%)		4	0-5

1. According to EU regulation REACH Annex XVII point 47 Chromium VI compounds

NORCEM
HEIDELBERGCEMENT Group

Norcem AS, Postboks 142, Lilleaker, 0216 Oslo
Tlf. 22 87 84 00 firmapost@norcem.no www.norcem.no

B.3 CEM II



Produktdatablad

STANDARDSEMENT FA justert

CEM II/B-M (V-L) 42,5 R

Sist revidert september 2023

Sementen tilfredsstiller kravene i NS-EN 197-1:2011 til Portland blandingssement CEM II/B-M (V-L) 42,5 R.

Egenskap		Deklarerte data	Krav ifølge NS-EN 197-1:2011
Finhet (Blaine m ² /kg)		470	
Spesifikk vekt (kg/dm ³)		3,00	
Volumbestandighet (mm)		1	≤ 10
Begynnende styrking (min)		150	≥ 60
Trykkfasthet (MPa)	1 døgn	19	
	2 døgn	29	≥ 20
	7 døgn	40	
	28 døgn	53	≥ 42,5 ≤ 62,5
Sulfat (% SO ₃)		≤ 4	≤ 4
Klorid (% Cl ⁻)		≤ 0,085	≤ 0,10
Vannløselig krom (ppm Cr ⁶⁺)		≤ 2	≤ 2 ¹
Alkalier (% Na ₂ O _{equiv})		1,2	
Klinker (%)		78	65-79
Flygeaske (%)		13	21-35
Kalksteinsfiller (%)		9	

1. I henhold til EU forordning REACH Vedlegg XVII punkt 47 krom VI-forbindelser.

Heidelberg Materials

P.b. 143 Lilleaker, N-0216 Oslo

www.sement.heidelbergmaterials.no

B.4 Dynamon SX-23



PRODUCT DESCRIPTION

Dynamon SX-23 is a very effective superplasticizing admixture based on modified acrylic polymers. The product is part of the **Dynamon System**. This system is based on DPP technology (Designed Performance Polymers) developed by Mapei, where the properties of the admixtures are custom built for different kinds of concrete. The **Dynamon System** is developed from Mapei's own composition and production of monomers.

APPLICATION AREAS

Dynamon SX-23 is specially designed for ready-mix concrete production and can be used to increase the workability for all types of concrete and/or reduce water consumption.

Some special areas of application

- Watertight concrete that requires high or very high strength and strict requirement to concrete durability in aggressive environments.
- Concrete with high workability requirements.
- Self-compacting concrete with somewhat longer open times. If necessary, this type of concrete can be stabilised with a viscosity enhancing admixture, such as **Viscofluid** or **Viscostar**.
- Frost resistant concrete – in combination with an air entraining agent like **Mapeair**. The type of air entraining is chosen based on the properties of the other ingredients.
- Concrete for flooring to create a more pliable concrete with greater workability. High dosages of the product and low temperatures can lead to a certain retardation of the concrete.

Dynamon SX-23 differs greatly from superplasticizing admixtures based on sulphonated melamines and naphthalenes, as well as from first-generation acrylic-based polymers – by having a higher water-reducing effect and a longer open time. The necessary dosage to achieve the desired workability/water reduction will be significantly lower when using **Dynamon SX-23**, than with older types of superplasticizing admixtures.

The time of dosing **Dynamon SX-23** is not so important, but the shortest mixing time is generally obtained when adding **Dynamon SX-23** after at least 80 % of the mixing water is added. It is advisable to do some preliminary testing to obtain optimal utilization of the mixing equipment.

PROPERTIES

Dynamon SX-23 is a water soluble product of active acrylic polymers that effectively disperses cement within the mixture.

This effect can be utilised in three ways:

1. To reduce the amount of mixing water, but at the same time maintain the concrete workability. Lower w/c ratio gives increased strength, reduced permeability and improved durability.
2. To increase workability compared to concrete with the same w/c ratio. The strength remains the same but ease of placement is improved.



3. To reduce both the water and the cement without altering the mechanical strength. Through this method it is possible to reduce costs (less cement), shrinkage (less water) and also the risk of temperature gradients due to the lower heat of hydration. This last effect is particularly important for concrete containing a high percentage of cement.

COMPATIBILITY WITH OTHER PRODUCTS

Dynamon SX-23 can be combined with Mapei's other concrete additives, for example accelerators like **Mapefast** and setting retardants like **Mapetard**.
The product can also be combined with air entraining agents for production of frost-resistant concrete, **Mapeair** products. Selecting the type needed is done based on the properties of the other ingredients.
When combining products, it is recommended that testing is done to obtain the desired effect in the mixture. You may also contact our technical department.

DOSAGE

Dynamon SX-23 is added to achieve the desired effect, strength, durability, workability and cement reduction by varying its dosage between 0.3 and 2.0 % of the amount of cement + fly ash + microsilica.
Higher dosages increase the concrete's open time, which means the time where the concrete can be worked. A higher dosage and a lower concrete temperature will cause some retardation.
Test mixtures using the selected parameters are always recommended.

PACKAGING

Dynamon SX-23 is available in 25 liter cans, 200 liter drums, 1000 liter IBC tanks and in tank.

STORAGE

Dynamon SX-23 must be stored at temperatures between +8 and +35°C, and will retain its properties for at least 12 months when stored unopened in original packaging. If the product is exposed to direct sunlight, colour variation may occur, but this will not affect the technical properties of the product.

SAFETY INSTRUCTIONS FOR PREPARATION AND INSTALLATION

Instructions for the safe use of our products can be found on the latest version of the SDS available from our website www.mapei.no

PRODUCT FOR PROFESSIONAL USE.

TECHNICAL DATA (typical values)

PRODUCT IDENTITY	
Appearance:	liquid
Colour:	yellow-brown
Viscosity:	low viscosity; <30 mPa·s
Solids content (%):	23.0 ± 1.1
Density (g/cm ³):	1.05 ± 0.02
pH:	6 ± 1
Chloride content (%):	< 0.05
Alkali content (Na ₂ O-equivalents) (%):	< 2.0



WARNING

Although the technical details and recommendations contained in this product data sheet correspond to the best of our knowledge and experience, all the above - information must, in every case, be taken as merely indicative and subject to confirmation after long-term practical application: for this reason, anyone who intends to use the product must ensure beforehand that it is suitable for the envisaged application: in every case, the user alone is fully responsible for any consequences deriving from the use of the product.

Please refer to the current version of the technical data sheet, available from our web site www.mapei.no

LEGAL NOTICE

The contents of this Technical Data Sheet ("TDS") may be copied into another project-related document, but the resulting document shall not supplement or replace requirements per the TDS in effect at the time of the MAPEI product installation. For the most up-to-date TDS and warranty information, please visit our website at www.mapei.no

ANY ALTERATIONS TO THE WORDING OR REQUIREMENTS CONTAINED IN OR DERIVED FROM THIS TDS SHALL VOID ALL RELATED MAPEI WARRANTIES.

6874-7-2017-gb

Any reproduction of texts, photos and illustrations published here is prohibited and subject to prosecution



B.5 Mapei air



AREA OF USE

Mapeair® 25 is a surface active agent which promotes the formation of small air bubbles and is used to improve the frost resistance of concrete and mortar.

Mapeair® 25 also gives improved workability and reduces the risk of segregation. The product is usually used in combination with MAPEI's plasticising or superplasticising admixtures.

Mapeair® 25 is based on synthetic tensides and tall oil derivatives.

TECHNICAL CHARACTERISTICS

Concrete always contains a certain amount of air (1 - 3 %). In order to meet the usual requirements of 4 - 6 % air in fresh concrete, **Mapeair® 25** is added, which produces smaller and more evenly distributed air bubbles, which leads to improved freeze-thaw resistance.

Air introduced during mixing is transformed into small evenly distributed pores in the presence of **Mapeair® 25**. The measured pore volume and spacing factor in hardened concrete is given in the technical data. These entrained air bubbles also improve the workability and reduce the amount of water required. Increased air content leads generally to a decrease in compressive strength. A general guide is that 1% of air reduces the compressive strength by 5%. This is partly compensated for by the reduced need for water and by adding plasticising and/or superplasticising admixtures.

Mapeair® 25 will also improve stability during transportation by reducing the risk of segregation for concrete containing a low volume of fine particles and actively preventing bleeding (transportation of water to the surface of fresh concrete).

WORKING INSTRUCTIONS

Mapeair® 25 is delivered ready for use and can be added directly into the mixer. To obtain an even distribution of air from batch to batch, it is important that **Mapeair® 25** is added at the same stage of the mixing procedure each time. The dosage required to give the desired air content varies with aggregates, cement type and quantity present. Other additives may also have an influence. It is important that the addition of **Mapeair® 25** is determined by trial mixing and that the air content in the fresh concrete is checked regularly.

DOSAGE

0.05 - 0.5 kg % weight of cement. As the quantity of **Mapeair® 25** used is usually small, dilution with water is an advantage. Use 1 part **Mapeair® 25** to 9 or 19 parts water for a more reliable dosage. The product dissolves easily in water. Stir before use to ensure a homogenous mixture.

ATTENTION

Variations in other components in the concrete can greatly influence the formation of air bubbles in concrete. In some cases duration of transport and transportation equipment used can produce variations in air content. If the mixing time has been too short the total measured air content may increase from production to delivery, whereas in most cases a



reduction of air content is observed. Normally this reduction is the result of the release of larger, undesirable air bubbles. The producer must therefore base his calculations on experience with the particular constituents used.

PACKAGING

Mapecair® 25 is available in 25 liter cans, 200 liter drums, 1000 liter IBC tanks and in tank.

STORAGE

The product must be stored at temperatures between +8°C and +35°C, and will retain its properties for at least one year if stored unopened in its original packaging. If the product is exposed to direct sunlight, colour variation may occur, but this will not affect the technical properties of the product.

SAFETY INSTRUCTIONS FOR PREPARATION AND INSTALLATION

Instructions for the safe use of our products can be found on the latest version of the SDS available from our website www.mapei.no

PRODUCT FOR PROFESSIONAL USE.

TECHNICAL DATA (typical values)

PRODUCT IDENTITY	
Type:	liquid
Colour:	pale yellow/brown
Viscosity:	low viscosity < 10 mPa·S
Solid content, (%):	6
Density, (g/cm ³):	1.00 ± 0.02
pH:	9.0 ± 1
Chloride content, (%):	≤ 0.05
Alkali content (Na ₂ O-equivalent), (%):	≤ 1.0
CHARACTERISTICS OF CONCRETE CONTAINING MAPEAIR® 25:	
Volume of air in concrete mixture EN 12350-7:	6 % at dosage 0.05 % weight of cement (reference 2.2 %)
Spacing factor in hardened concrete, EN 480-11 (mm):	0.190 (requirement < 0.200)
Specific surface, EN 480-11, (mm ² /mm ³):	25.2 (requirement > 25)
Frost resistance (scaling) – EN 12390-9 (kg/m ²):	0.05 (best classification < 0.1: excellent)

WARNING

Although the technical details and recommendations contained in this product data sheet correspond to the best of our knowledge and experience, all the above - information must, in every case, be taken as merely indicative and subject to confirmation after long-term practical application: for this reason, anyone who intends to use the product must ensure beforehand that it is suitable for the envisaged application: in every case, the user alone is fully responsible for any consequences deriving from the use of the product.

Please refer to the current version of the technical data sheet, available from our web site www.mapei.no

LEGAL NOTICE

The contents of this Technical Data Sheet ("TDS") may be copied into another project-related document, but the resulting document shall not supplement or replace requirements per the TDS in effect at the time of the MAPEI product installation. For the most up-to-date TDS and warranty information, please visit our website at www.mapei.no

ANY ALTERATIONS TO THE WORDING OR REQUIREMENTS CONTAINED IN OR DERIVED FROM THIS TDS SHALL VOID ALL RELATED MAPEI WARRANTIES.



C Full mix design for 1 m³ concrete

	REF-360	M18/6-360	M18/6-300	M25/10-360
W/B ratio	0.40	0.40	0.47	0.42
W/C ratio	0.48	0.47	0.55	0.54

BINDER CONTENT								
	[kg/m ³]	[w%]	[kg/m ³]	[w%]	[kg/m ³]	[w%]	[kg/m ³]	[w%]
CEM I	0	0	287	79.8	239	79.8	246	68.2
CEM II	360	100	0	0	0	0	0	0
LP	0	0	8	2.2	7	2.2	24	6.8
VPI	0	0	65	18	54	18	90	25
Total SCM content	86.4	24	86.5	24	72.2	24	125.6	35
Total binder materials	360	100	360	100	300	100	360	100

AGGREGATES CONTENT								
	[kg/m ³]	[w%]	[kg/m ³]	[w%]	[kg/m ³]	[w%]	[kg/m ³]	[w%]
BS sand 0-8mm	849	49.0	856	49.0	891	49.0	861	49.0
RB agg 8-22mm	808	43.0	814	43.0	840	43.0	811	43.0
Crushed 4-8mm	148	8.00	149	8.00	152	8.00	147	8.00

ADDITIVES CONTENT				
	[kg/m ³]	[kg/m ³]	[kg/m ³]	[kg/m ³]
Dinamon SX-32	4.32	4.80	3.60	4.32
Mapei Air	0.14	0.14	0.16	0.14

WATER CONTENT				
	[kg/m ³]	[kg/m ³]	[kg/m ³]	[kg/m ³]
Free water	143	136	132	132

D W/C-ratio and W/B ratio calculations

The formulas for the W/B ratio and the W/C ratio are the following:

$$wbr = \frac{W}{(C + k * A)} \qquad wcr = \frac{W}{C}$$

With:

wbr	Water/binder-ratio
W	Free water [kg/m ³]
C	Cement [kg/m ³]
k	k-value
A	Additional binder [kg/m ³]

With:

wcr	Water/cement-ratio
W	Free water [kg/m ³]
C	Cement [kg/m ³]

According to EN-206 the k-values for the used materials are the following:

Name of binder	k-value
Norcem CEM I	1
Norcem CEM II	1
LP	0.3
VPI	0.7

The calculations for REF-360 are the following:

W/C factor

$$wcr = \frac{W}{C} = \frac{143}{295} = 0.48$$

Note: the cement content equals: binder – FA content

W/B factor

$$wbr = \frac{W}{(C + k * A)} = \frac{143}{(287 * 1)} = 0.40$$

The calculations for M18/6-360 are the following:

W/C factor

$$wcr = \frac{W}{C} = \frac{136}{287} = 0.47$$

W/B factor

$$wbr = \frac{W}{(C + k * A)} = \frac{136}{(287 + 0.3 * 8 + 0.7 * 65)} = 0.40$$

The calculations for M18/6-300 are the following:

W/C factor

$$wcr = \frac{W}{C} = \frac{132}{239} = 0.55$$

W/B factor

$$wbr = \frac{W}{(C + k * A)} = \frac{132}{(239 + 0.3 * 7 + 0.7 * 54)} = 0.47$$

The calculations for M18/6-300 are the following:


W/C factor

$$wcr = \frac{W}{C} = \frac{132}{246} = 0.54$$

W/B factor

$$wbr = \frac{W}{(C + k * A)} = \frac{132}{(246 + 0.3 * 24 + 0.7 * 90)} = 0.42$$

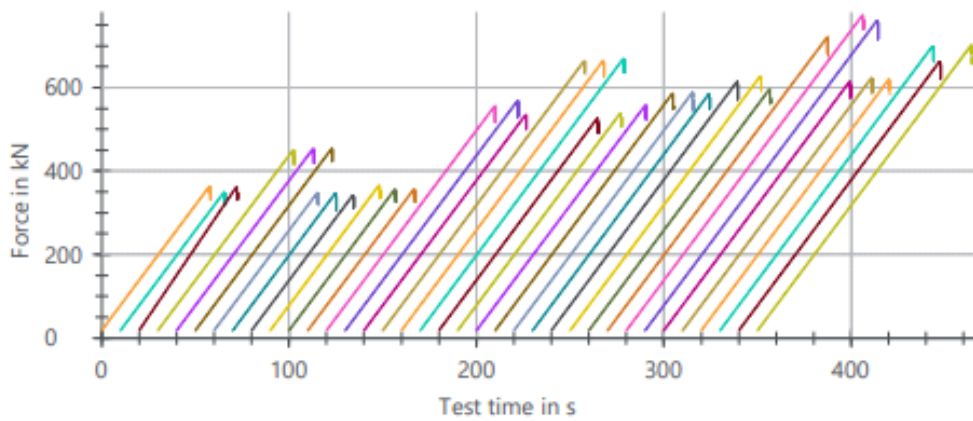
E Compressive strength results

	Print date: 25.04.24
Test report	
Test report :	Customer :
Tester :	Test standard : EN196
Test speed : 0.6 N/mm ² s	
Test results:	

Legend	No.	Date/Clock time	ID	S ₀ mm ²	h mm	m g	ρ g/cm ³	F _{max} kN	σ _m MPa
	1	15/02/2024 12:59:51	A-ref mix-2d	10007.00	104.0	2432	2.3362	363.03	36.28
	2	15/02/2024 13:06:48	B-ref mix-2d	9981.00	103.0	2411	2.3449	348.14	34.88
	3	15/02/2024 13:10:48	C-ref mix-2d	9985.00	103.9	2422	2.3351	361.08	36.16
	4	16/02/2024 14:13:11	A-mix 1-2d	9983.01	100.1	2390	2.3903	449.55	45.03
	6	16/02/2024 14:18:41	B-mix 1-2d	9973.02	100.6	2384	2.3769	452.63	45.39
	7	16/02/2024 14:25:01	C-mix 1-2d	9980.01	104.8	2498	2.3878	452.28	45.32
	8	21/02/2024 12:52:52	A-mix 2-2d	9984.01	102.5	2431	2.3757	346.86	34.74
	9	21/02/2024 12:58:06	B-mix 2-2d	10010.99	101.9	2427	2.3788	345.32	34.49
	10	21/02/2024 13:07:29	C-mix 2-2d	9994.99	102.9	2463	2.3943	341.16	34.13
	11	22/02/2024 10:39:18	A-mix 3-2d	9988.00	102.3	2409	2.3572	364.53	36.50
	12	22/02/2024 10:43:57	B-mix 3-2d	9980.01	102.0	2382	2.3402	355.04	35.57
	13	22/02/2024 10:47:44	C-mix 3-2d	9964.03	101.2	2385	2.3660	355.46	35.67
	14	12/03/2024 11:20:12	D-ref mix-28d	9988.00	103.0	2415	2.3474	554.99	55.57
	15	12/03/2024 11:25:31	E-ref mix-28d	9981.01	103.6	2415	2.3346	567.62	56.87
	16	12/03/2024 11:30:52	F-ref mix-28d	9990.40	105.6	2407	2.2809	534.27	53.48
	17	13/03/2024 11:03:02	D-mix 1-28d	10016.69	106.0	2478	2.3346	663.35	66.22
	18	13/03/2024 11:07:55	E-mix 1-28d	10021.00	103.6	2442	2.3532	663.81	66.24
	19	13/03/2024 11:12:59	F-mix 1-28d	10021.00	104.9	2487	2.3660	668.81	66.74
	20	18/03/2024 10:12:10	D-mix 2-28d	10033.03	101.0	2423	2.3908	525.43	52.37
	21	18/03/2024 10:17:17	E-mix 2-28d	10000.00	103.8	2499	2.4075	538.41	53.84
	22	18/03/2024 10:21:22	F-mix 2-28d	9982.01	103.8	2487	2.4003	556.96	55.80
	23	19/03/2024 12:09:41	D-mix 3-28d	10009.70	99.8	2358	2.3618	585.18	58.46
	24	19/03/2024 12:14:31	E-mix 3-28d	9983.01	103.4	2426	2.3497	587.88	58.89
	25	19/03/2024 12:18:52	F-mix 3-28d	10046.05	100.6	2394	2.3691	584.06	58.14
	26	09/04/2024 14:49:41	G-REF mix-56d	10031.99	103.6	2413	2.3225	613.29	61.13
	27	09/04/2024 14:55:28	H-REF mix-56d	10009.00	105.4	2469	2.3393	626.73	62.62
	28	09/04/2024 15:00:59	I-REF mix-56d	9998.00	102.9	2421	2.3525	595.77	59.59
	29	10/04/2024 13:15:41	G-MIX 1-56d	9997.00	101.0	2382	2.3582	720.91	72.11
	30	10/04/2024 13:20:47	H-MIX 1-56d	9993.00	105.2	2455	2.3365	772.51	77.31
	31	10/04/2024 13:26:31	I-MIX 1-56d	10002.00	102.8	2442	2.3755	760.28	76.01
	32	15/04/2024 13:00:35	G-MIX 2-56d	10028.02	101.3	2439	2.4019	613.44	61.17
	33	15/04/2024 13:05:27	H-MIX 2-56d	10010.00	102.1	2452	2.3978	622.57	62.19
	34	15/04/2024 13:18:08	I-MIX 2-56d	10023.01	100.2	2404	2.3942	618.70	61.73
	35	16/04/2024 12:16:52	G-MIX 3-56d	10020.01	102.6	2434	2.3668	698.64	69.72
	36	16/04/2024 12:21:40	H-MIX 3-56d	10028.02	100.8	2385	2.3588	662.15	66.03
	37	16/04/2024 12:35:45	I-MIX 3-56d	9996.00	102.2	2411	2.3614	700.82	70.11

$\epsilon_{b,03}$			$\epsilon_{b,03}$			$\epsilon_{b,03}$			$\epsilon_{b,03}$		
Legend	No.	%	Legend	No.	%	Legend	No.	%	Legend	No.	%
	1	-		11	-		20	-		29	-
	2	-		12	-		21	-		30	-
	3	-		13	-		22	-		31	-
	4	-		14	-		23	-		32	-
	6	-		15	-		24	-		33	-
	7	-		16	-		25	-		34	-
	8	-		17	-		26	-		35	-
	9	-		18	-		27	-		36	-
	10	-		19	-		28	-		37	-

Series graph:



Statistics:

Series	ρ	F_{max}
$n = 36$	g/cm^3	kN
\bar{x}	2.3623	543.66
s	0.0269	133.91
V [%]	1.14	24.63

F Chloride migration results

Prove	Slopt	Testlet	Diameter (mm)	Height L(mm)	Voltage V(volts)	I _{0-30V} (mA)	T1 (°C)	Duration time (h)	I ₀ (mA)	Tf (°C)	Chloride penetration depth (mm)							Average	Dissm (Stcm/Sec)	Average Dism (Stcm/Sec)	Age days	Std	CoV	Notes	
											1	2	3	4	5	6	7								
A, ref			100.07	50.1	30	59.0	22.5	24	52.0	24.3	23.3	23.5	23.1	24.3	22.4	25.6	22.8	23.56	23.40	11,04201012	10.18	28	0.80	7.83	REF (28d) A
B, ref		28d	100.2	51.3	30	57.0	22.2	24	50.0	24.5	22.7	19.3	22.7	20.6	21.9	20.3	19.9	21.05	23.35	10.01					REF (28d) B
C, ref			99.81	50.8	30	49.0	22.2	24	44.0	24.3	20.1	19.4	22.4	20.3	20.2	19.8	19.2	20.19	23.25	9.47					REF (28d) C
A, M1			100.3	50.7	25	52.0	22.5	25	47.0	23.9	20.1	18.6	15.9	17.1	21.3	17.4	21.7	18.87	23.20	10.13					MIX 1 (28d) A
B, M1		28d	100.04	50.4	25	51.0	22.2	25	48.0	23.8	21.7	21.2	21.3	20.7	19.0	22.4	20.7	21.02	23.00	11.30					MIX 1 (28d) B
C, M1			99.85	50.0	25	51.0	22.1	25	49.0	24.0	19.4	22.7	17.7	18.7	16.4	17.4	20.9	19.02	23.05	10.09					MIX 1 (28d) C
A, M2			100.34	50.7	25	55.0	20.6	24	54.0	23.5	18.3	21.5	19.6	21.4	19.4	22.2	21.9	20.59	22.05	11.56					MIX 2 (28d) A
B, M2		28d	99.76	50.4	25	54.0	20.5	24	52.0	23.8	24.5	22.5	22.0	21.5	24.3	21.1	23.3	22.74	22.15	12.79					MIX 2 (28d) B
C, M2			100.39	50.3	25	47.0	20.6	24	43.0	23.5	22.1	21.0	22.3	25.0	20.9	20.5	19.0	21.52	22.05	12.02					MIX 2 (28d) C
A, M3			100.19	50.0	30	59.0	21.7	24	52.0	24.0	21.3	18.0	19.9	19.6	19.2	15.9	20.9	19.25	22.85	8.87					MIX 3 (28d) A
B, M3		28d	99.63	50.4	30	57.0	21.5	24	50.0	23.6	18.5	18.7	16.5	18.2	15.4	17.6	16.4	17.16	22.55	7.89					MIX 3 (28d) B
C, M3			100.24	49.6	30	45.0	21.8	24	44.0	23.6	14.7	20.3	17.6	22.6	17.2	21.0	19.1	18.92	22.70	8.63					MIX 3 (28d) C
A, ref			100.02	50.0	35	39.0	21.8	24	36.0	23.4	18.9	17.7	13.8	17.8	16.3	21.2	14.1	17.11	22.60	6.70					REF (56d) A
B, ref		56d	100.02	50.1	35	40.0	21.6	24	37.0	23.3	13.2	11.0	11.9	15.6	17.5	10.9	14.6	13.54	22.45	5.22					REF (56d) B
C, ref			100.04	50.6	35	37.0	21.3	24	34.0	23.0	16.5	12.3	15.7	11.5	14.1	17.2	13.9	14.44	22.15	5.64					REF (56d) C
A, M1			100.46	50.2	35	50.0	20.6	24	45.0	23.3	16.4	16.0	16.7	14.6	14.3	16.9	18.8	16.23	21.95	6.34					MIX 1 (56d) A
B, M1		56d	100.12	50.3	35	43.0	20.2	24	41.0	23.5	16.2	11.7	12.6	11.3	13.7	12.4	15.0	13.28	21.85	5.12					MIX 1 (56d) B
C, M1			99.89	50.1	35	38.0	20.0	24	36.0	23.3	13.0	13.7	14.4	13.5	17.9	17.9	15.9	15.20	21.65	5.90					MIX 1 (56d) C
A, M2			100.01	50.4	30	51.0	23.4	24	44.0	23.5	15.7	14.4	13.9	16.5	14.4	14.8	13.1	14.67	23.45	6.67					
B, M2		56d	100.35	50.4	30	42.0	23.4	24	38.0	23.7	19.5	17.5	15.9	15.5	16.8	14.7	18.1	16.85	23.55	7.75					
C, M2			100.1	49.6	30	40.0	23.3	24	30.0	23.5	16.3	16.0	15.6	16.0	15.5	17.5	19.8	16.69	23.40	7.55					
A, M3			100.03	51.2	40	35	22.0	24	39.0	22.4	12.2	11.1	14.2	14.9	13.0	10.8	17.0	13.29	22.20	4.58					
B, M3		56d	100.08	50.0	40	36	21.5	24	42.0	22.4	16.7	15.3	16.1	14.5	14.1	16.2	10.1	14.69	21.95	4.98					
C, M3			100.47	50.8	40	35	21.5	24	36.0	22.3	10.9	11.4	8.7	10.2	10.8	12.8	10.1	10.69	21.90	3.59					

G F-T result graphs and tables

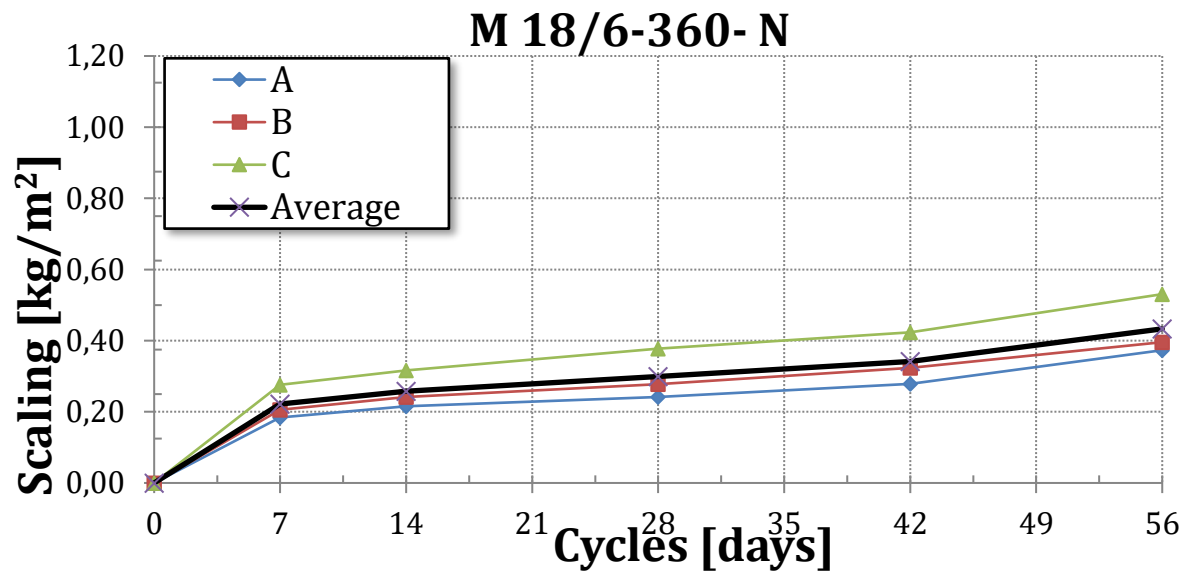
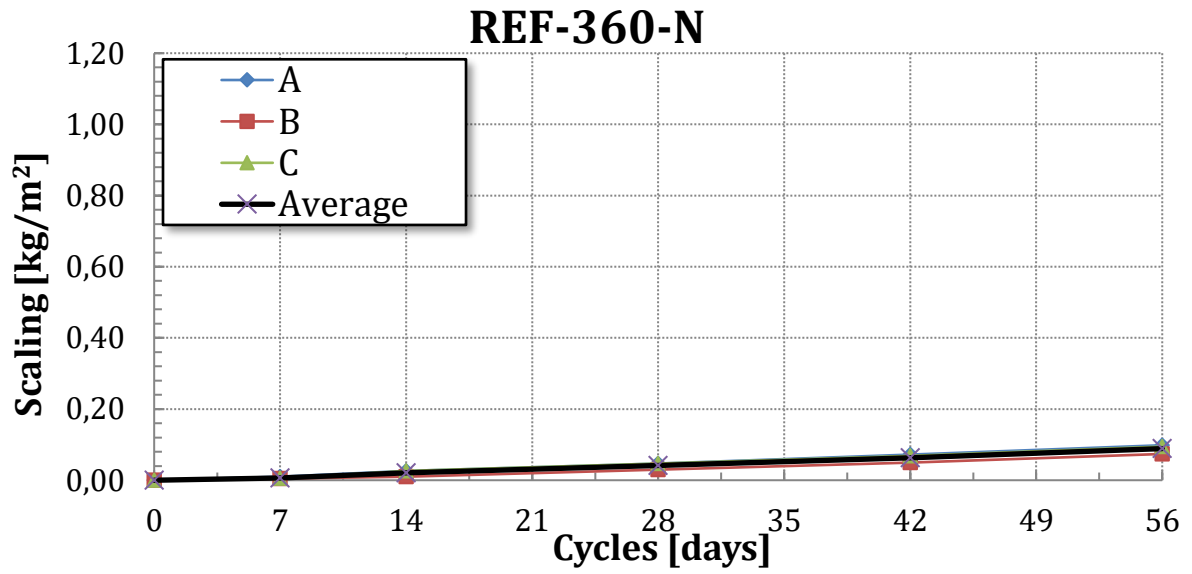
G.1 Normal curing samples

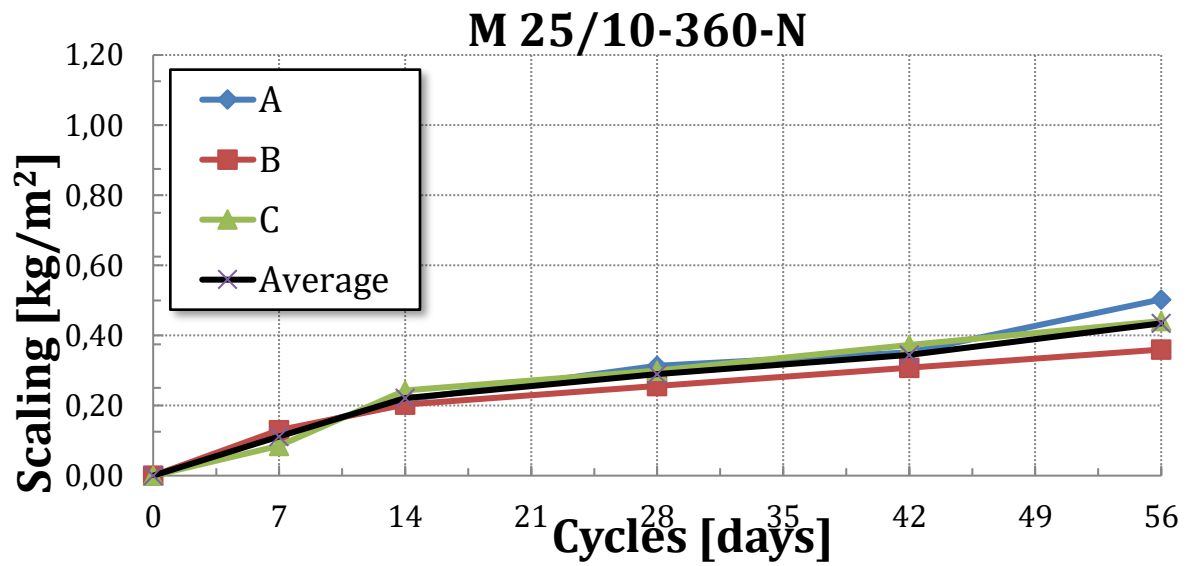
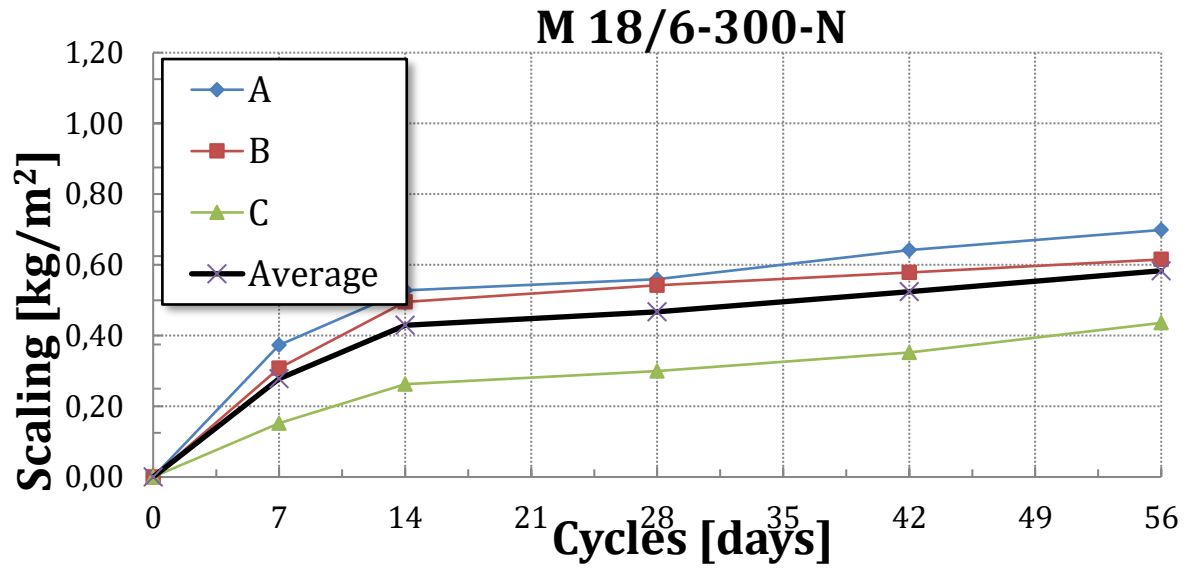
REF-360-N				
	A	B	C	Average
Length	14,0	14,5	13,7	
Width	13,8	14,0	13,9	
Area	193	203	190	
Bowl	2,9	2,9	2,9	
7d	3,1	3	3	
14d	3,4	3,1	3,4	
28d	3,8	3,5	3,8	
42d	4,3	3,9	4,2	
56d	4,8	4,4	4,7	
0	0	0	0	0
7	0,01	0,00	0,01	0,01
14	0,03	0,01	0,03	0,02
28	0,05	0,03	0,05	0,04
42	0,07	0,05	0,07	0,06
56	0,10	0,07	0,09	0,09
56d/28d	2,11	2,50	2,00	2,20

M 18/6-360-N				
	A	B	C	Average
Length	14,2	13,9	14,1	
Width	13,4	14,0	13,9	
Area	190	195	196	
Bowl				
7d	3,5	4	5,4	
14d	4,1	4,7	6,2	
28d	4,6	5,4	7,4	
42d	5,3	6,3	8,3	
56d	7,1	7,7	10,4	
0	0	0	0	0
7	0,18	0,21	0,28	0,22
14	0,22	0,24	0,32	0,26
28	0,24	0,28	0,38	0,30
42	0,28	0,32	0,42	0,34
56	0,37	0,40	0,53	0,43
56d/28d	1,54	1,43	1,41	1,46

M 18/6-300-N				
	A	B	C	Average
Length	13,9	13,7	13,7	
Width	13,9	14,0	13,9	
Area	193	192	190	
Bowl	2,9	2,9	2,9	
7d	10,1	8,8	5,8	
14d	13,1	12,4	7,9	
28d	13,7	13,3	8,6	
42d	15,3	14	9,6	
56d	16,4	14,7	11,2	
0	0	0	0	0
7	0,37	0,31	0,15	0,28
14	0,53	0,50	0,26	0,43
28	0,56	0,54	0,30	0,47
42	0,64	0,58	0,35	0,52
56	0,70	0,62	0,44	0,58
56d/28d	1,25	1,13	1,46	1,28

M 25/10-360-N				
	A	B	C	Average
Length	13,6	13,7	13,2	
Width	13,6	14,0	13,4	
Area	185	192	177	
Bowl	2,9	2,9	2,8	
7d	5,1	5,4	4,3	
14d	6,9	6,8	7,1	
28d	8,7	7,8	8,1	
42d	9,4	8,8	9,4	
56d	12,2	9,8	10,6	
0	0	0	0	0
7	0,12	0,13	0,08	0,11
14	0,22	0,20	0,24	0,22
28	0,31	0,26	0,30	0,29
42	0,35	0,31	0,37	0,34
56	0,50	0,36	0,44	0,43
56d/28d	1,60	1,41	1,47	1,49





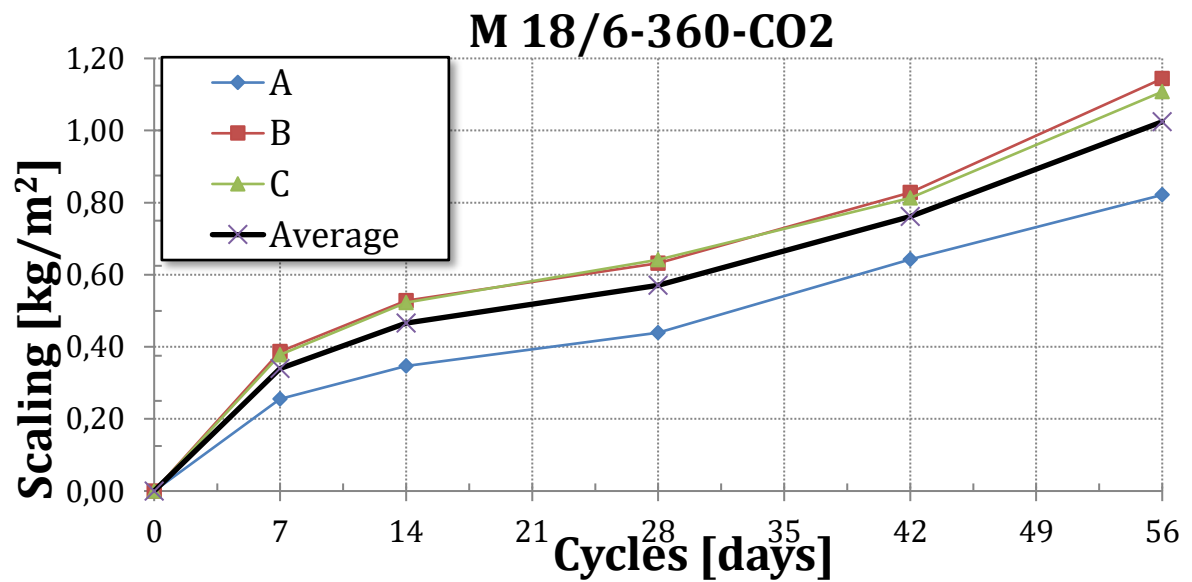
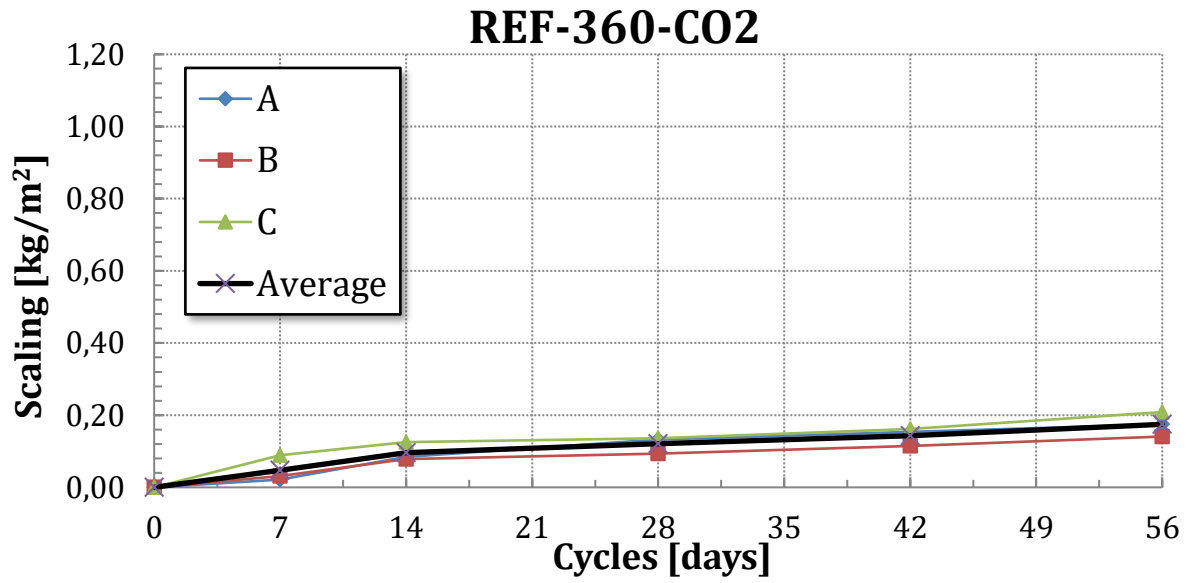
G.2 CO₂-curing samples

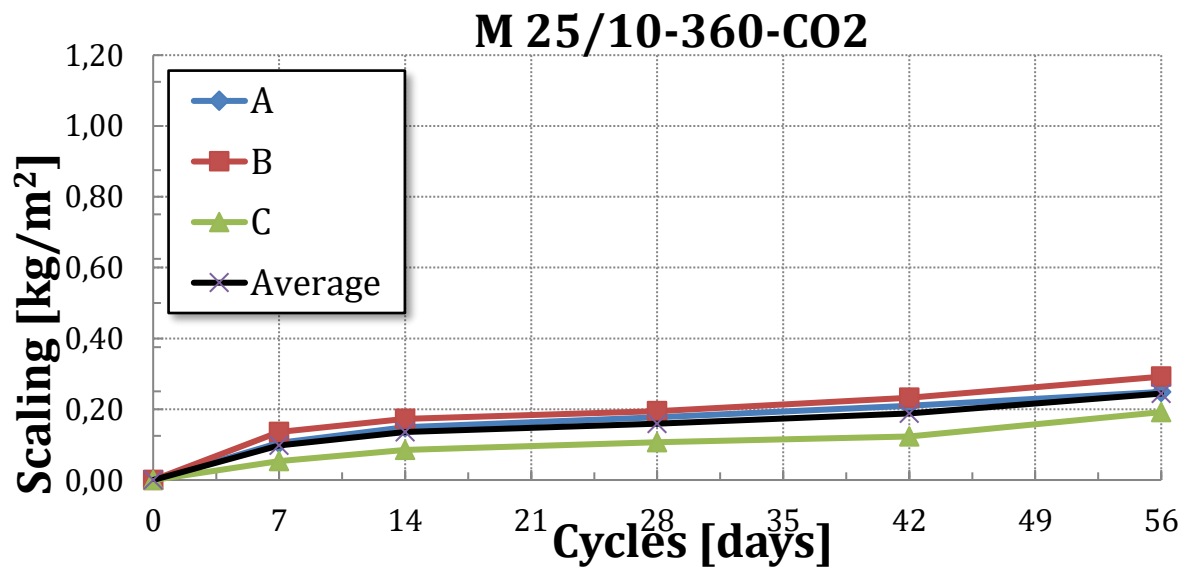
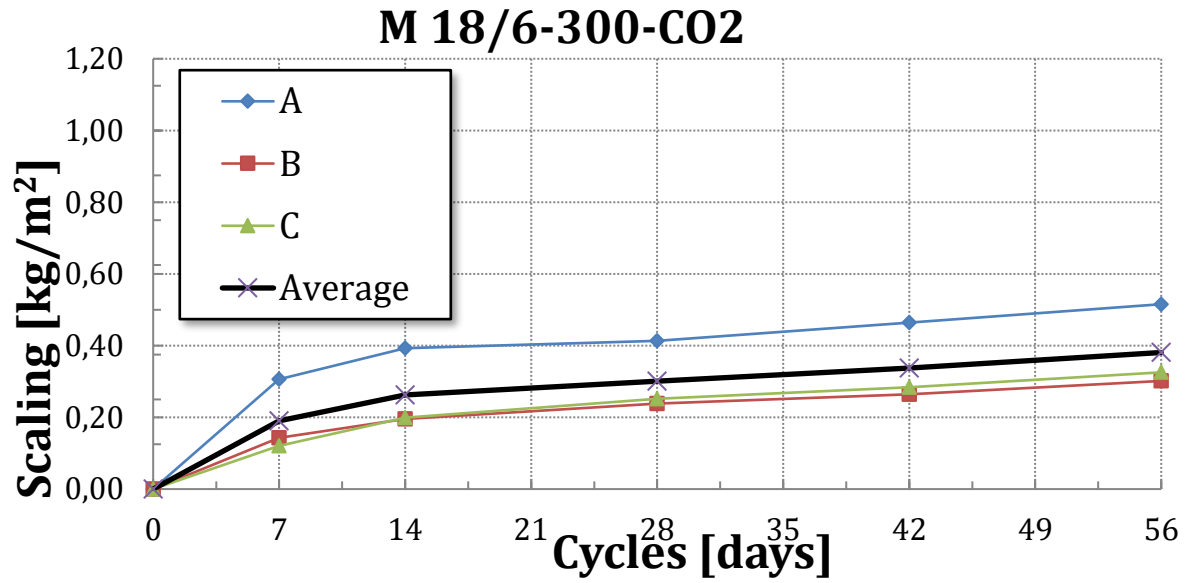
REF-360-CO ₂				
	A	B	C	Average
Length	13,6	13,7	13,7	
Width	13,9	14,0	14,0	
Area	189	192	192	
Bowl	2,8	2,8	2,9	
7d	3,2	3,4	4,6	3,7333333
14d	4,4	4,3	5,3	
28d	5,3	4,6	5,5	
42d	5,7	5	6	
56d	6,1	5,5	6,9	
0	0	0	0	0
7	0,02	0,03	0,09	0,05
14	0,08	0,08	0,13	0,10
28	0,13	0,09	0,14	0,12
42	0,15	0,11	0,16	0,14
56	0,17	0,14	0,21	0,17
56d/28d	1,32	1,50	1,54	1,45

M 18/6-360-CO ₂				
	A	B	C	Average
Length	14,0	13,6	14,0	
Width	14,0	13,5	13,8	
Area	196	184	193	
Bowl	5,8	5,7	5,8	
7d	10,8	12,8	13,1	
14d	12,6	15,4	15,9	
28d	14,4	17,3	18,2	
42d	18,4	20,9	21,5	
56d	21,9	26,7	27,2	
0	0	0	0	0
7	0,26	0,39	0,38	0,34
14	0,35	0,53	0,52	0,47
28	0,44	0,63	0,64	0,57
42	0,64	0,83	0,81	0,76
56	0,82	1,14	1,11	1,02
56d/28d	1,87	1,81	1,73	1,80

M 18/6-300-CO ₂				
	A	B	C	Average
Length	13,7	13,5	13,6	
Width	14,3	14,0	14,0	
Area	196	189	190	
Bowl	5,8	5,8	5,8	
7d	11,8	8,5	8,1	
14d	13,5	9,5	9,6	
28d	13,9	10,3	10,6	
42d	14,9	10,8	11,2	
56d	15,9	11,5	12	
0	0	0	0	0
7	0,31	0,14	0,12	0,19
14	0,39	0,20	0,20	0,26
28	0,41	0,24	0,25	0,30
42	0,46	0,26	0,28	0,34
56	0,52	0,30	0,33	0,38
56d/28d	1,25	1,27	1,29	1,27

M 25/10-360-CO ₂				
	A	B	C	Average
Length	13,4	13,7	13,6	
Width	13,5	13,5	13,8	
Area	181	185	188	
Bowl	5,8	5,8	5,7	
7d	7,7	8,3	6,7	
14d	8,5	9	7,3	
28d	9	9,4	7,7	
42d	9,6	10,1	8	
56d	10,3	11,2	9,3	
0	0	0	0	0
7	0,11	0,14	0,05	0,10
14	0,15	0,17	0,09	0,14
28	0,18	0,19	0,11	0,16
42	0,21	0,23	0,12	0,19
56	0,25	0,29	0,19	0,24
56d/28d	1,41	1,50	1,80	1,57





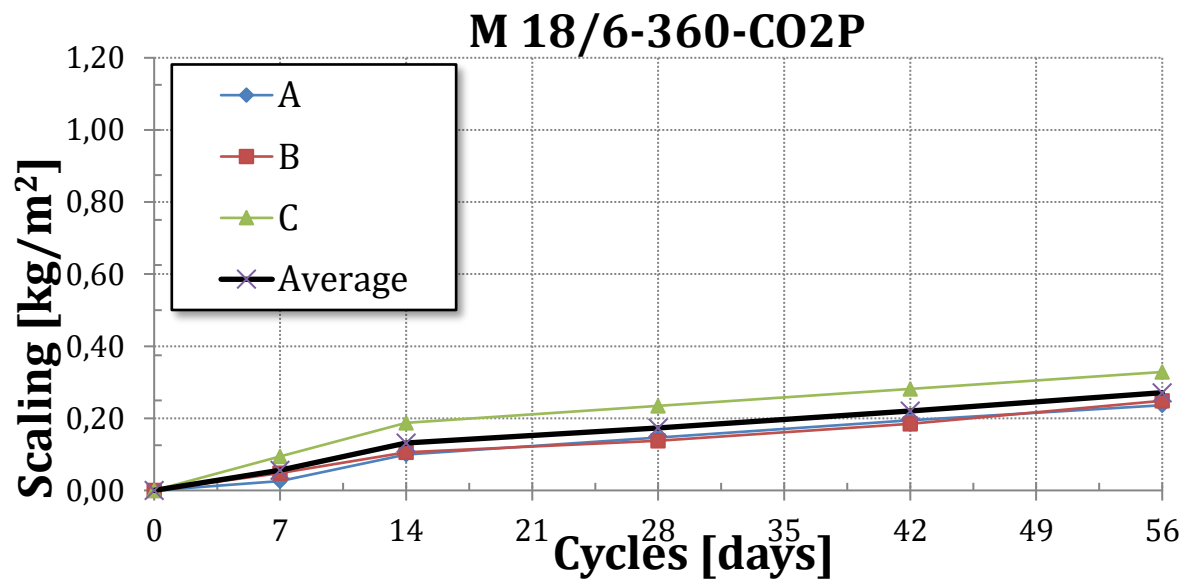
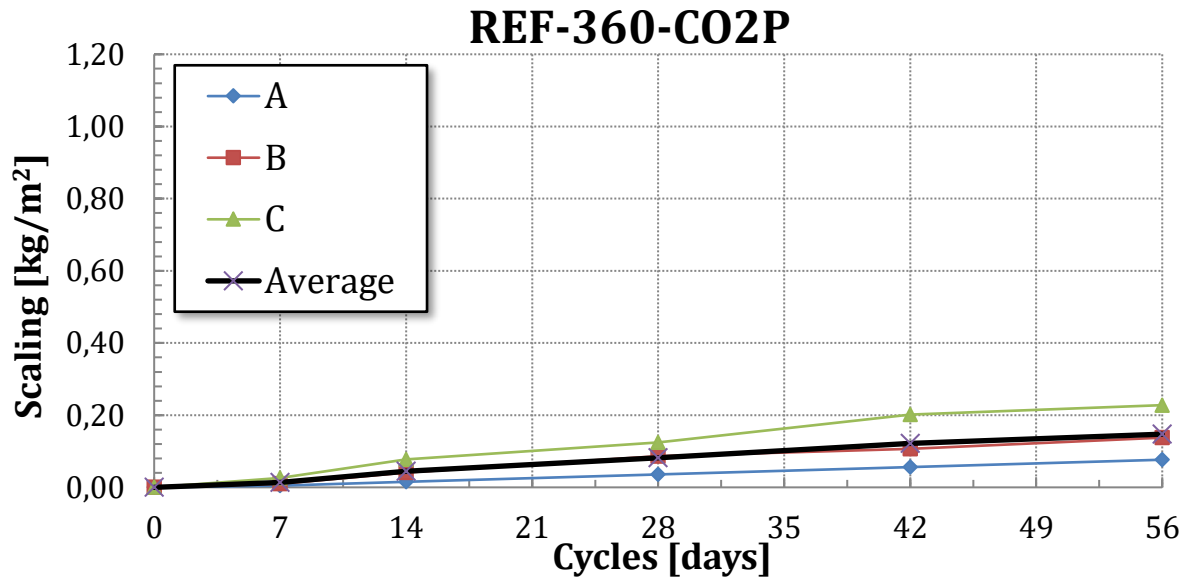
G.3 Prolonged CO₂-curing samples

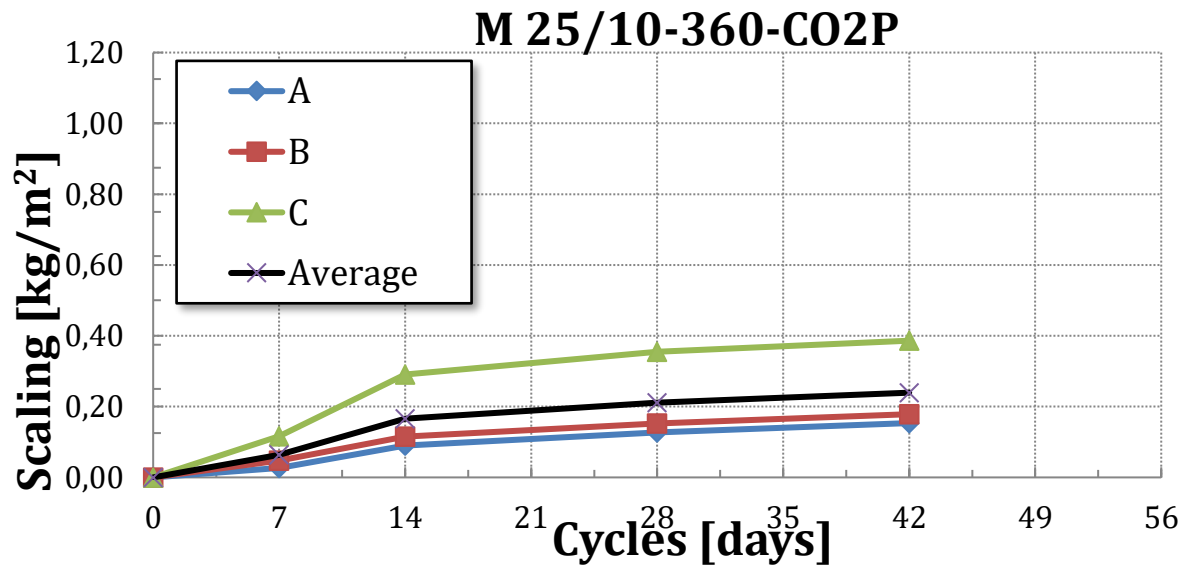
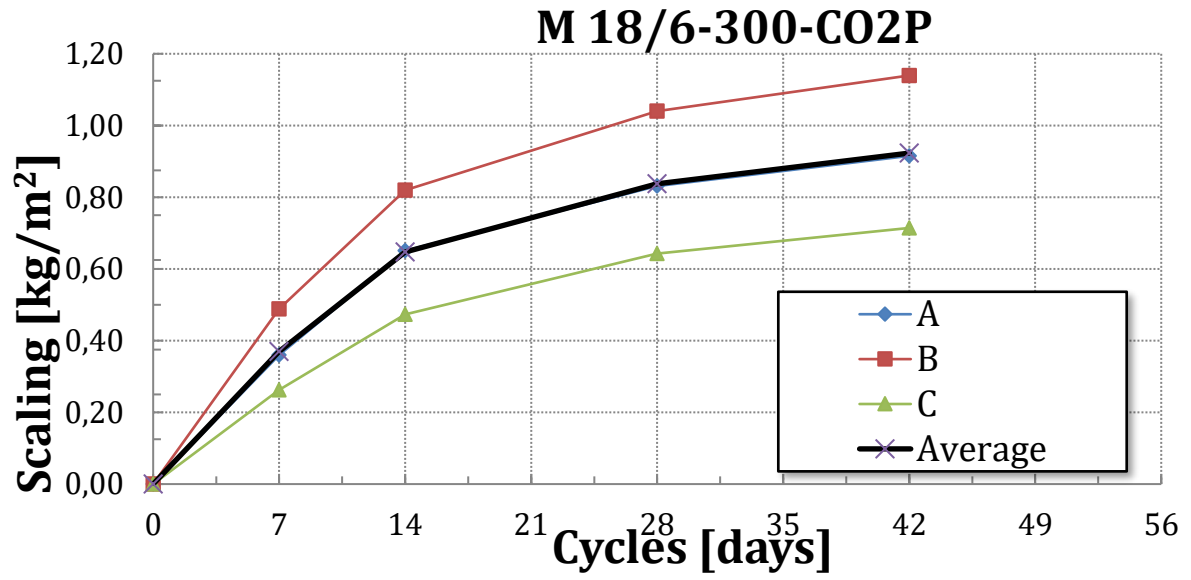
REF-360-CO2P				
	A	B	C	Average
Length	14,0	14,0	14,0	
Width	14,0	14,0	13,8	
Area	196	196	193	
Bowl	5,8	5,8	5,7	
7d	5,9	6	6,2	
14d	6,1	6,6	7,2	
28d	6,5	7,5	8,1	
42d	6,9	7,9	9,6	
56d	7,3	8,5	10,1	
0	0	0	0	0
7	0,01	0,01	0,03	0,01
14	0,02	0,04	0,08	0,04
28	0,04	0,09	0,12	0,08
42	0,06	0,11	0,20	0,12
56	0,08	0,14	0,23	0,15
56d/28d	2,14	1,59	1,83	1,85

M 18/6-360-CO2P				
	A	B	C	Average
Length	13,7	13,5	14,0	
Width	13,9	14,0	13,7	
Area	190	189	192	
Bowl	5,8	5,7	5,7	
7d	6,3	6,6	7,5	
14d	7,7	7,7	9,3	
28d	8,6	8,3	10,2	
42d	9,5	9,2	11,1	
56d	10,3	10,4	12	
0	0	0	0	0
7	0,03	0,05	0,09	0,06
14	0,10	0,11	0,19	0,13
28	0,15	0,14	0,23	0,17
42	0,19	0,19	0,28	0,22
56	0,24	0,25	0,33	0,27
56d/28d	1,61	1,81	1,40	1,60

M 18/6-300-CO2P				
	A	B	C	Average
Length	14,0	13,8	13,9	
Width	13,5	13,8	14,0	
Area	189	190	195	
Bowl	5,7	5,7	5,7	
7d	12,5	15	10,8	
14d	18	21,3	14,9	
28d	21,4	25,5	18,2	
42d	23	27,4	19,6	
56d				
0	0	0	0	0
7	0,36	0,49	0,26	0,37
14	0,65	0,82	0,47	0,65
28	0,83	1,04	0,64	0,84
42	0,92	1,14	0,71	0,92
56	-0,30	-0,30	-0,29	-0,30
56d/28d	-0,36	-0,29	-0,46	-0,37

M 25/10-360-CO2P				
	A	B	C	Average
Length	13,5	13,6	13,6	
Width	14,0	14,0	13,9	
Area	189	190	189	
Bowl	5,7	5,7	5,7	
7d	6,2	6,6	7,9	
14d	7,4	7,9	11,2	
28d	8,1	8,6	12,4	
42d	8,6	9,1	13	
56d				
0	0	0	0	0
7	0,03	0,05	0,12	0,06
14	0,09	0,12	0,29	0,17
28	0,13	0,15	0,35	0,21
42	0,15	0,18	0,39	0,24
56	-0,30	-0,30	-0,30	-0,30
56d/28d	-2,38	-1,97	-0,85	-1,73





H Pictures of F-T samples after testing

H.1 Normal curing samples



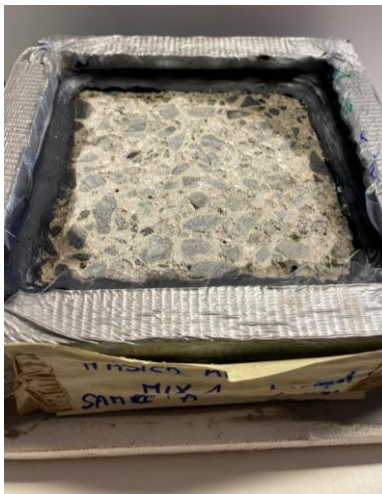
REF-360-N: Sample A-56d



REF-360-N: Sample B-56d



REF-360-N: Sample C-56d



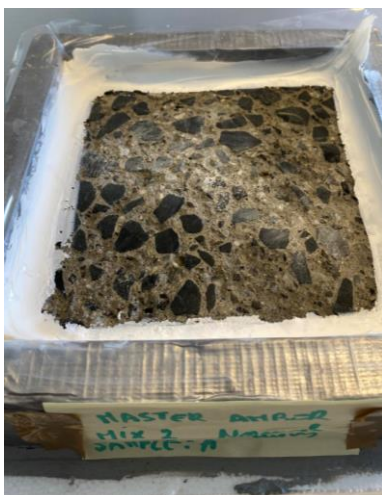
M 18/6-360-N: Sample A-56d



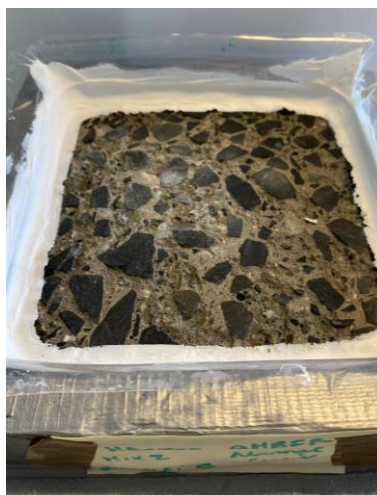
M 18/6-360-N: Sample B-56d



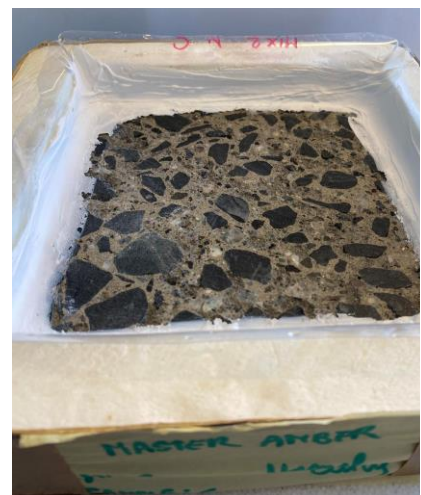
M 18/6-360-N: Sample C-56d



M 18/6-300-N: Sample A-56d



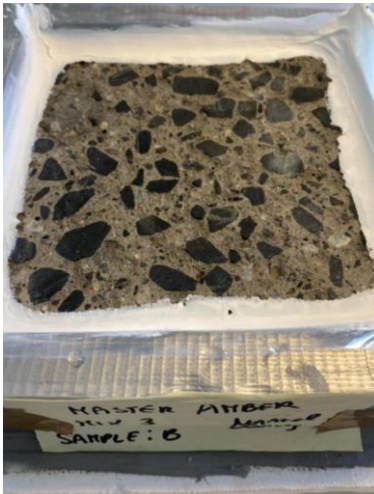
M 18/6-300-N: Sample B-56d



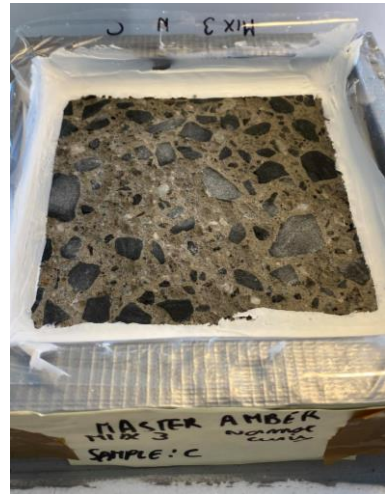
M 18/6-300-N: Sample C-56d



M 25/10-360-N: Sample A-56d



M 25/10-360-N: Sample B-56d



M 25/10-360-N: Sample C-56d

H.2 CO₂ curing samples



REF-360-CO2: Sample A-56d



REF-360-CO2: Sample B-56d



REF-360-CO2: Sample C-56d



M 18/6-360-CO2: Sample A-56d



M 18/6-360-CO2: Sample B-56d



M 18/6-360-CO2: Sample C-56d



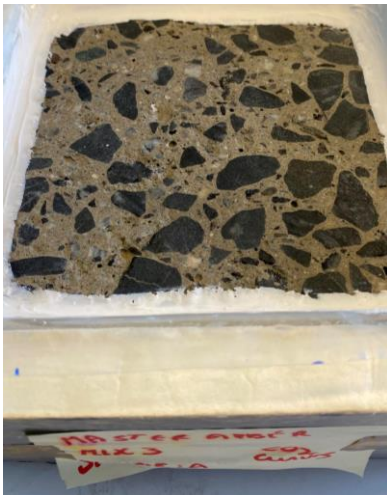
M 18/6-300-CO2: Sample A-56d



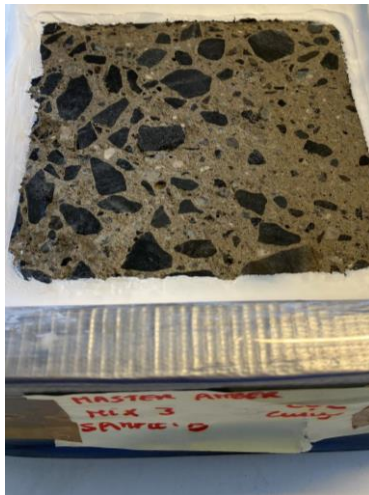
M 18/6-300-CO2: Sample B-56d



M 18/6-360-CO2: Sample C-56d



M 25/10-360-CO2: Sample A-56d



M 25/10-360-CO2: Sample B-56d



M 25/10-360-CO2: Sample B-56d

H.3 CO₂ and prolonged curing samples



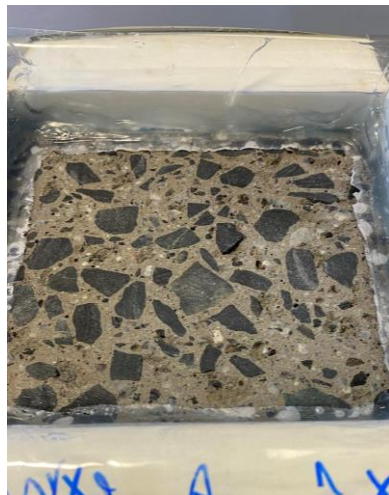
REF-360-CO₂P: Sample A-56d



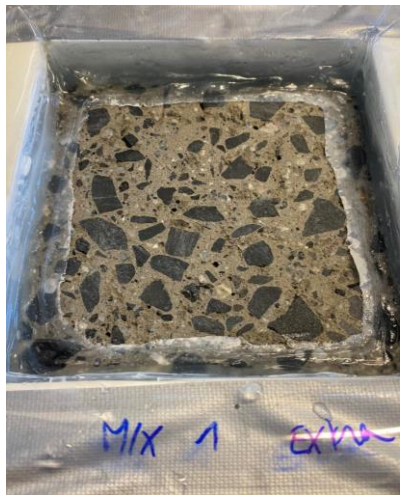
REF-360-CO₂P: Sample B-56d



REF-360-CO₂P: Sample C-56d



M 18/6-360-CO₂P: Sample A-56d



M 18/6-360-CO₂P: Sample B-56d



M 18/6-360-CO₂P: Sample C-56d



M 18/6-300-CO₂P: Sample A-42d



M 18/6-300-CO₂P: Sample B-42d



M 18/6-300-CO₂P: Sample C-42d



25/10-360-CO2P: Sample C-42d

M




M 25/10-360-CO2P: Sample C-42d




M 25/10-360-CO2P: Sample C-42d

I Spacing factor and air percentage analysis on hardened concrete


I.1 REF-360

 TÆKNISSETUR		Date: 31.5.2024
ASTM C457/C457M-16 Microscopical Determination of Parameters of the Air-Void System in Hardened Concrete		
Consultant	The Arctic University of Norway	
Sender	Iveta Novakova/ Amber Steelandt	
Project:	Ar2CorD - Master thesis	
Mixing date:	13.2.2024	
Sample ID:	Ar2corD REF	
Method:	ASTM C457/457M-16 Procedure B	
Operated by:	Kjartan Björgvin Kristjánsson	
Description of sample:	Slab from the end of a 150 mm cube	
Direction of traverse:	Perpendicular to packing direction	
Number of points:	1410	
Magnification:	80 x	
Results		
Specific Surface (α):	33 mm⁻¹	
Spacing Factor (L):	0,14 mm	
Percent air (A):	<u>5,3 %</u>	


I.2 M 18/6-360

 TÆKNISSETUR		Date: 31.5.2024
ASTM C457/C457M-16 Microscopical Determination of Parameters of the Air-Void System in Hardened Concrete		
Consultant	The Arctic University of Norway	
Sender	Iveta Novakova/ Amber Steelandt	
Project:	Ar2CorD - Master thesis	
Mixing date:	14.2.2024	
Sample ID:	Ar2corD Mix 1	
Method:	ASTM C457/457M-16 Procedure B	
Operated by:	Kjartan Björgvin Kristjánsson	
Description of sample:	Slab from the end of a 150 mm cube	
Direction of traverse:	Perpendicular to packing direction	
Number of points:	1380	
Magnification:	80 x	
Results		
Specific Surface (α):	22 mm⁻¹	
Spacing Factor (L):	0,26 mm	
Percent air (A):	<u>3,8 %</u>	

I.3 M 18/6-300

 TÆKNISETUR		Date: 31.5.2024
ASTM C457/C457M-16 Microscopical Determination of Parameters of the Air-Void System in Hardened Concrete		
Consultant	The Arctic University of Norway	
Sender	Iveta Novakova/ Amber Steelandt	
Project:	Ar2CorD - Master thesis	
Mixing date:	19.2.2024	
Sample ID:	Ar2corD Mix 2	
Method:	ASTM C457/457M-16 Procedure B	
Operated by:	Kjartan Björgvin Kristjánsson	
Description of sample:	Slab from the end of a 150 mm cube	
Direction of traverse:	Perpendicular to packing direction	
Number of points:	1420	
Magnification:	80 x	
Results		
Specific Surface (α):	22 mm⁻¹	
Spacing Factor (L):	0,25 mm	
Percent air (A):	<u>4,0 %</u>	

I.4 M 25/10-360

 TÆKNISETUR		Date: 31.5.2024
ASTM C457/C457M-16 Microscopical Determination of Parameters of the Air-Void System in Hardened Concrete		
Consultant	The Arctic University of Norway	
Sender	Iveta Novakova/ Amber Steelandt	
Project:	Ar2CorD - Master thesis	
Mixing date:	20.2.2024	
Sample ID:	Ar2corD Mix 3	
Method:	ASTM C457/457M-16 Procedure B	
Operated by:	Kjartan Björgvin Kristjánsson	
Description of sample:	Slab from the end of a 150 mm cube	
Direction of traverse:	Perpendicular to packing direction	
Number of points:	1460	
Magnification:	80 x	
Results		
Specific Surface (α):	28 mm⁻¹	
Spacing Factor (L):	0,16 mm	
Percent air (A):	<u>6,0 %</u>	

J Placement of samples in the F-T chambers

F-T chamber 1

M 25/10-360-CO2	M 18/6-300-CO2
M 25/10-360-CO2	M 25/10-360-CO2
REF-360-CO2P	REF-360-CO2P
REF-360-CO2P	M 18/6-360-CO2P
M 18/6-360-CO2P	M 18/6-300-CO2P
M 18/6-360-CO2P	M 18/6-300-CO2P
M 18/6-300-CO2P	M 25/10-360-CO2P
M 25/10-360-CO2P	M 25/10-360-CO2P
DUMMY	DUMMY
DUMMY	DUMMY

F-T chamber 2

M 18/6-360-CO2	M 18/6-300-CO2
M 18/6-360-CO2	M 18/6-300-CO2
M 18/6-360-N	M 18/6-360-N
M 18/6-360-N	REF-360-N
REF-360-N	M 18/6-300-N
REF-360-N	M 18/6-300-N
M 18/6-300-N	M 25/10-360-N
M 25/10-360-N	M 25/10-360-N
REF-360-CO2	REF-360-CO2
M 18/6-360-CO2	REF-360-CO2



Optimization of freeze-thaw durability testing for low-carbon concrete with VPI

Amber Steelandt^{1,2}, Veerle Boel¹ and Iveta Nováková²

¹*Ghent university, Department of Structural Engineering and Building Materials, Ghent, Belgium*

²*UIT The Arctic University of Norway, Department of Building, Energy and Material Technology, Narvik, Norway*

Abstract- Concrete, the most widely used building material, significantly impacts the environment, with cement production contributing up to 8% of global CO₂ emissions. To address this, low-carbon concrete (LCC) mixes with supplementary cementitious materials (SCMs) have been developed. Fly ash (FA) is a well-established SCM, but with the decline of coal-fired power plants, alternatives like volcanic pozzolans from Iceland (VPI) are needed. This research evaluated the durability of concrete with VPI through freeze-thaw (F-T) resistance, compressive strength, and chloride migration tests. Results showed VPI enhanced long-term strength more than FA, although higher VPI percentages reduced strength. VPI significantly improved chloride migration resistance, with higher percentages yielding greater resistance. Concrete with VPI performed well in F-T tests but generally worse than FA. Different curing methods significantly influenced F-T performance, with the effect dependent on factors such as air percentage, spacing factor, W/B ratio, specific surface area, and pore size distribution.

Keywords- Low carbon concrete, supplementary cementitious materials, volcanic pozzolan, VPI, fly ash, freeze-thaw, chloride migration, compressive strength

1 Introduction

The production of cement accounts for approximately seven to eight percent of the world's annual CO₂ emissions. [1] However, it wasn't until the 1990s that the construction industry, including the cement industry, began to acknowledge its environmental impact. [2] In response to these environmental concerns, researchers have embraced the task of investigating alternatives to traditional cement in concrete production. This exploration has led to the formulation of low-carbon concrete (LCC), achieved by incorporating supplementary cementitious materials (SCMs) alongside ordinary Portland cement (OPC). [3] The most widely recognized and utilized SCM is Fly-ash (FA). [4]

However, the availability of FA is decreasing due to the phasing out of coal-fired power plants. [4] This necessitates the exploration of alternative materials like

natural pozzolans (NP). Within the group of the NP, volcanic pozzolans (VP) have emerged as a promising candidate for fulfilling the role of SCMs in concrete production. [5] As new types of SCMs, including VP, are being investigated, there is a pressing need for further research into their durability characteristics. Many natural SCMs remain unexplored, with limited data available regarding their durability performance. The properties of concrete are dependent on various factors such as curing conditions, the input materials, and the ratios in which they are used. [6]

2 Materials and Methods

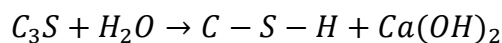
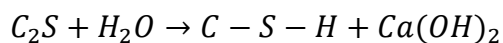
2.1 Materials

2.1.1 Ordinary Portland cement

Ordinary Portland cement (OPC) is produced from Portland clinker, which is manufactured using either the wet or dry milling process. In both methods, limestone

(CaCO₃), clay, and other clay-like materials are added into a rotating kiln. Water is included in the wet milling process. To produce OPC, the resulting clinker is ground, and gypsum (CaSO₄) is added. This final step ensures the desired properties of the cement. The fundamental elements of OPC include calcium silicates (C₂S, C₃S) and calcium aluminates (C₃A, C₄AF), which are generated through the heat-induced reactions among the existing oxides present in the Portland clinker. [7]

When OPC is used to make concrete, the calcium silicates will initiate a hydration reaction when combined with water leading to the formation of calcium silicate hydrate (C-S-H gel) and calcium hydroxide (Ca(OH)₂) as shown in the following reactions [6]:



The C-S-H gel plays a crucial role in interconnecting particles within the concrete, thereby influencing its strength and durability. The calcium hydroxide on the other hand is a by-product that does not directly influence the strength of the concrete. It does however, contribute to the alkalinity of the concrete.[6]

2.1.2 Fly ash

Fly ash, a by-product of power plants generating pulverized coal is the most dominantly used SCM when making low-carbon concrete. [8] It is a pozzolanic binder which means that it reacts chemically with calcium hydroxide in the presence of water.[9] There are two categories in which fly ash can be classified. These are class C fly ash and class F fly ash. Class C stands for high calcium fly ash that contains more than 20% limestone, whilst class F is low calcium fly ash that contains less than 7 % limestone.[8] Class F fly ash is typically produced by burning high-quality coals, such as anthracite and bituminous coals.

These ashes possess pozzolanic properties, which means they react with calcium hydroxide (Ca(OH)₂) and water to form compounds that contribute to the hardening of concrete. However, Class F fly ash lacks inherent cementitious characteristics and thus requires mixing with either OPC or limestone powder (LP) to create concrete. On the other hand, Class C fly ash is generated from the combustion of lower-quality coals, including lignite and sub-bituminous coal. This class of FA not only exhibits pozzolanic properties but also possesses cementitious properties. As a result, Class C fly ash may not necessarily require the addition of OPC or LP to initiate the hydraulic reactions necessary for concrete formation. [9] Class F fly ash is used the most to produce LCC since it is easier to find and has a slower hardening process than class C. [8] The FA used in this paper was already incorporated into the cement type. The FA-cement used to make the reference mix in this paper was CEM II produced by “Heidelberg sement Norge”.

2.1.3 Limestone powder

Limestone powder (LP) does not contain hydraulic or pozzolanic properties. This binder will enhance some properties that cement has, leading to good processability. [7] LP is almost inert but it does partially react with aluminates, producing carbo-aluminate and carbo-silicate hydrates. LP will also dilute the binder phase in concrete which contributes to a higher porosity.[10] When LP is added to concrete it can increase early-age strength when SCMs are used. [10, 11]

2.1.4 Volcanic pozzolan

Materials of a volcanic origin do not automatically possess pozzolanic activity, which is a requirement for their consideration as a SCM. Therefore, only the volcanic materials that have been tested for pozzolanic activity are classified as a volcanic pozzolan (VP) and can be used as a SCM. [12] A study conducted by Hamada et al. (2023) [5]states that volcanic pozzolans vary in chemical composition depending on

their origin. Consequently, outcomes obtained with one type of volcanic pozzolan may diverge from those obtained with another type. The main components of all volcanic pozzolans are silicon dioxide (SiO_2), alumina oxide (Al_2O_3) and ferric oxide (Fe_2O_3). Additionally, notable constituents include calcium oxide (CaO), magnesium oxide (MgO), sodium oxide (Na_2O), potassium oxide (K_2O) and sulfur trioxide (SO_3). The components can be determined using either x-ray fluorescence (XRF), x-ray diffraction (XRD) or other suitable techniques.

The VP used in this paper originates from “Lambafell” in Iceland and is referred to as volcanic Pozzolan Iceland (VPI). The VP found at Lambafell are geologically classified as hyaloclastites, a type of volcanic rock, typically associated with explosive eruptions. Hyaloclastites are created during volcanic eruptions that take place underwater, beneath ice, or when lava flows on land meet the sea or other bodies of water. The lava and rock fragments that are created due to the explosive eruption will mix with the water or ice, forming hyaloclastites through rapid cooling and solidification. [4] The specific properties of VPI are shown in Table 1.

Table 1: properties of VPI

Properties	VPI
Specific weight [g/cm^3]	2.98
Specific surface, Blaine [m_2/kg]	686
SiO_2 [w%]	47.42
Al_2O_3 [w%]	13.35
Fe_2O_3 [w%]	12.32
CaO [w%]	10.98
K_2O [w%]	0.41
Na_2O [w%]	1.88
MgO [w%]	11.29
TiO_2 [w%]	1.66
P_2O_5 [w%]	0.19
Mn_2O_3 [w%]	0.21
Cl [w%]	0.02
$\text{Na}_2\text{O Eq}$ [w%]	2.15

2.1.5 Sample preparation

Four mixes were prepared according to a mix design delivered by Iveta Nováková, researcher at UiT and are shown in Table 2. One mix contained FA-cement (REF-360) and the other three contained VPI. The total amount of binder was either 300 or 360 kg/m^3 and is placed in the name of the samples. M 18/6-360 and M 18/6-300 were made with 18% of the total binder mass being VPI and 6% being LP. M 25/10-360 was made with 25% of the total binder mass being VPI and 10% being LP.

Table 2: mix design [kg/m^3]

	REF-360	M18/6-360	M18/6-300	M25/10-360
CEM I	-	287	239	246
CEM II	360	-	-	-
LP	-	8	7	24
VPI	-	65	54	90
Water	143	136	132	132
Sand:0-8mm	849	856	891	861
Agg:8-22mm	808	814	840	811
Agg:4-8mm	148	149	152	147
SP*	4.32	4.80	3.60	4.32
Air entrainer	0.14	0.14	0.16	0.14

*SP= superplasticizer

2.2 Methods

2.2.1 Tests conducted to determine important concrete properties

A slump test was conducted according to NS-EN 12350-2 [13] to determine the workability of the concrete. Secondly, an air percentage test was performed according to NS-EN 12350-7 [14] to determine the air in the concrete. The slump class that was aimed for was S4 (200-220mm) and the air percentage 4-6%.

However, due to issues with the air pressure gauge, the measured air percentages were unreliable. Consequently, the air content was tested on hardened concrete following ASTM C457/457M-16 Procedure B [15]. This test was conducted by Kjartan Björgvin Kristjánsson, lab researcher in Iceland.

Additionally, the spacing factor and specific surface were determined. The air

percentages presented in the results are those obtained using ASTM C457/457M-16 Procedure B. The original air percentages measured according to NS-EN 12350-7 are excluded due to their inaccuracy.

Additionally, a density evaluation was performed on the hardened concrete samples.

2.2.2 Compressive strength test

Compressive strength tests were conducted according to EN 12390-3 [16] for all the mixes at 2, 28 and 56 days. Three cubes were tested per mix for each age. Up until testing the test pieces were cured in water with a temperature of 20°C. For these tests cubes of 100 x 100 x 100 mm were used.

2.2.3 Chloride migration test

Chloride migration testing was performed according to NT-build-492 [17]. The mixes were tested at both 28 and 56 days. The pieces were cured in water with a temperature of 20°C up until testing and were cut one day before testing took place. When the samples were cut they were placed inside a vacuum pump according to the preparation specifications for this test that are given in the standard.

2.2.4 Freeze-thaw test

Freeze-thaw (F-T) testing was conducted according to SN-EN12390-9 [18]. The standard defines that 4 test pieces should be tested per mix but due to limited space and the use of multiple different curing methods it was decided to use three cubes per mix and curing method instead.

Three types of curing methods were implemented to research their influence on the F-T test results. These curing methods, their code names and the standard they were based on are shown in Table 3.

Table 3: curing methods for F-T

Curing method	Code name	Standard
Normal curing	N	SN-EN12390-9 [18]
CO ₂ -curing (1% CO ₂)	CO2	SS137003 [19]
Prolonged CO ₂ -curing with one week extra in CO ₂ -chamber (1% CO ₂)	CO2P	Executed according to SS137003 [19] But length of prolonged curing determined in collaboration with Ar2CorD*

*information about Ar2CorD in the acknowledgements

3 Results and Discussion

3.1 Important concrete properties

Some important concrete properties are given in Table 4.

Table 4: important concrete properties

	REF-360	M18/6-360	M18/6-300	M25/10-360
Slump [mm]	220	220	220	220
Air [%]	5.3	3.8	4.0	6.0
Mapair [kg/m ³]	0.14	0.14	0.16	0.14
SP [kg/m ³]	4.32	4.80	3.60	4.32
Spacing factor [mm]	0.14	0.26	0.25	0.16
Specific surface [mm ⁻¹]	33	22	22	28
W/B ratio	0.40	0.40	0.47	0.42
W/C ratio	0.48	0.47	0.55	0.54

3.2 Density evaluation

The results for the density evaluation of hardened concrete are shown in Table 5

Table 5: density evaluation

Mix name	Density 2 days [kg/m ³]	Density 28 days [kg/m ³]	Density 56 days [kg/m ³]
REF-360	2340	2345	2345
M 18/6-360	2385	2390	2395
M 18/6-300	2385	2400	2400
M 25/10-360	2355	2360	2365

3.3 Compressive strength

The compressive strength results are shown in Figure 1. All the mixes can reach a strength class of C40/50 after 28 days.

M 18/6-360 and M25/10-360 had a higher compressive strength than REF-360 at all the testing ages, whereas M 18/6-300 had a lower compressive strength. Since M 18/6-300 has less binder than the other mixes, it is normal for the compressive strength to be lower.

According to Hossain & Lachemi (2007) [20] the compressive strength of concrete with VA will decrease with the increase of the VA substitution percentage compared to concrete with only OPC. A similar study that was conducted by Aziz et al. (2021) [21] concludes the same thing. The results from this research also find a similar trend. The compressive strength of M 25/10-360 is lower than the compressive strength of M 18/6-360 which both have the same amount of binder but a different substitution percentage of OPC.

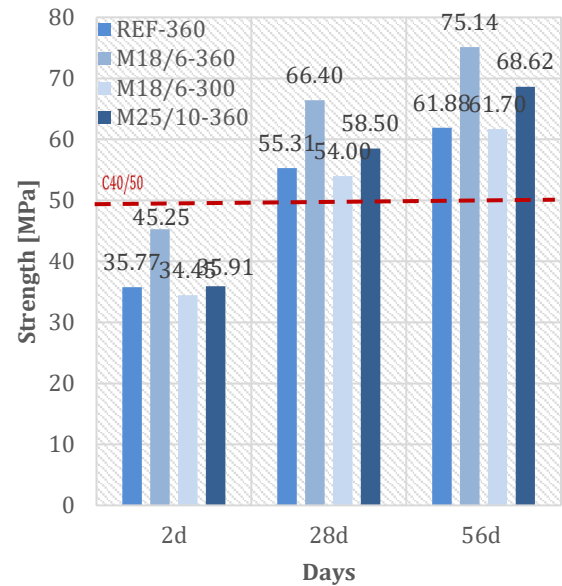


Figure 1: compressive strength results

3.4 Chloride migration

The results for the chloride migration test are given in Figure 2. When looking at the results it is noticeable that M 25/10-360 was highly chloride resistant at 28 days and could be classified as very high resistant at 56 days. The three other mixes were classified as moderate resistant to chloride migration at 28 days and high resistant after 56 days.

It is noticeable that M 18/6-360 and M 18/6-300 are both in the same chloride resistance category as the reference mix. Meaning, the reference mix which contains fly-ash cement does not necessarily perform better than the mixes with VPI. M 25/10-360 even surpasses the reference mix in terms of chloride migration resistance.

Celik et al. (2014) [22] attributed the improved resistance to the lower porosity of concrete with SCMs, meaning it has fewer gel pores for chloride to penetrate. Additionally, adding LP can form carboaluminates, further reducing pore size and blocking chloride entry. These results are clearly supported by the findings in this study.

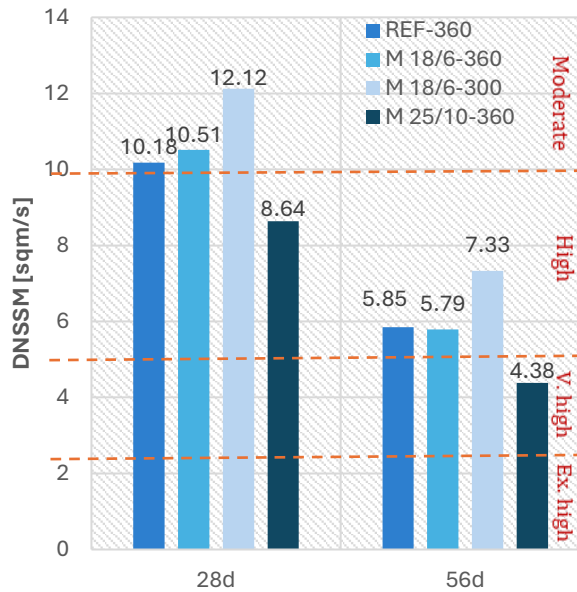


Figure 2: chloride migration results

3.5 Freeze-thaw

According to EN12390-9 [23] the limit for scaling when doing F-T testing for a concrete slab is 1 kg/m^2 . NS-EN 206 [24] says that the scaling cannot surpass 0.50 kg/m^2 for concrete slabs. The primary requirement for determining freeze-thaw resistance will be the 0.50 kg/m^2 limit, although the 1 kg/m^2 limit will also be considered. The F-T results for REF-360, M 18/6-360, M 18/6-300 and M 25/10-360 are respectively shown in Figure 3, 4, 5 and 6. Some of the mixes did not have data for 56 days due to time constraints.

To avoid confusion, the basics regarding F-T performance are briefly explained. A higher air content leads to better F-T performance because it provides space for the water inside the pores to expand, thereby releasing pressure [25]. The spacing factor refers to the average distance between the added air voids and is optimal for F-T when it is lower than 0.20 mm [26]. The specific surface refers to the total surface area of air voids per unit volume of concrete, indicating the fineness or coarseness of the air-void system. A specific surface value greater than 25 mm^{-1} is considered beneficial for F-T performance [15]. A higher W/B ratio leads to the formation of more capillary pores,

which is not beneficial for F-T performance since these pores can absorb water. [27] The pore size distribution refers to the distribution of different sizes of pores within the concrete. This distribution can change when the pores get filled and their sizes reduce, which can occur, for example, through CO_2 curing. [27]

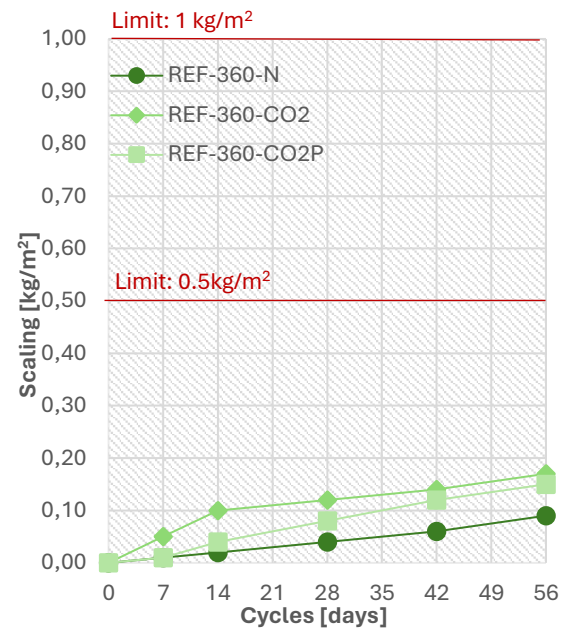


Figure 3: F-T results for REF-360

REF-360 had a W/B ratio of 0.4, which is relatively low and therefore results in the formation of fewer capillary pores. This positively influences the F-T resistance. The air percentage in this mix was 5.3% which is also very beneficial for F-T performance. Additionally, the spacing factor was 0.14 mm , below the optimal threshold of 0.22 mm , and the specific surface area was 33 mm^{-1} , exceeding the ideal minimum of 25 mm^{-1} . The pore size distribution was likely very good as well due to the low W/B ratio. Although normal curing performs slightly better than the other two curing conditions, the difference is negligible. In other words, the scaling with CO_2 and prolonged CO_2 curing is worse but still within acceptable limits. The slightly worse performance of CO_2 curing is likely because more gel pores than capillary pores were filled with CaCO_3 , resulting in an uneven pore size distribution

and thus worse F-T results. The F-T performance improves slightly with prolonged CO₂ curing. This improvement could be attributed to the fact that the CO₂ had more time to fully penetrate the concrete, leading to an overall better pore size distribution.

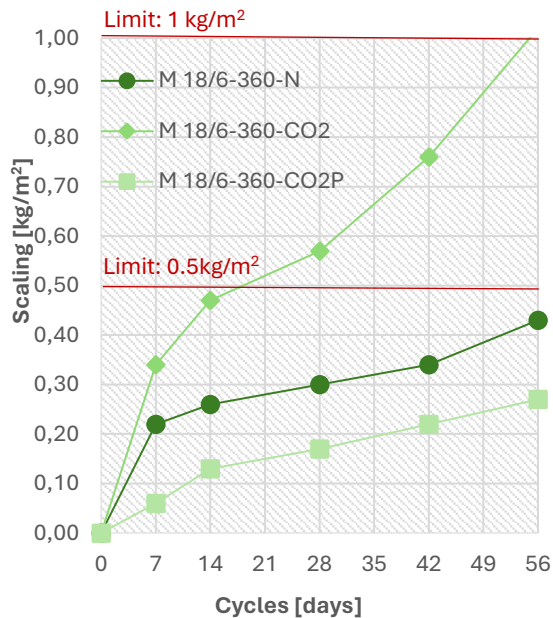


Figure 4: F-T results for M 18/6-360

M 18/6-360 had a W/B ratio of 0.4, an air content of 3.8% and a spacing factor of 0.26 mm. The relatively low W/B ratio suggests that fewer capillary pores were formed, which is beneficial for F-T performance. However, the low air content and spacing factor higher than 0.20 mm contributes to worse F-T results. Additionally, the specific surface area was 22 mm⁻¹ which is lower than ideal minimum of 25 mm⁻¹ and therefore also contributes worse F-T resistance.

For M 18/6-360, the standard CO₂ curing leads to the formation of CaCO₃, which fills the pores. The poor F-T performance under standard CO₂ curing suggests that more gel pores, rather than capillary pores, were filled, or that the filling of pores was unevenly distributed. However, prolonged CO₂ curing performs better, staying below the limits. This improvement is likely

because the extended time in the CO₂ chamber allows for more thorough and uniform penetration of CO₂, resulting in better F-T resistance.

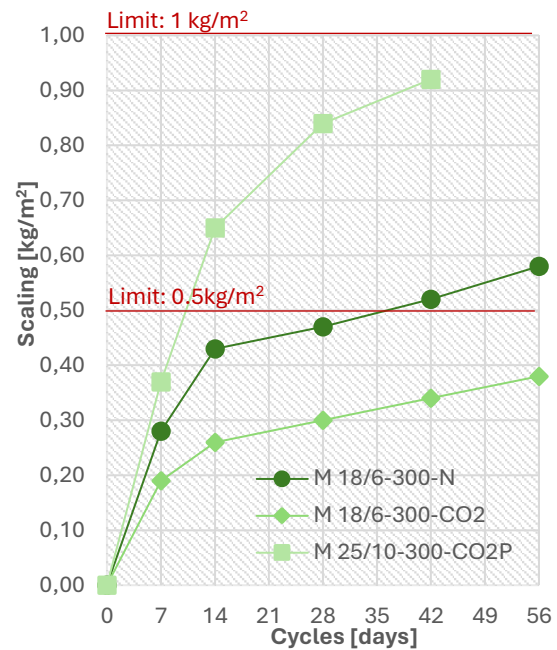


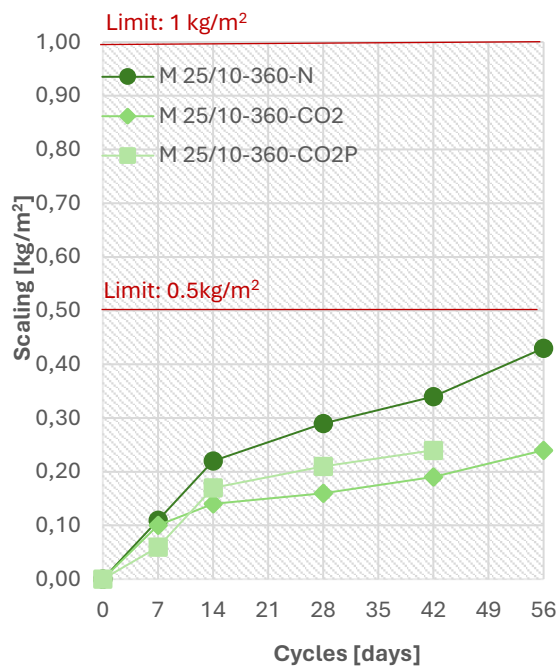
Figure 5: F-T results for M 18/6-300

M 18/6-300 surpasses the limit of 0.5 kg/m² for both normal curing and prolonged curing. The results for CO₂ curing however, stay below the limits for all the cycles. In this case the CO₂ curing most likely filled the capillary pores, resulting in less water absorption and thus better F-T results. The normal curing performs well up until 42 cycles, when it eventually exceeds the limit of 0.5 kg/m². However, it does not exceed the limit of 1 kg/m² at any time. The worst performance is this of the prolonged CO₂ curing, which exceeds the limit of 0.5 kg/m² relatively quick.

M 18/6-300 had an air percentage of 4% which is not very high but can still contribute to better F-T performance. However, the mix does have a relatively high W/B ratio (0.47) which can lead to the formation of more capillary pores. The air percentage might explain why the concrete doesn't exceed the limit for normal curing at first despite the fact that there are probably more capillary pores present in the concrete. However, this

mix does have a spacing factor of 0.25 mm and a specific surface of 22 mm⁻¹. Both of these values are not optimal and also contribute to worse F-T performance.

CO₂ curing likely produced the best results for M 18/6-300 because the capillary pores were partially filled with CaCO₃, improving the F-T performance by reducing the pore size. However, the fact that prolonged CO₂ curing resulted in the worst performance suggests that the extended time in the CO₂ chamber led to excessive carbonation, which may have filled both gel and capillary pores unevenly. This uneven pore structure might have led to poorer F-T performance.



M 25/10-360 contained a relatively high substitution percentage of 25% VPI. The VPI reacts with Ca(OH)₂ to form additional compounds that fill the capillary pores, resulting in consistently excellent F-T performance that remains below the limit at all times. Additionally, the mix had a measured air content of 6%, which is relatively high and contributes to a good spacing factor (0.16 mm) and thus to the good F-T results. The W/B ratio was 0.42, which could lead to the formation of more capillary pores but the higher VPI content

effectively fills these pores. Generally speaking, this mix likely had an optimal pore size distribution.

It is noticeable that normal curing for M 25/10-360 resulted in the poorest performance among the three methods, whereas the standard CO₂ curing performed the best. CO₂ curing results in the creation of CaCO₃ which ideally fills up the capillary pores, which is likely the case for this mix. The high VPI percentage and the high air percentage already contribute to really good F-T performance, but the extra filling of the capillary pores due to the CO₂ curing added to this even more. The prolonged CO₂ curing performs slightly worse than the standard CO₂ curing. This could be attributed to over carbonization which lead to an uneven pore distribution.

Table 6 gives an overview of the curing method that performed best and the one that performed worst for all of the mixes. Hereby W= worst, B= Best and M= middle. The absence of a visible pattern in these results is evident, making it worthwhile to discuss several potential factors that could have contributed to this lack of pattern.

Table 6: best and worst curing method for each mix

	REF-360	M 18/6-360	M 18/6-300	M 25/10-360
N	B	M	M	W
CO2	W	W	B	B
CO2P	M	B	W	M

There is no universal curing condition that suits all concrete mixes, even those made with the same type of binder. This variability is evident in Table 24, which shows that the optimal curing conditions differ significantly across the three mixes made with VPI. Each mix responds differently, highlighting the complexity of the F-T mechanism. More research is needed to obtain additional test results that can help form explanations, especially concerning curing conditions performed according to

Swedish standards, as these results do not show a clear pattern.

4 Conclusions

In this study, the durability performance of concrete incorporating VPI was investigated, with a primary focus on F-T resistance. This research was conducted as part of the larger collaborative project Ar2CorD, aiming to optimize LCC through the utilization of various SCMs, including VPI.

The findings revealed that the compressive strength decreased with higher substitution percentages of OPC. Even with a lower binder content, mixes with VPI showed comparable compressive strength to those with higher binder content, suggesting a significant contribution of VPI to strength development through pozzolanic reactions.

Furthermore, the chloride resistance of concrete mixes varied, with M 25/10-360 demonstrating high resistance at 28 days and very high resistance at 56 days, while the other mixes exhibited moderate to high resistance over time. Generally, the inclusion of VPI resulted in good chloride resistance, with higher resistance observed at higher VPI substitution percentages.

For F-T resistance, all tested mixes performed relatively well, with VPI mixes showing higher scaling compared to FA mixes under all curing conditions. However, the choice of curing condition significantly influenced F-T performance. While some mixes surpassed scaling limits under certain conditions, they remained within acceptable limits for others.

In conclusion, concrete incorporating VPI demonstrated good durability performance overall, affirming its suitability as an SCM in concrete applications. However, the complexity of F-T mechanisms and the variability of mix responses highlight the need for further research.

5 Further research

Future research endeavors should focus on exploring different types of volcanic pozzolans, investigating the influence of various curing methods, conducting comparative studies with other SCMs, and expanding the database of test results to optimize the application of volcanic pozzolans in concrete construction.

Research of SCMs with curing conditions according to Swedish standards should also be further investigated. Additional studies in this area can provide valuable insights for optimizing concrete performance.

Author Contributions

Conceptualization, A.S., I.N. and V.B.; Data curation, A.S.; Investigation, A.S., I.N. and V.B.; Writing-original draft, A.S.; Supervision, V.B. and I.N.

Declaration of Conflict of Interests

The authors declare that they have no known competing financial interests or personal relationships that could have appeared to influence the work reported in this paper

Acknowledgements

This research is included in the master's dissertation submitted in order to obtain the academic degree of Master of Science in de "industriële wetenschappen: bouwkunde". It is part of the Ar2CorD project, a collaboration project between different Nordic countries to research the optimization of LCC with the use of both known and unknown SCMs.

References

- [1] N. B. Singh, M. Kumar, and S. Rai, "Geopolymer cement and concrete: Properties," (in English), *Materials Today-Proceedings*, Proceedings Paper vol. 29, pp. 743-748, 2020, doi: 10.1016/j.matpr.2020.04.513.
- [2] P. V. Nidheesh and M. S. Kumar, "An overview of environmental sustainability in cement and steel

- production," (in English), *Journal of Cleaner Production*, Review vol. 231, pp. 856-871, Sep 2019, doi: 10.1016/j.jclepro.2019.05.251.
- [3] P. D. Nukah, S. J. Abbey, C. A. Booth, and G. Nounu, "Optimisation of Embodied Carbon and Compressive Strength in Low Carbon Concrete," (in English), *Materials*, Article vol. 15, no. 23, p. 32, Dec 2022, Art no. 8673, doi: 10.3390/ma15238673.
- [4] H. m. Norge. "vulkansk pozzolan aske fra island i fremtidens sementer?" https://www.sement.heidelbergmaterials.no/no/vulkansk_aske (accessed.
- [5] H. M. Hamada, F. Abed, S. Beddu, A. M. Humada, and A. Majdi, "Effect of Volcanic Ash and Natural Pozzolana on mechanical properties of sustainable cement concrete: A comprehensive review," (in English), *Case Studies in Construction Materials*, Review; Early Access vol. 19, p. 14, 2023 2023, Art no. e02425, doi: 10.1016/j.cscm.2023.e02425.
- [6] S.Druart and L.Taerwe, *betontechnologie*, 6th ed. Brussel: Belgische betongroepering, 2018, p. 817.
- [7] V. Boel, "Microstructuur van zelfverdichtend beton in relatie met de gaspermeabiliteit en duurzaamheidsaspecten," PHD, university of Ghent, Ghent, 2006. [Online]. Available: <http://hdl.handle.net/1854/LU-4271638>
- [8] Z. G. Ralli and S. J. Pantazopoulou, "State of the art on geopolymers concrete," (in English), *International Journal of Structural Integrity*, Article vol. 12, no. 4, pp. 511-533, Aug 2021, doi: 10.1108/ijsi-05-2020-0050.
- [9] J. R. Shania Zehra Naqvi , and Kamal K. Kar, "coal-based fly ash,"
- [10] M. Marinkovic, A. Radovic, and V. Carevic, "Carbonation of limestone powder concrete: state-of-the-art overview," (in English), *Gradevnski Materijali I Konstrukcije-Building Materials and Structures*, Review vol. 66, no. 2, p. 13, Jun 2023, Art no. 2300005m, doi: 10.5937/grmk2300005m.
- [11] K. Celik, R. Hay, C. W. Hargis, and J. Moon, "Effect of volcanic ash pozzolan or limestone replacement on hydration of Portland cement," (in English), *Construction and Building Materials*, Article vol. 197, pp. 803-812, Feb 2019, doi: 10.1016/j.conbuildmat.2018.11.193.
- [12] F. J. Jubera-Pérez et al., "Pozzolanic activity of volcanic ashes produced by the eruption of the Tajogaite Volcano in La Palma, Canary Islands," (in English), *Construction and Building Materials*, Article vol. 419, p. 11, Mar 2024, Art no. 135498, doi: 10.1016/j.conbuildmat.2024.135498 .
- [13] NS-EN 12350-2, 2019.
- [14] NS-EN 12350-7, 2019.
- [15] ASTM C457/457M-16, 2024.
- [16] EN 12390-3, 2019.
- [17] NT-build-492, 2018.
- [18] SN-EN 12390-9, 2016.
- [19] SS137003, 2004.
- [20] K. M. A. Hossain and M. Lachemi, "Fresh, Mechanical, and Durability Characteristics of Self-Consolidating Concrete Incorporating Volcanic Ash," (in English), *Journal of Materials in Civil Engineering*, vol. 22, no. 7, pp. 651-657, Jul 2010, doi: 10.1061/(asce)mt.1943-5533.0000063.
- [21] M. M. Aziz, A. Moundi, D. Dawai, B. Ntieche, B. M. G. Koungang, and F. Michel, "Effect of the use of volcanic pozzolan from Mbepit Massif (West-Cameroon) on the mechanical properties of mortar and composite cements production," (in

- English), Engineering Research Express, Article vol. 3, no. 1, p. 8, Mar 2021, doi: 10.1088/2631-8695/abe954.
- [22] K. Celik et al., "High-volume natural volcanic pozzolan and limestone powder as partial replacements for portland cement in self-compacting and sustainable concrete," (in English), Cement & Concrete Composites, vol. 45, pp. 136-147, Jan 2014, doi: 10.1016/j.cemconcomp.2013.09.003
- [23] EN 1504-9, 2008.
- [24] NS-EN 206, 2022.
- [25] G. D. Schutter, damage to concrete structures. (in english), 2013, p. 209.
- [26] R. J. Wang, Z. Y. Hu, Y. Li, K. Wang, and H. Zhang, "Review on the deterioration and approaches to enhance the durability of concrete in the freeze-thaw environment," (in English), Construction and Building Materials, Review vol. 321, p. 24, Feb 2022, Art no. 126371, doi: 10.1016/j.conbuildmat.2022.126371
- [27] P. Taylor et al., Entrained air-void systems for durable highway concrete, n. a. press, ed., 2021. [Online]. Available: <https://nap.nationalacademies.org/catalog/26071/entrained-air-void-systems-for-durable-highway-concrete>.